EXPERIMENTAL AND ANALYTICAL STUDIES OF DROP-SIZE DISTRIBUTIONS IN HYDROCARBON FERMENTORS

A Thesis Submitted
in partial Fulfilment of the Requirements
for the Degree of

DOCTOR OF PHILOSOPHY

By

RAKESH KUMAR BAJPAI

DEPARTMENT OF CHEMICAL ENGINEERING

INDIAN INSTITUTE OF TECHNOLOGY KANPUR

OCTOBER 1975

CHE-1995-D-BAJ-EXP

46109

TO THOSE

WHO ALWAYS SACRIFICE

AND DEMAND NOTHING

C E R T I F I C A T E

This is to certify that the present work, "EXPERIMENTAL AND ANALYTICAL STUDIES OF DROP-SIZE DISTRIBUTIONS IN HYDROCARBON FERMENTORS " has been carried out under my supervision and that this work has not been submitted elsewhere for a degree.

D. Ramkrishna
Professor
Department of Chemical Engineering

ACKNOWLEDGEMENTS

The author is indebted to Professor D. Ramkrishna for suggesting the research topic and continuous close guidance all along the work. He also wishes to express his deep sense of gratitude to Dr. A. Prokop (Institute of Microbiology, Czechoslovak Academy of Sciences, Prague, Czechoslovakia) for untiring supervision and constant encouragement in addition to providing facilities for experimental work during author's stay in Czechoslovakia.

Dr. A. Einsele (Institute of Microbiology, ETH, Zürich), Dr. H.W.D. Katinger (Institute of Microbiology, Vienna, Austria), and Dr. H. Sawistowski (Imperial College, London, U.K.) provided the necessary experimental data available in their laboratories and the author is very grateful to them.

The help provided by Professor J.D. Borwankar, Dr. P.C. Joshi (both of Department of Mathematics, IIT-Kanpur), Professor A.P. Kudchadker, Dr. A.K. Gupta, and Dr. B.H. Shah at various stages of the research work is gratefully acknowledged.

The technical staff of Department of Technical Microbiology, MBÚ, ČSAV, Prague, ČSSR, esp. Mrs. Pisařiková and Mr. Turčič provided their valuable support in conducting experimental work, which is very much appreciated.

Thanks are also due to the authorities and staff of Computer Centre, I.I.T., Kanpur for providing the necessary computer time.

Financial support provided by the organizers of the UNESCO and WHO sponsored 'Post Graduate Course in Microbiology', for author's stay in Czechoslovakia is acknowledged.

Finally, the author expresses his thanks to Messrs. B.S. Pandey, D.S. Panesar, Hari Ram, and Jai Ballabh Ghoshal for their assistance in preparing this manuscript.

Author

TABLE OF CONTENTS

* * *

LIST OF TABLES

* * *

LIST OF FIGURES

* * *

NOMENCLATURE AND GLOSSARY OF ABBREVIATIONS

Nomenclatures

a_1	maximum surface biomass density, dimensionless	defined in Appendix E
a_2	mass transfer parameter, dimensionless	
a_3	desorption parameter, dimensionless	
a_4	adsorption parameter, dimensionless	
a_5	equilibrium constant for the distribution of substrate between the two phases, dimensionless	
a_k	saturation constant for growth of biomass on interface, dimensionless	
$a_{k'}$	saturation constant for growth of biomass in continuous phase, dimensionless	
A	surface area of a drop of volume v	cm^2
A_t	state of system at any time t	
b	constant, Equation (3.1.14)	cm
d	diameter of a drop of volume v	cm
d_{21}	(μ_2/μ_1) mean diameter	cm
d_{32}	(μ_3/μ_2) mean diameter, also known as Sauter-mean diameter	cm
$f(v)$, $f_n(v)$; $f_N(v)$	drop-size distributions	cm^{-3}
f_A	surface area distribution of dispersed phase drops	cm^{-2}
$F(v)$, $F_N(v)$	cumulative drop-size distribution	
$g(v', v''; x)$	probability density of sizes of a new droplet pair due to C-R event involving v' and v'', Equation (3.1.5)	cm^{-3}

k	constant, Equation (3.1.14)	dimensionless
k_a	adsorption constant	$L_{CP}/gm_{DW}/hr$
k_c	coalescence-redispersion frequency, defined by Erickson, et al. (1970)	hr^{-1}
k_d	desorption constant	hr^{-1}
k_m	mass transfer coefficient	cm/hr
k_s	saturation constant for growth of biomass on dispersed phase	$gm_{substrate}/cm^3_{DP}$
$k_{s'}$	saturation constant for growth of biomass in aqueous phase	$gm_{substrate}/L_{DP}$
m	exponent of size in interaction frequency, Equation (3.1.4)	
M	sequence of random numbers for the probability of formation of a daughter droplet	
n	number density distribution of drop-sizes, also, biomass density (dispersed phase)	cm^{-3} gm_{DW}/cm^2_{DP}
n'	biomass density in continuous phase	gm_{DW}/L_{CP}
n_∞	maximum surface biomass density	gm_{DW}/cm^2_{DP}
N	total number of drops in the system; also number of data sets	
N_s	number of simulations	
p	probability that the random variable X has a negative sign	
P	cumulative probability of signs of X; also represents the probability that no particulate event occurs in the given interval of time	
$q(v',v'')$	interaction frequency for the droplet pair of sizes v' and v", Equation (3.1.4)	hr^{-1}
S	concentration of substrate in dispersed phase,	$gm_{substrate}/cm^3_{DP}$

S'	concentration of substrate in aqueous phase	$gm_{substrate}/L_{CP}$
$S_{eq'}$	equilibrium concentration of substrate in aqueous phase	$gm_{substrate}/L_{CP}$
t	time	hr
T	sequence of random numbers for interval of quiescence	
u	sequence of random numbers for coalescence of a pair of droplets	
v	volume of a droplet	cm^3
V	volumes of various phases	cm^3
w	constant coalescence frequency	hr^{-1}
w_o	Proportionality constant in drop interaction frequency, Equation (3.1.4)	
We	Weber number	
x	random variable	
Y	growth constant	$gm_{DW}/gm_{substrate}$
x,y,z	intermediate variables	

Greek Symbols

α, β	constant	
θ	holding time in CFSTV	hr
σ	surface tension	dynes/cm
ϕ	dispersed phase fraction	
φ	transformed drop-size distribution, Equation (3.1.8)	

μ	moments of drop-size distribution; also specific growth rate of biomass	hr^{-1}
χ^2	Chi-square	
ρ_s	density of substrate	$gm_{substrate}/cm^3$
τ	time	

Subscripts

-, +	number of times the property takes negative or positive sign
o,1,2, ...,m	order of moment
c	continuous phase property
d	dispersed phase property
max	maximum value of the property
o	properties at time t=0

Superscripts

',,"	properties pertaining to different elements; Also represents continuous phase property
*	equilibrium value of the property
~	steady state property

Glossary of Abbreviations

C-R	coalescence-redispersion
CFSTV	constant flow stirred tank vessel
CP	continuous phase
CRF	coalescence-redispersion frequency
CS	circulation $stirring_{(adj)}$ - and circulation $stirrer_{(noun)}$

DM	detergent method
DP	dispersed phase
DSD	drop-size distribution
DW	dry weight
EM	encapsulation method
exp	exponential
FBT	flat-blade turbine
GM	gelation embedding method
HMDA	hexamethylene di-amine
IQ	interval of quiescence
SC	sebacoyl chloride
SDS	sodium dodecyl sulfate

SYNOPSIS

EXPERIMENTAL AND ANALYTICAL STUDIES OF DROP-SIZE DISTRIBUTIONS IN HYDROCARBON FERMENTORS

A Thesis Submitted
In Partial Fulfilment of the Requirements
For the Degree of
DOCTOR OF PHILOSOPHY

by

RAKESH KUMAR BAJPAI

to the

Department of Chemical Engineering
Indian Institute of Technology, Kanpur

October 1975

Hydrocarbon fermentation is a subject of intensive research because of its anticipated potential of producing Single-Cell protein. The system consists of hydrocarbons dispersed in the aqueous medium in the form of drops, aqueous medium itself, microbial cells, and air bubbles. Stirred vessels with specially designed agitators for vigorous mixing of the different phases are commonly used for this purpose. Hydrocarbon drops continuously coalesce and redisperse giving rise to a distribution of drop sizes. Simultaneously, the microorganisms consume hydrocarbons either directly from the drop-interface or those dissolved in the aqueous medium. Therefore a thorough knowledge of drop-interaction processes and the drop-size distributions is essential before a

rational design and scale-up of hydrocarbon fermentors may be attempted.

The present study has attempted to characterize the nature of drop-interactions and the drop-size distributions obtained in hydrocarbon fermentors and related systems. A coalescence-redispersion (C-R) model has been proposed for drop-interactions and its predictions have been verified for a large number of experimental data obtained during the course of this investigation and from the literature. Experimental measurements for drop-interaction frequencies have been carried out using a new method based upon the C-R model. The model has finally been used, together with the growth equations, for a Monte-Carlo simulation of growth of biomass in hydrocarbon fermentors.

Chapter II describes a method for experimental measurement of drop-size distributions in liquid-liquid agitated systems. A detergent stabilization method was chosen because of its applicability to drop-size measurement in hydrocarbon - water systems both in the absence and the presence of biological growth. This method consists of sampling a small amount of dispersion in a mildly agitated concentrated solution of detergent followed by microphotography. A high degree of reproducibility could be obtained by this method. All the experimental work was carried out in a three-litre fermentor fitted with a Waldhof-agitator.

Drop-size distribution data experimentally observed in gas-oil and in n-alkane fermentations were obtained from various

sources (Prokop and Ludvík, 1973; Blanch and Einsele, 1973; and Katinger, 1973) and an attempt was made to empirically correlate them with experimental conditions. It was found that the number density distributions for different experimental conditions of speeds of rotation, dispersed phase fractions, sizes of vessels, and different times of fermentation, when normalized with the Sauter-mean diameter, reduce to a single normalized distribution. Thus the Sauter-mean diameter emerged as a possible basis for scale-up of hydrocarbon fermentors. The Sauter-mean diameter was correlated with parameters describing experimental conditions in the circulation-stirring systems. The exponent of dependence upon Weber number in particular was found to be $-(0.1-0.3)$ instead of -0.6 obtained for flat-blade turbine systems. Another observation which emerged out of the studies was that the concentration as well as the physiological state of the biomass strongly affect the Sauter-mean diameter.

In Chapter III, a coalescence-redispersion model for drop-interactions is discussed. The model views the drop-phenomena as a single step coalescence-redispersion process between any two droplets which results in redistribution of mass between them. The population balance equation for batch vessels at equilibrium drop-size distribution is amenable to analytical solution and for the case of constant coalescence frequency, the model predicts an <u>exponential</u> equilibrium distribution of drop sizes. Experimental data for drop-size distributions, collected in laboratory during

the present investigation for n-alkane-water system mixed by a Waldhof-agitator, and for various other systems available in the literature (Brown and Pitt, 1972; Luhning and Sawistowski, 1971; Shinnar, 1961; and Prokop and Ludvík, 1973), were satisfactorily predicted by the model. On comparing the model predictions with those of the drop-size distributions proposed by vanHeuven and Hoevenaar (1968) and Bayens (1967), a χ^2-sign test rated the C-R model better than the latter two. The model predictions for Waldhof-agitated systems (or circulation stirring systems) were found to improve when the coalescence frequency was assumed to be a function of drop-sizes.

Based upon the C-R model, a method was proposed for the measurement of coalescence frequency. It requires measurement of transient-state drop-size distributions in a stirred batch vessel, or steady state DSDs of in- and out-going streams in a continuous flow stirred tank vessel. From the data obtained in the batch vessel, the coalescence frequency can be calculated by the slope of the straight line obtained by plotting the second moments of drop-size distributions vs time lapsed since the start of the stirring. In this connection, the experimental data were obtained for n-alkane-water system agitated by a Waldhof-mixer. The results show that instead of a power function dependence of coalescence frequency upon the speed of rotation as normally observed for flat-blade turbine systems, the Waldhof-agitated systems

are characterized by a linear dependence of drop-interaction frequency on the speed of rotation.

Finally, the C-R model has been used to represent the drop-phenomena in hydrocarbon fermentors while attempting to predict their behavior. A Monte-Carlo simulation procedure has been utilized for this purpose and the results are presented in Chapter IV. The nature and significance of interactions between dispersed phase drops has been investigated. The results of computer simulation confirm the empirically observed self preserving nature of drop-size distributions in batch hydrocarbon fermentors. A study of the contribution of continuous phase growth towards overall biomass growth has also been attempted.

* * *

CHAPTER I

INTRODUCTION

World-wide protein shortage has stimulated a vigorous search for new sources of protein supply, in the last fifteen years. By the end of this century, the demand for protein is estimated to be around 65 million tons, of which only 43 million tons is expected to be met by conventional means (Vilenchich and Akhtar, 1971). In order to overcome such high deficiencies, it is evident that every possible means be tapped to the utmost. Microorganisms which contain proteins as much as sixty percent of their dry weight, will play an important role in meeting the requisite demand in future. A strong case for their cultivation is presented by high rates of multiplication of microorganisms, relatively small floor-space requirements and a high efficiency of conversion of substrate to proteins. In addition to hydrocarbons, other carbon substrates for the growth of microbes are methanol, ethanol, natural gas, and glucose. Hydrocarbon fermentation has, however, the additional advantage that it results in improved quality of the petroleum product used for the supply of C-substrate. In India, there is a potential for producing 6 lakh (600,000) tons of pure proteins from Assam crudes alone (Iyengar, et al., 1968).

Hydrocarbon fermentation involves four phases which contribute to the growth of microorganisms. These are the gas

phase (air), the aqueous phase (medium), the dispersed phase (oil), and the solid phase (cells). Transfer of oxygen and C-substrate across interfaces, sometimes more than one, before being consumed by the cells, makes the analysis of these systems extremely complicated. However, we shall restrict our attention in the present study to substrate limited growth alone. In other words, oxygen concentration in the system is assumed to be above the critical level all the time. Hydrocarbons being sparingly soluble in aqueous medium, exist in the form of drops. These drops are present in a turbulent environment, and continuously coalesce and redisperse. The cells consume the hydrocarbons either directly from the interface or those dissolved in the continuous phase. The substrate limited growth in hydrocarbon fermentors is influenced by distribution of drop sizes, frequency of coalescence and breakup of drops, distribution of biomass between the continuous phase and the dispersed phase interface, mass transfer between phases, and distribution of substrate in the dispersed phase. Rational choice of hydrocarbon-fermentor design and scale-up has so far been hindered by inadequate knowledge of drop phenomena in these systems. The present study attempts to throw some light upon the nature of these processes by proposing a simple model for drop-interactions, and explains the drop-size distributions observed in hydrocarbon fermentors and similar systems. Further it demonstrates the applicability of the model by simulating the drop phenomena

and growth in hydrocarbon fermentors on a computer. Coalescence-redispersion frequencies needed in the course of simulation have been experimentally measured.

The literature reports various attempts to model the growth phenomena in hydrocarbon fermentors. Erickson et al. (1969 a,b,c) have proposed models for growth on single hydrocarbon drops. These models were used to examine the effects of interfacial area, substrate solubility in the aqueous medium, the mass transfer coefficient, and the saturation constant in the kinetic equations on the growth behavior. Erickson et al.(1970) and Humphrey and Erickson (1972) extended these models to cases where swarms of drops exist. These models take into account the distribution of drop sizes, the rate of adsorption of cells on the drop surface, the rate of desorption of cells from the drop surface, substrate transport between the phases, and growth kinetics. The effect of coalescence and redispersion of drops was also considered. A discrete uniform distribution and a discrete normal distribution obtained from an experimentally observed distribution curve (Chen and Middleman, 1967) were used as drop-size distributions by Erickson et al.(1970) and relative importance of each parameter encountered in the system was investigated. Drop-size distributions were found to affect the batch growth profoundly. It was reported that in the presence of a drop-size distribution and little or no drop-interaction, the large drops require more time for their

substrate to be consumed than the smaller drops, thus increasing the time required to complete the fermentation.

Shah et al. (1972 a) utilized the model for simulating the performance of hydrocarbon fermentors and estimated the parameters in the model. For parameter estimation, they used the experimental data of Prokop et al. (1971) who studied the effects of inoculum size, dispersed phase volume, and substrate concentration on the batch growth of Candida lipolytica on a model system composed of n-hexadecane dissolved in dewaxed gas-oil. It was pointed out that either continuous phase growth or growth on small segregated drops or both, contribute significantly towards the linear growth rate especially when the dispersed phase substrate concentration is large. Accurate knowledge of drop-size distribution and drop-phenomena was emphasized for the sake of better prediction.

Stamatoudis and Tavlarides (1973) have also highlighted the importance of accurate knowledge of drop-size distributions. Drop phenomena have been simulated using a Monte-Carlo method developed by Zeitlin and Tavlarides (1972). This study which utilized the experimental data of Prokop et al. (1971), Moo-Young et al. (1971 a,b), and Wang and Ochoa (1972) for estimation of the parameters, concluded that changes of total interfacial area with the different drop-size distributions were responsible for significant differences in prediction of various size-distribution models. Moo-Young and coworkers (1971 a,b) studied

the influence of cell-drop interactions on growth in hydrocarbon fermentors. This investigation found that a model which assumed that the oil drops were smaller than the yeast cells, gave a better fit to the experimental data. The importance of small accommodated drops was also advanced by Aiba et al. (1969 a,b).

1.1 Drop-Size Distributions (DSD) in Hydrocarbon Fermentation:

Recently, a number of experimental studies have reported drop-size distribution data measured in hydrocarbon fermentation systems. Prokop et al.(1972), and Prokop and Ludvík (1973) have presented drop-size distributions observed in batch fermentations of Candida lipolytica on gas-oil and n-alkanes dissolved in dewaxed gas-oil. These observers found that the distributions are positively skewed and that a very large number of very small drops ($< 3\mu m$) exist. Some distributions, however, showed a bimodal shape at size frequency less than 1%. Distributions of drop sizes in samples taken from different positions of large vessels did not show any spatial dependence. Dispersed phase fraction and inoculum size were found to have a strong influence over the drop-size distributions. Distributions taken at various times during the course of fermentation were widely different, thus emphasizing the influence of biomass concentration on the distributions. The physiological state of biomass also seems to exercise significant effect on the dispersion quality. Katinger (1973) reported similar observations from his study of

DSDs during fermentation of gas-oil as well as of n-hexadecane. Blanch and Einsele (1973) measured DSDs during the growth of C.tropicalis on pure n-hexadecane both in circulation-stirring as well as in flat-blade turbine systems. Highly skewed distributions were obtained which were affected by biomass concentration and the physiological state of the system. Sauter-mean diameter in the circulation-stirring systems was not found to be well correlated with Weber number.

Yoshida and Yamada (1971), and Podlech and Borzani (1972) measured distributions in similar pure chemical systems. Yoshida and Yamada (1971) studied dispersion of kerosene in water in gas-bubble columns and in a vessel agitated by a turbine type of mixer. Sauter-mean diameter which did not depend upon sampling position, was found to be influenced by power input and dispersed phase fraction. Podlech and Borzani (1972) studied distribution of diesel oil in distilled water using a radiometric technique. An empirical parameter was described to characterize the drop-size distributions which were found to be unsymmetrical.

Wang and Ochoa (1972) measured distribution of n-hexadecane drop sizes during active growth of Candida intermedia. Both the presence of cells and the presence of synthetic detergent, were found to influence the specific surface area of the hydrocarbon. However, the distribution of droplet diameters was not affected by changes in cell concentration above 0.5 grams (dry weight) per liter of broth.

1.2 Aim and Scope of the Present Work:

The present work aims at developing a quantitative understanding of the agglomerative and break-up processes in the dispersed liquid phase in hydrocarbon fermentors. Thus it attempts to resolve a major snag in the theoretical modelling of substrate limited growth in these vessels, namely: lack of adequate knowledge of drop-phenomena and drop-size distributions. It is proposed to find a suitable model of drop-phenomena and to carry out the necessary experimental work to verify the predictions of the model. In view of previous experience (reported in literature) concerning mathematical intractability of such models, it is desired that the model be simple enough so that it can be used along with transport and growth processes to predict the performance of n-alkane and gas-oil fermentors. This study also aims to investigate the effect of various factors, for example, dispersed phase mixing, nature of drop interactions, adsorption/desorption kinetics, upon the growth of biomass on hydrocarbons.

The break-up of subject matter in various chapters is as follow :

Chapter II discusses the development of techniques for the measurement of drop-size distributions in systems with and without biomass. Empirical studies dealing with experimentally observed DSDs in hydrocarbon fermentors and the correlations, have also been presented in this chapter.

Coalescence-redispersion model and its implications have been discussed in Chapter III. It includes development of the model, its analysis and verification, and the measurement of coalescence-redispersion frequency.

Results of computer simulation experiments have been presented in Chapter IV.

Chapter V summarizes the conclusions and recommendations for further research work.

* * *

CHAPTER II

EXPERIMENTAL AND EMPIRICAL STUDIES

This chapter deals with experimental and empirical studies of the drop-size distributions in agitated hydrocarbon - water systems, with and without biological matter. The first part discusses the methods of measurement of distributions of drop sizes in liquid-liquid dispersions and their applicability to the systems of interest in this study. In the second part, an empirical analysis of drop-size distribution data obtained in n-alkane and gas-oil fermentors available from the literature, is described and correlations are developed. The purpose of this study was to look for certain general trends which may be useful for the scale-up of these fermentors.

2.1 Measurement of Drop-Size Distributions (DSDs):

It is primarily performed by physical means, e.g. by microscopic inspection, by Coulter counters, by light transmission or light scattering techniques, by direct photography, and by sedimentation analysis. The choice of a particular method normally depends upon the dispersed phase system under consideration and the facilities available. Shah et al.(1972 b) have reviewed the various alternatives and their applicability.

Photography and microscopic inspection constitute the methods most commonly used for this purpose. Shinnar (1961) used

direct microscopic inspection to measure drop-size distributions of Shell-wax dispersed in water in a heated vessel. Cooling the sample taken out of the system fixed the dispersion, which could then be observed under a microscope, and be counted. For a system not so easily stabilized, different methods of stabilization were devised. Madden and McCoy (1964) used an interfacial polycondensation method for this purpose. vanHeuven and Hoevenaar (1968) used a concentrated detergent solution to stabilize the samples taken from the dispersion. Aiba et al. (1969 a,b) used direct microscopic observation of samples taken from n-alkane fermentors to establish distribution of drop-sizes in it. Since the possibility of coalescence could not be negated in this process, Yoshida and Yamada (1971) used a flow cell adjoining the vessel to photograph the dispersions in kerosene-water system. Similar arrangement was used by Blanch and Einsele (1973) to photograph n-alkane droplets in fermentation.

Katinger (1970) employed a gelatin embedding method to stabilize samples of dispersions. It consisted of taking a small sample directly from the fermentor into a semi-molten gelatin solution which was then immediately solidified by dipping into ice-water. The drops were prevented from coalescing by the high viscosity and the stabilizing effect of solidifying gelatin. This method was further improved by Prokop et al. (1972) to measure drop-size distributions in gas-oil fermentation.

Direct photography of drops in an agitated system has been utilized by many research workers to measure drop-size distributions. Kintner et al. (1961) have presented a review of these techniques adopted to bubble and drop research. Brown and Pitt (1972) have employed this method for the study of kerosene dispersed in water systems. Photographs were taken using a photoelectric probe with a synchronized photo-flash. Chen and Middleman (1967), Ward (1964), and Scott et al. (1958) also followed similar methods for their studies. Sedimentation analysis which takes advantage of the specific weight difference between dispersed and continuous phases, was developed by Wang and Ochoa (1972) for n-alkane fermentation. A combination of sedimentation analysis with radioactive tracer in simulated systems was employed by Podlech and Borzani (1972) also. Unfortunately, in biological systems, flocks consisting of hydrocarbon droplets, cells and air bubbles, prevent free rise of oil droplets due to the buoyancy forces, thus interfering with accurate measurement of DSD. On the other hand, microscopic methods enable direct measurement of DSD even in the presence of these disturbing factors and have, therefore, been selected for use in this investigation.

Here, the detergent method (DM), the gelatin method (GM), and the encapsulation method (EM) have been compared for their applicability to hydrocarbon-water systems with and without biomass. During the course of laboratory experimentation in the

present investigation, GM and EM were found to be of restricted utility, while DM was found applicable to both the systems and satisfactory for most of the working conditions. As a result, detergent method (DM) was selected for all the subsequent experimentation.

All the experiments were performed in a three-litre fermentor. The system was agitated by a Waldhof-type of agitator whose details are given in Figure 2.1.1. Dimensions of fermentor are given in Table II-1.1. A constant speed motor with facilities

TABLE II-1.1: DIMENSIONS OF FERMENTOR

Fermentor volume	3,000 ml
Operating volume	1,500 - 2,000 ml
Fermentor diameter	128 mm
Fermentor height	255 mm
Impeller type	modified Waldhof mixer
Impeller diameter/fermentor diameter	0.47
Height of impeller from bottom	46 mm
Impeller height	78 mm
Number of baffles	4
Baffle height	55 mm
Baffle width/fermentor diameter	0.1

to control the speed of shaft rotation from 250 rpm to 1300 rpm was utilized. Actual speed of rotation during an experiment was

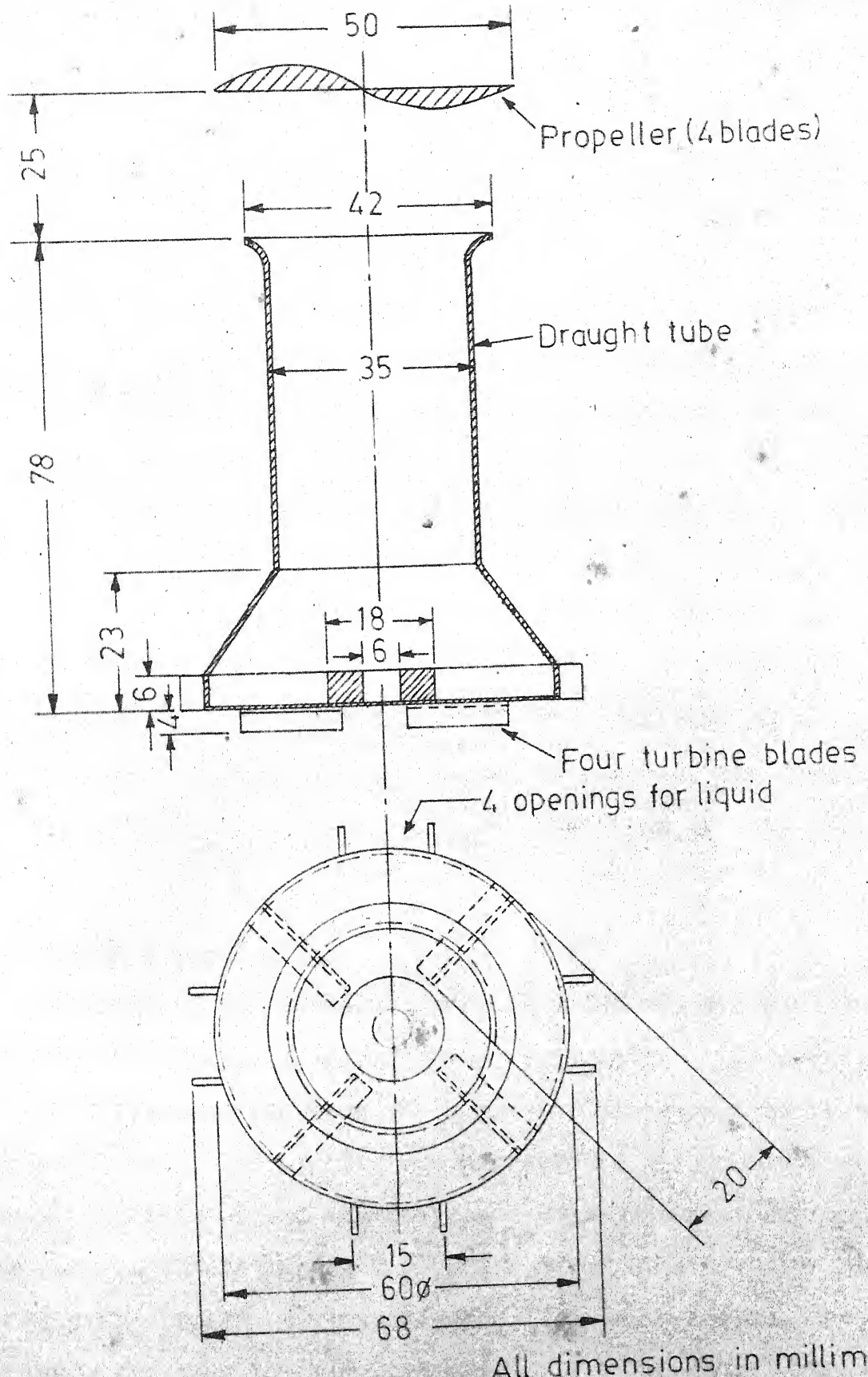

Fig. 2.1.1 - Modified Waldhof agitator.

[Ref: Prokop et al. 1972]

measured using a stroboscope. In all the experiments, total liquid level was initially kept at a level of two litres, and therefore an air-liquid interface was always present. Sampling was carried out from near the tip of the agitator and the length of the sampling tube was kept as small as possible so as to minimize coalescence in the sampling tube.

Distilled water was used as continuous phase in all the experiments. Dispersed phase consisted of either a mixture of n-alkane or gas-oil. Both the n-alkane mixture and the gas-oil were obtained by distillation of a Romashkin (USSR) crude oil. Spectrum of paraffins in n-alkane mixture ranged from C_7 to C_{27}, but the bulk constituted of C_{14} - C_{21}. In gas-oil, the distillation cut consisted of as much as 20% paraffins between C_{13} to C_{24}.

2.1.1 Detergent Method (DM):

This method was first utilized by vanHeuven and Hoevenaar (1968) and is based upon the property of lowering of interfacial tension by detergents between the phases. Detergent molecules, by virtue of their hydrophilic and hydrophobic groups, form an electrostatic film around the drops and thus prevent them from coalescing when the stirring has been reduced to a very low level or even completely stopped. The dispersion-sample, once stabilized, can then be microphotographed and counted.

Some amount of dispersion (10-25 ml) was sampled into approximately the same volume of highly concentrated solution of Sodium Dodecyl Sulphate (SDS) which was kept mildly agitated in order to prevent coalescence of drops before they are completely mixed with the detergent. A drop of the stabilized sample was quickly put on a grooved microscope-slide and covered with a microscope cover-glass, taking care not to retain any air-bubble below the cover-glass. Once the air-liquid interface has thus been eliminated, the distribution could be obtained subsequently by counting as it was observed that the distribution did not change (indicating that no coalescence of the drops occurred) even 48 hours after preparing the slide.

For microphotography, the dispersion was placed under a Rathenow ROW microscope which was fitted with a camera. With a 100X magnification, many photographs were taken from different portions of the sample on the slide and at different depths of focus.* The exposure time for OR WO - NP15 film was usually 1/5 second. The film was developed using OR WO - R09 fine grain developer. Positive prints were prepared on normal Bromofort BEH O Forte paper for an additional 5X enlargement. Thus the total magnification was 500X, and 1 mm on prints corresponded to 2μm. For measurement of distributions, 1000-1500 drops of varying sizes were counted from the prints considering only those in sharp focus.

---

*See Appendix G for sample photographs

The detergent method could be used for both pure chemical as well as fermentation systems. For fermentation systems, it was found to be especially good because the microbial cells present on the surface of the drops, were displaced from the interface in the presence of detergent, and during microphotography all the cells were present at a focus different from that for drops. It resulted in a more authentic identification of small drops.

2.1.2 Gelatin-Embedding Technique (GM):

The stabilization of the dispersions in this method is provided by the solidifying-gelatin in which the drops of the dispersed phase are embedded. An 8% gelatin solution is prepared and poured into petri-dishes to a 2-3 mm thick layer. Just before sampling, these petri-dishes are put in hot water so as to melt the gelatin. Sampling is carried out in the petri-dishes when the gelatin is just in a semi-molten state. After sampling, the petri-dishes are quickly immersed into ethanol-dry ice mixture which freezes the gelatin and the dispersion with it. The state of gelatin just before the sampling is an important factor in deciding the quality of the dispersion sample. If the gelatin solution is too fluid, dispersion gets thoroughly mixed in it and creates difficulties under the microscope as the drops get distributed over a wider thickness thus producing only very few drops at any depth of focus. Too fluid a gelatin

solution may take a finite time before solidifying and the drops have a chance to coalesce during the process. On the other hand, if the gelatin gets over-solidified before sampling, the dispersion does not get mixed with gelatin properly and therefore the sample does not represent the dispersion in the vessel. Also, the petri-dishes must not be kept in ethanol-dry ice mixture for too long; otherwise gelatin would crystallize thus obscuring the observation of the drops. The rest of the process is same as in the detergent stabilization method.

2.1.3 Encapsulation Method (EM):

The dispersed phase drops present in the dispersion are stabilized by coating them with a polymer film. Advantage is taken of a fast surface polycondensation reaction which deposits a nylon film at the surface. The reagents used in the study were Sebacoyl chloride (soluble in dispersed hydrocarbon phase) and Hexamethylene diamine (in the aqueous phase). Sodium hydroxide was used as the acid acceptor. Sebacoyl chloride (SC) was added to the dispersed phase before mixing it with the aqueous phase. The polycondensation reaction was initiated by adding 50 ml. of Hexamethylene diamine (HMDA)/NaOH mixture to the system after the mixing was carried out for an appropriate time. After 5-10 seconds, the agitation was rapidly brought down from the prevailing rpm to 150-250 rpm and a sample was taken. Measurement of drop-size distribution was made in a way exactly similar to that in the

detergent stabilization method. Reaction mechanisms for these polycondensation reactions are discussed in detail by Morgan (1965). Reaction conditions were adapted to facilitate appropriate interfacial polycondensation keeping in mind the following requirements:

(a) Hydrolysis of SC dissolved in the hydrocarbon phase prior to the reaction is affected by its concentration in dispersed phase, speed of rotation and time of mixing. The rate of hydrolysis is dependent also upon the nature of dispersed phase and that of the aqueous medium. Unfortunately, both n-paraffins and the gas-oil seem to have a fairly low value of partition coefficient (Morgan, 1965) for Sebacoyl chloride and, therefore, chloride hydrolysis takes place to a considerable extent. For hydrocarbon-water systems, the hydrolysis was not found to be affected by the presence of salts either. This limited the time of mixing before reaction to 20-30 minutes, being shorter for higher concentrations of SC in dispersed phase. Fortunately, this time is sufficient to achieve stationary drop-size distributions for small dispersed phase fractions.

(b) Stoichiometry of the reaction of SC and HMDA must be found empirically, being a function of dispersed phase volume, speed of agitation, and the nature of dispersed phase. Especially, the latter affects the partition

coefficient of diamine between the two phases (Morgan, 1965). The concentration of the acid acceptor, NaOH, depends upon the concentration of HMDA.

(c) The conditions of the reaction must be chosen so that the polycondensation reaction occurs at the oil-water interface and a stable film is formed. It was observed that as soon as the agitation is brought down to a lower level, sampling of the stabilized dispersion into a concentrated detergent solution helps to preserve the dispersion even when the polymer film formed is weak.

The reaction of SC with HMDA is a very fast one and Morgan (1965) has discussed some of the basic conditions for it. The conditions employed in our study were as follows: dispersed phase 1-5% v/v for n-alkanes and 1-10% v/v for gas-oil; speed of rotation 700-1000 rpm; concentration of SC in the dispersed phase 0.5 and 1.0% v/v (higher for large dispersed phase fraction); HMDA and NaOH concentrations in water phase 0.35 - 1.0 M and 0.7 - 2.0 M, respectively. The process of counting the drop-size distributions from the stabilized dispersion was the same as that for the detergent method.

2.1.4 Comparison of Methods:

Experimental measurements of DSD in pure chemical and in fermentation systems were carried out. For pure chemical systems, only DM and EM were employed. Gelatin stabilization method could not be used as partial coalescence between dispersed phase drops could not be prevented. Samples of dispersions from biological systems were stabilized using DM and GM. For these systems, EM was not employed because of the suspected toxic effect of Sebacoyl chloride on the growth of biomass. Various distributions have been tabulated in Appendix A. The Sauter-mean diameters obtained from different methods during various experimental runs are tabulated in Table II-1.2. Reproducibility of Sauter-mean diameters was $\pm$10.0%. Figures 2.1.2 and 2.1.3 show the distributions obtained from some typical runs. Figure 2.1.2 presents a comparison of EM and DM for DSD samples taken from a dispersion of gas-oil in water in absence of cells. DSDs observed in a gas-oil fermentation experiment are illustrated in Figure 2.1.3. It follows from these figures that DM gives results fairly similar to those obtained by EM and GM, both of which can be considered as standard. EM and GM have been frequently used and reported in the literature (Madden and McCoy, 1964; Mlynek and Resnick, 1972; vanHeuven and Hoevenaar, 1968; Katinger, 1970; Prokop et al., 1972). However, these methods are rather cumbersome and of specific utility. On the other hand, DM can be used equally well for non-biological as well as biological systems,

TABLE II-1.2: COMPARISON OF SAUTER-MEAN DIAMETERS (IN μm) OBTAINED BY DIFFERENT METHODS

Sl.No.	Experiment No.	Mixing Conditions	Method of Stabilization		
			DM	GM	EM
1.	1	10% v/v gas-oil fermentation, 1000 rpm*	26.90 27.50 (repeated run)	29.80	--
2.	7	5% v/v gas-oil fermentation, 1000 rpm*	34.61	38.37	--
3.	3	4% v/v n-alkanes (0.5% SC in dispersed phase), 700 rpm	18.66	--	15.90
4.	6	8% v/v gas-oil (1% SC in dispersed phase), 1000 rpm	21.85	--	17.86
5.	9, 10	10% v/v gas-oil (1% SC in dispersed phase)	28.60 26.20 (repeated run)	--	21.80
6.	11, 16	5% v/v n-alkanes (1% SC in dispersed phase), 1000 rpm			
		20 minutes of mixing	29.50	--	25.50
		30 minutes of mixing	21.63	--	19.50

*Cell densities are different in experiments 1 and 7.

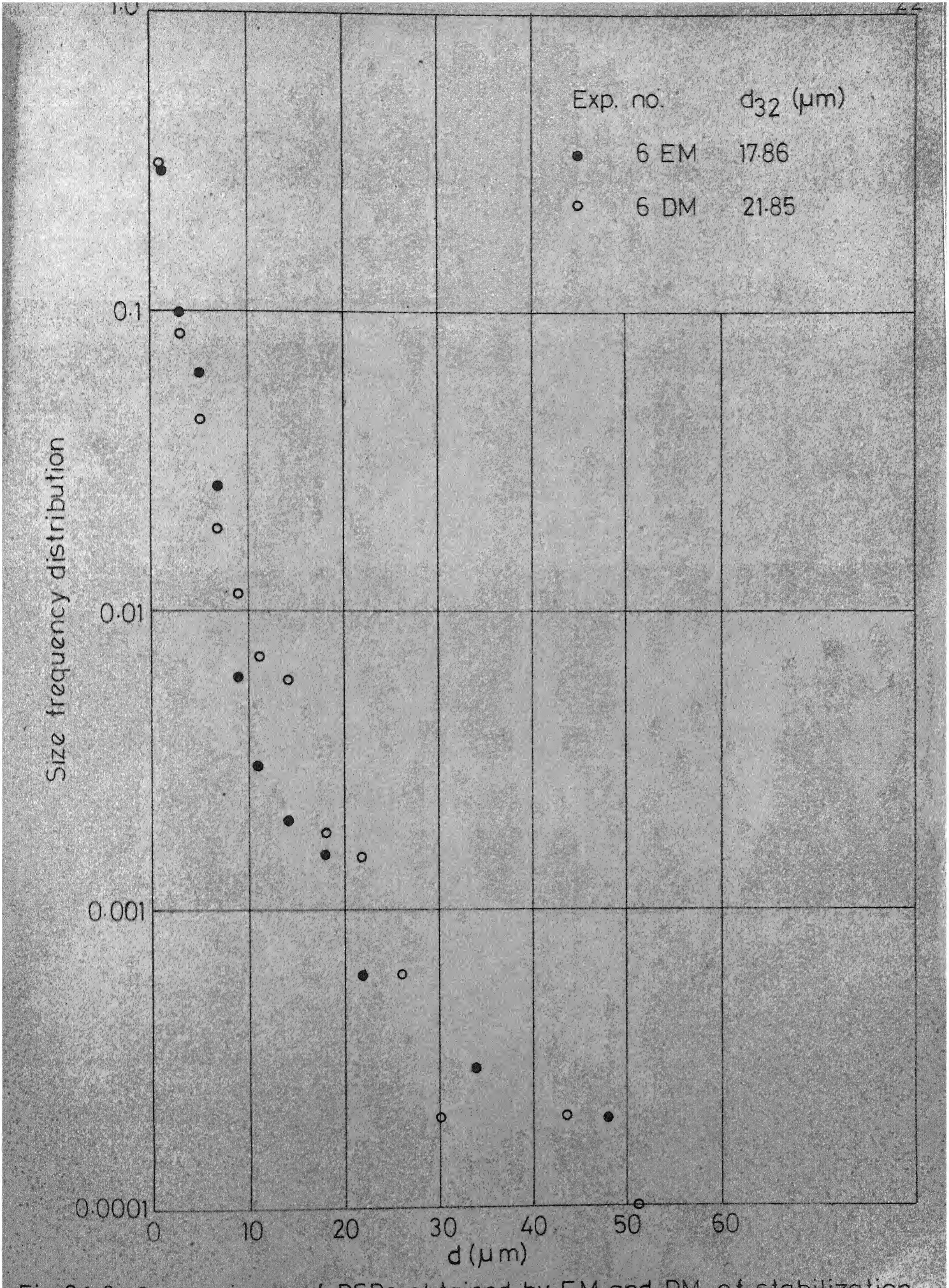

Fig. 2.1-2 - Comparison of DSDs obtained by EM and DM of stabilization of dispersions of gas-oil in water.

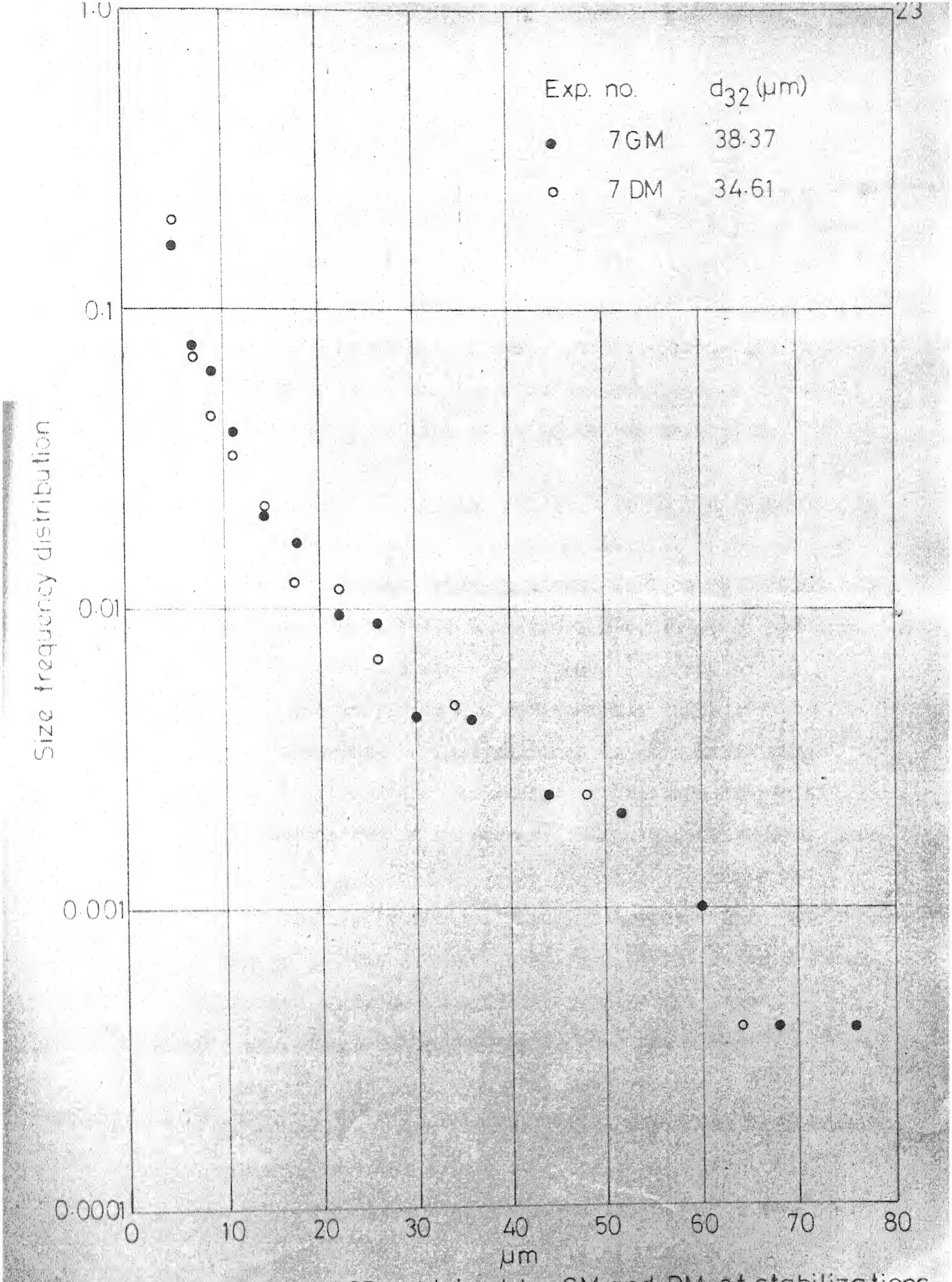

Fig. 2·1·3 – Comparison of DSDs obtained by GM and DM of stabilizations of dispersing from gas-oil fermentors.

and is relatively very simple in application. IM becomes very handy for measurement of transient state DSDs where samples need to be taken at very frequent intervals and thus results in saving a considerable amount of time. Especially in the presence of cells, it enables one to obtain better resolutions for small droplets, these being clouded by cells in the case of GM.

2.2 Drop-Size Distributions Observed in Hydrocarbon Fermentation:

Recently, a number of experimental studies have reported distribution of drop-sizes in hydrocarbon fermentors (Prokop and Ludvík, 1973; Katinger, 1973; Wang and Ochoa, 1972; Blanch and Einsele, 1973). From the results of these studies, it can be concluded that the drop-size distributions in these systems are influenced by a variety of factors, such as, dispersed phase fraction, speed of rotation, biomass concentration, state of fermentor broth, nature of dispersed and continuous phases, type of agitator, and the geometry of the vessel. The only previous attempt to theoretically predict these distributions during fermentation by Stamatoudis and Tavlarides (1973) using a Monte-Carlo simulation technique involved a prohibitive amount of computer time. These authors reported that the exact knowledge of DSD is important in predicting the performance of hydrocarbon fermentors accurately. Thus a need for an empirical drop-size distribution for at least a wide range of experimental conditions is obvious. In the absence of a theoretical model of prediction

of DSDs, such an attempt would eventually lead to incorporation of real size-distributions into a kinetic model for growth on hydrocarbons for extreme cases of complete mixing and complete segregation. Theoretical model is, however, still desirable in order to take into account the effect of interactions of dispersed phase drops which are crucial for correct prediction of growth of biomass (Chapter IV, Section 4.3) in hydrocarbon fermentors.

2.2.1 Normalized Drop-Size Distributions:

Drop-size distribution data observed in the hydrocarbon fermentation as well as from the simulated (i.e. similar pure chemical) systems were procured from different sources (Prokop and Ludvík, 1973; Katinger, 1973; Blanch and Einsele, 1973). The experimental conditions for which the data were collected form a wide spectrum. These studies were performed in the flat-blade turbine systems and in the circulation-stirring (i.e. Waldhof agitated) systems. The following general trends were obvious:

(a) The drop-size distributions in all the cases, are highly positively skewed. A very large number of extremely fine droplets exist in the system.

(b) Even in the case of gas-oil fermentation, the distribution of drop sizes becomes finer with growth in the fermentor.

(c) The distribution becomes coarser with increase in the dispersed phase fraction and finer with the speed of agitation.

(d) The effect of the speed of agitation is more pronounced in systems with flat-blade turbines than in those with Waldhof agitators.

As has been already observed, the drop-size distributions are influenced by a variety of factors which undergo a change during the course of fermentation. Figures 2.2.1 to 2.2.3 show the drop-size distributions for some experimental runs. In order to fit an empirical equation to these distributions, it was decided to normalize the DSDs with a suitable parameter thus reducing them into a set of normalized distributions. The choice of the normalizing parameter is often arbitrary and generally a matter of trial and error. Sauter-mean diameter was chosen to be the normalizing parameter because it is a mean property and can be separately correlated with the experimental parameters. Figures 2.2.4 to 2.2.10 present the normalized plots of DSDs collected by the different authors.

Figure 2.2.1 presents distributions obtained by Prokop and Ludvík (1973) at different times during the course of batch fermentation on model gas-oil. Shapes of these distributions change in time because of utilization of substrate and build-up of cell biomass and extracellular products in the system. As can be seen from Figure 2.2.4, these changes can be taken care of by

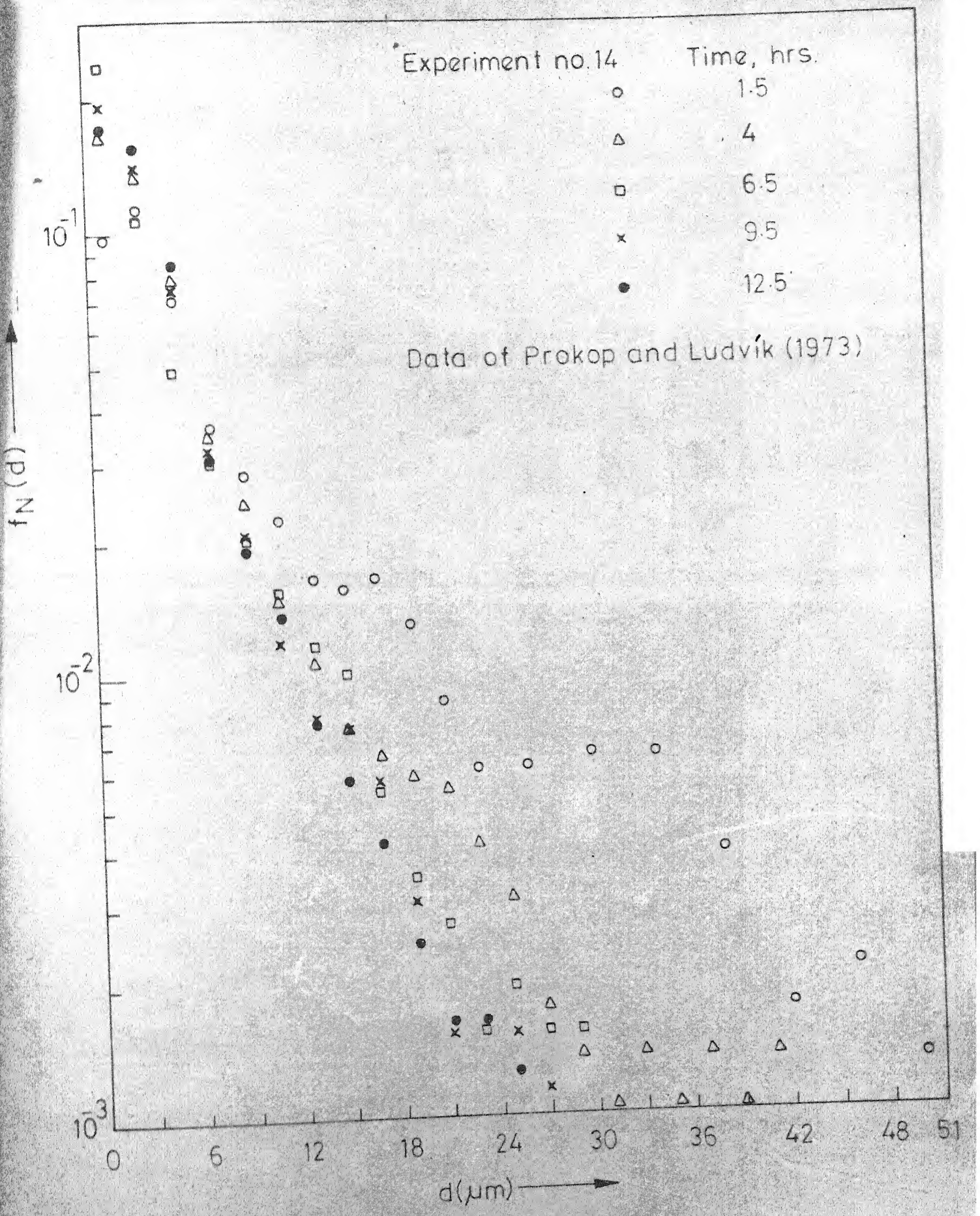

Fig 2.2.1-DSDs observed during batch cultivation of C. lipolytica on gas-oil.

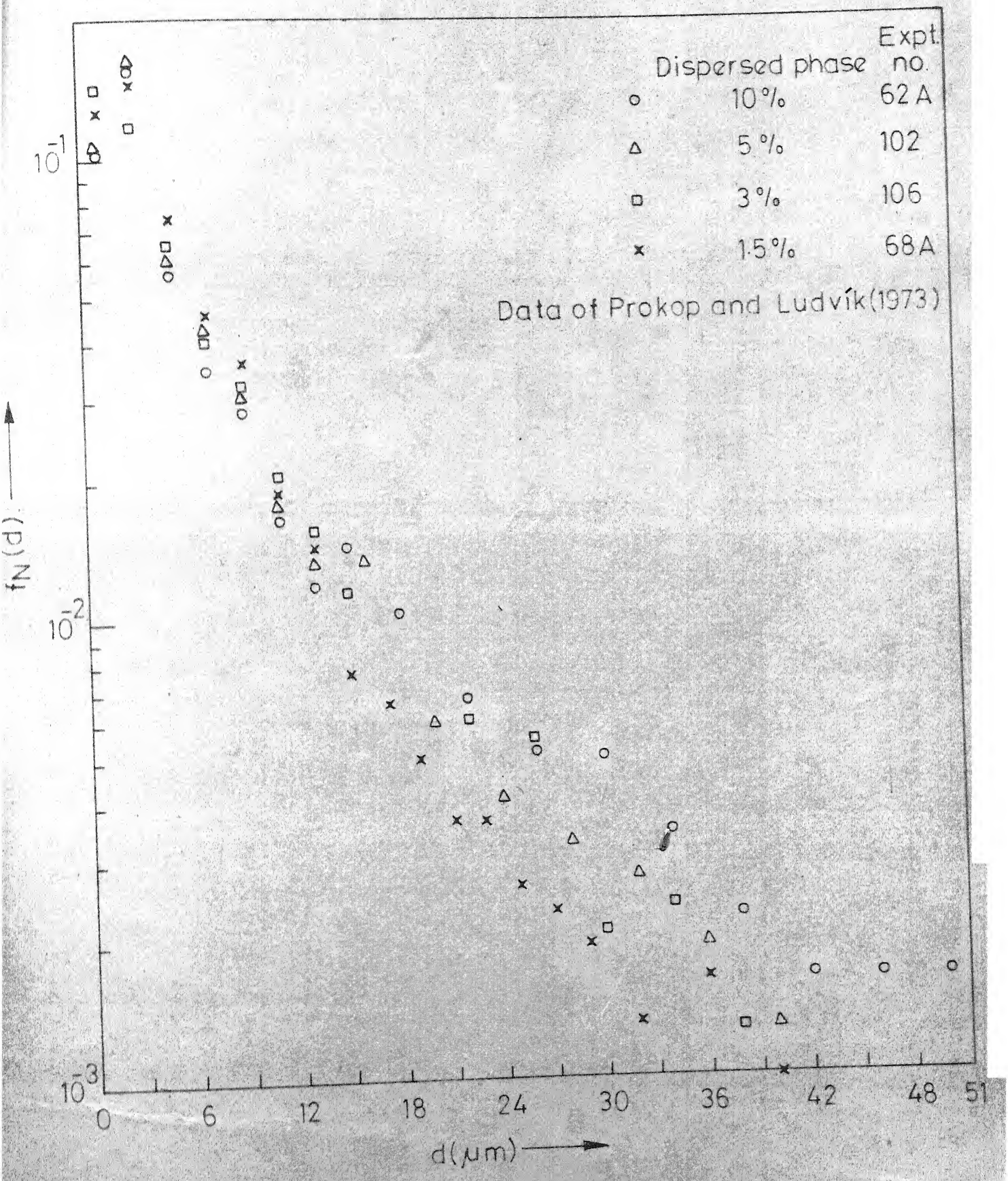

Fig. 2.2.2 - DSDs observed during cultivation of C. lipolytica on gas-oil.

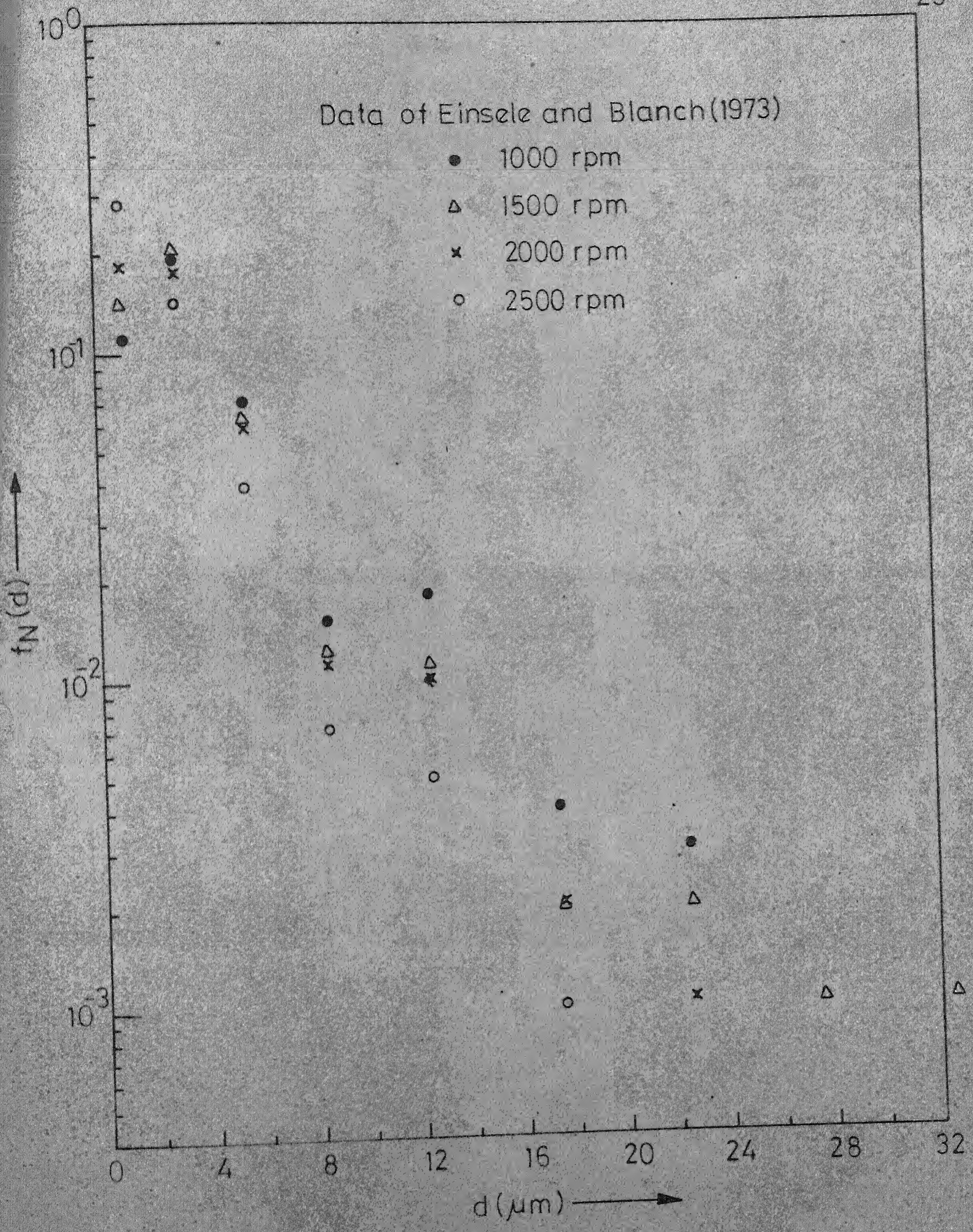

Fig. 2.2.3 - DSDs observed in dispersions of n-hexadecane in water by FBT.

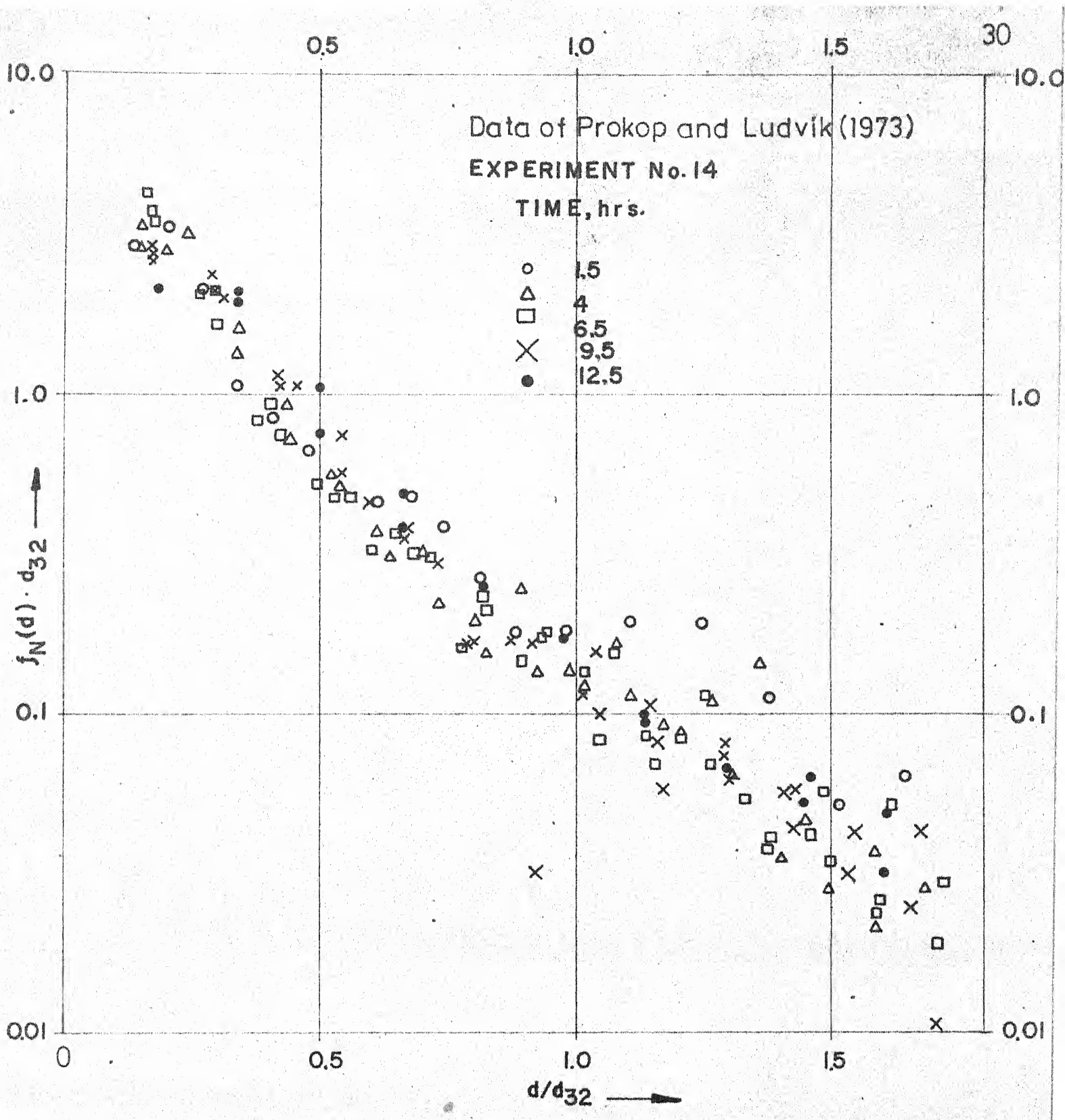

Fig. 2.2.4 - Normalized DSDs observed during batch cultivation of C. lipolytica on gas oil.

the proposed normalization. During the course of fermentation of gas-oil, the changes in dispersed phase fraction are rather small and the main contributing factor is the cell density. On the other hand, during n-hexadecane fermentation dispersed phase fraction also changes appreciably. In Figure 2.2.5 normalized distributions for this case are also shown.

Furthermore, the distributions are also affected by the initial dispersed phase fraction, ϕ_o, and the energy input (speed of rotation, N). Figures 2.2.6 to 2.2.9 present normalized distributions for these cases. The data reported in Figures 2.2.7 and 2.2.8 were collected for non-biological (n-hexadecane - water, no biomass) systems using circulation stirrer and flat-blade turbine, respectively (Blanch and Einsele, 1973). The data obtained by Katinger (1973) are shown in Figure 2.2.9 and these also conform to the previous observations. Also, the data were available for DSDs taken by Prokop and Ludvík (1973) from fermentors of different sizes. While the smaller fermentor was provided with a single Waldhof-agitator and a draught tube, the bigger fermentor was provided with a set of similar stirrers and draught tubes. DSDs obtained from these two fermentors showed considerable differences, but after normalization with the Sauter-mean diameter they could be reduced to one distribution. The normalized plots are presented in Figure 2.2.10. The fact that similar normalized distributions are obtained in vessels which are not only different in sizes but also in their geometry,

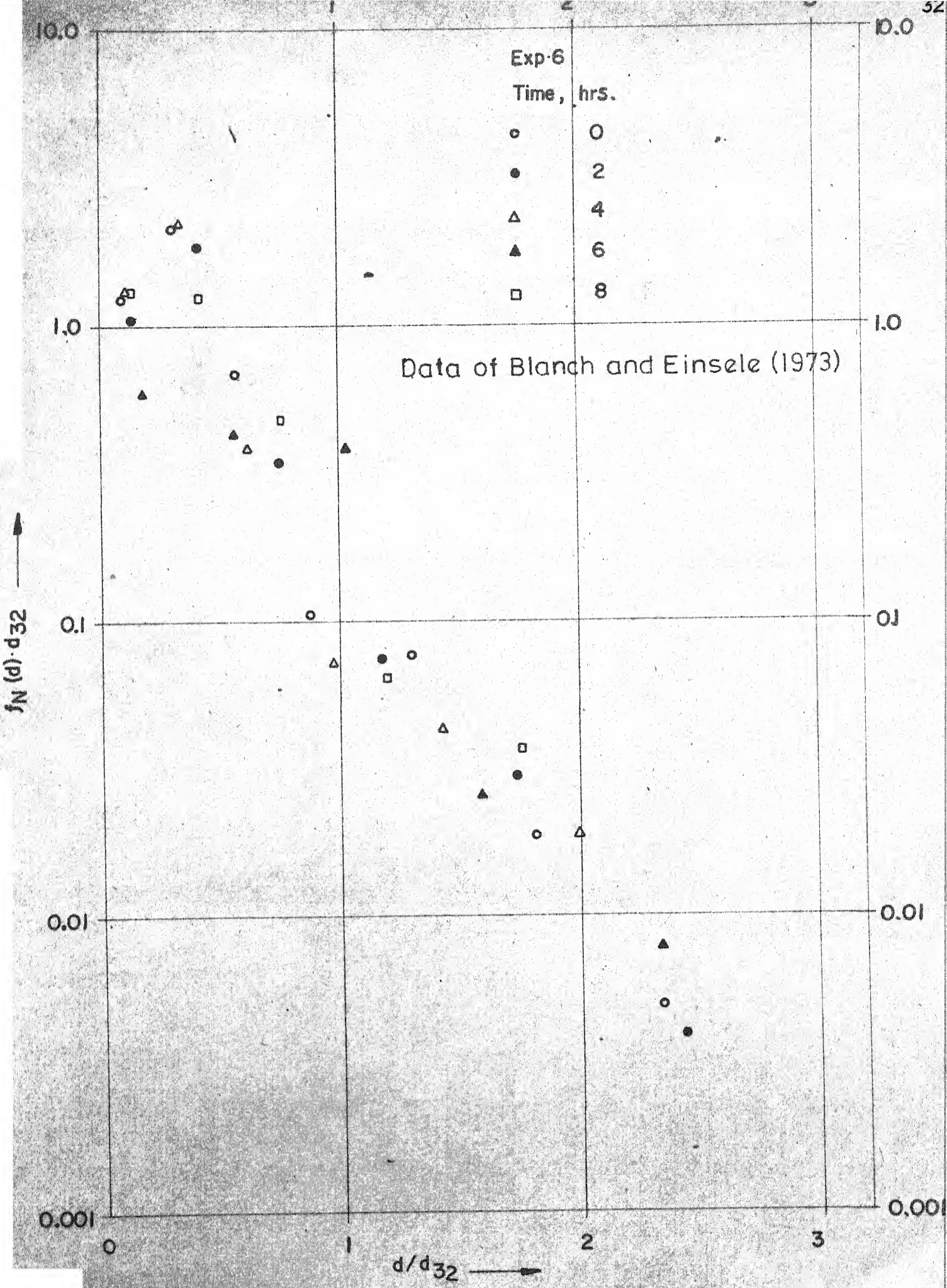

Fig. 2.2.5 - Normalized DSDs observed during n-hexadecane fermentation.

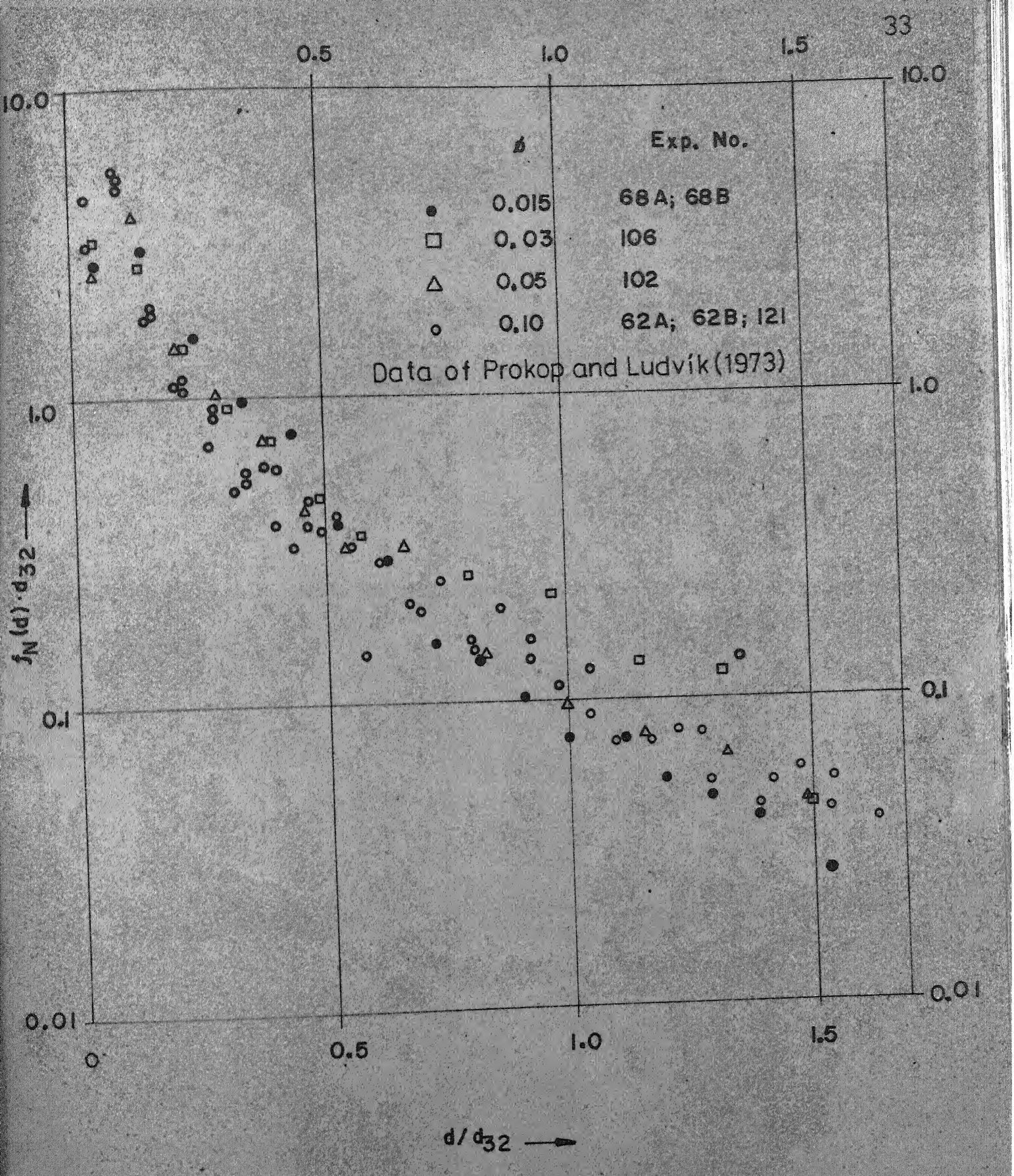

Fig. 2.2.6 - Normalized DSDs observed during cultivation of C. lipolytica on gas oil.

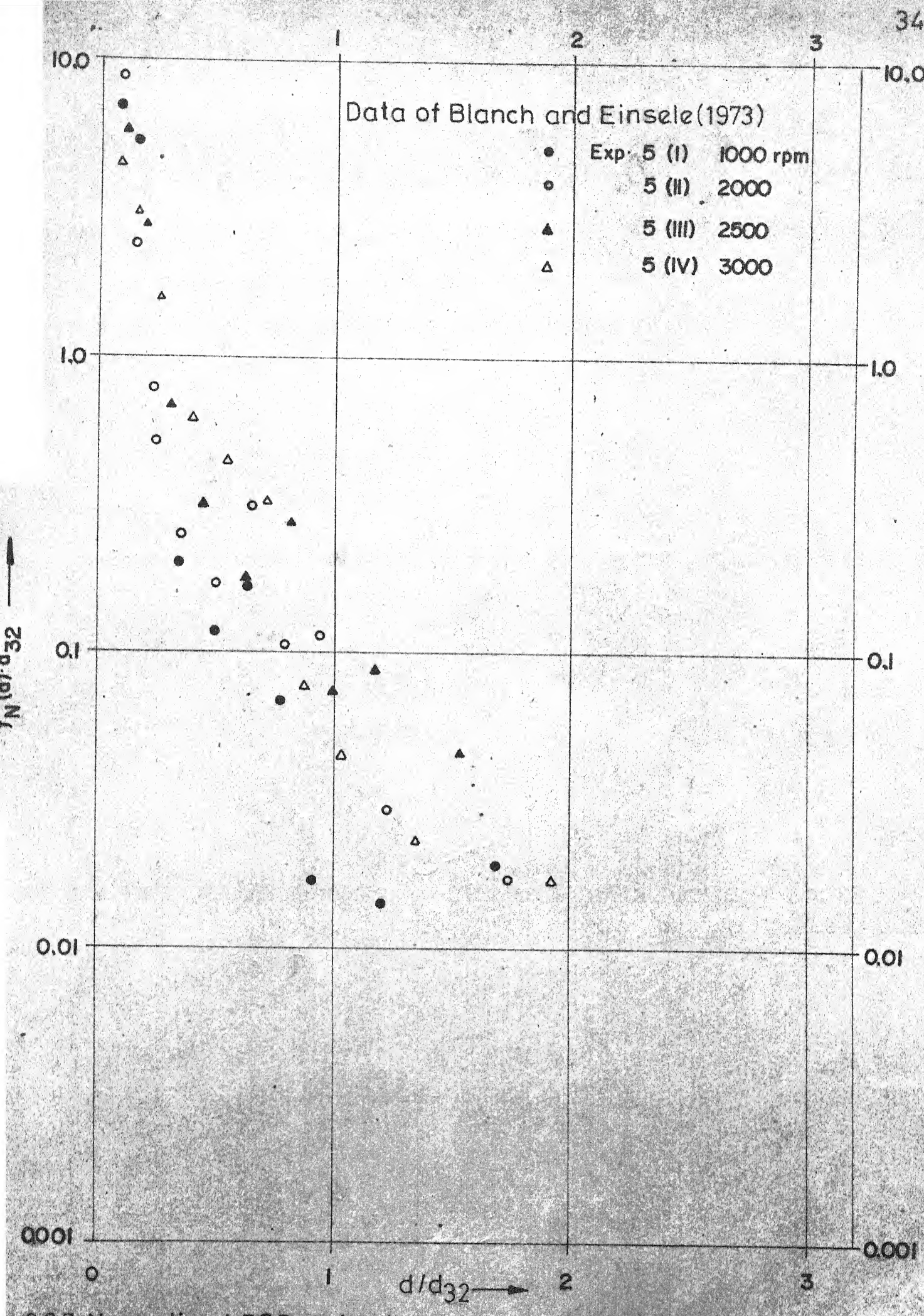

g. 2.2.7-Normalized DSDs of n-hexadecane dispersed in water by CS.

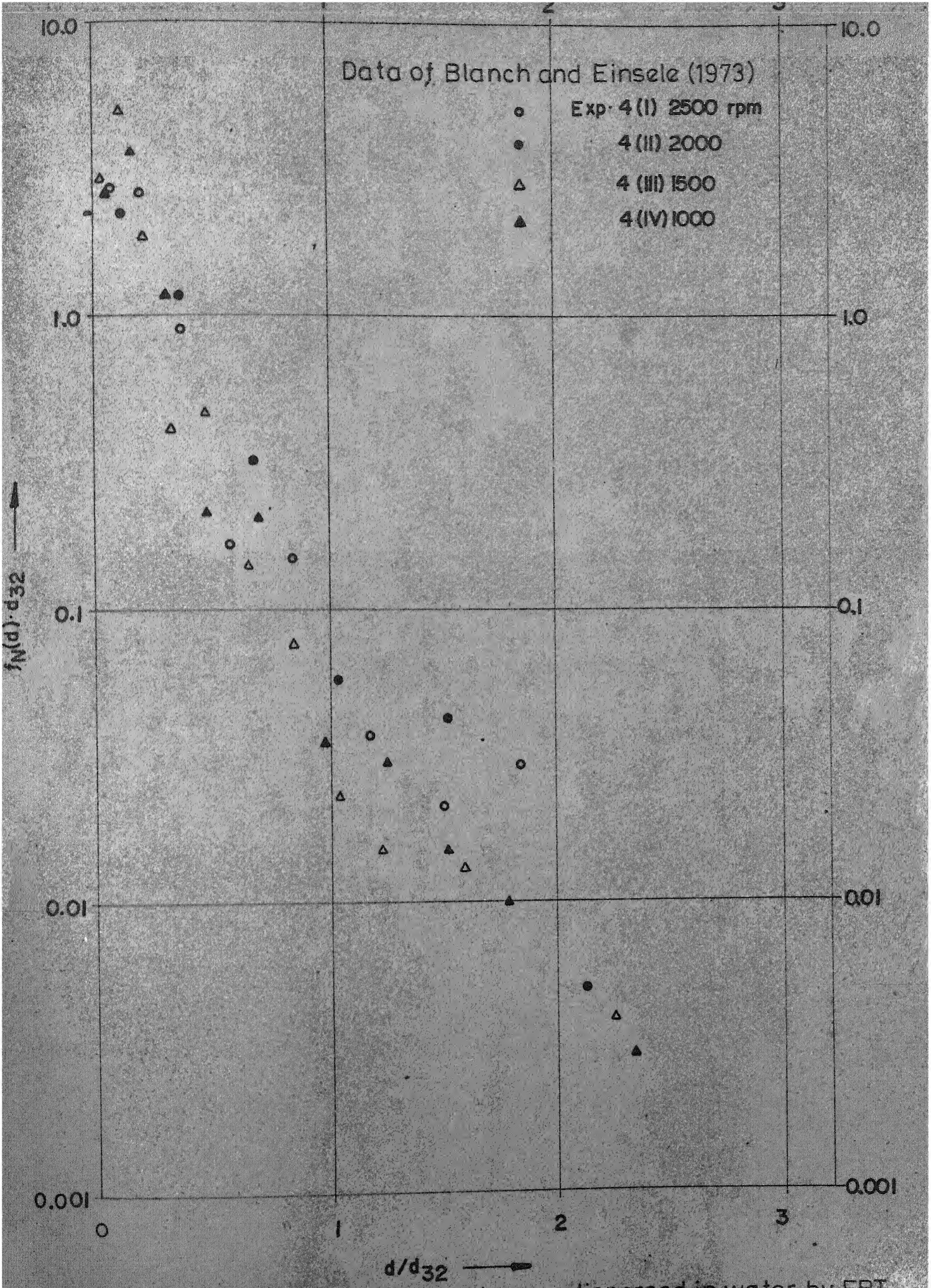

Fig. 2.2.8-Normalized DSDs of n-hexadecane dispersed in water by FBT.

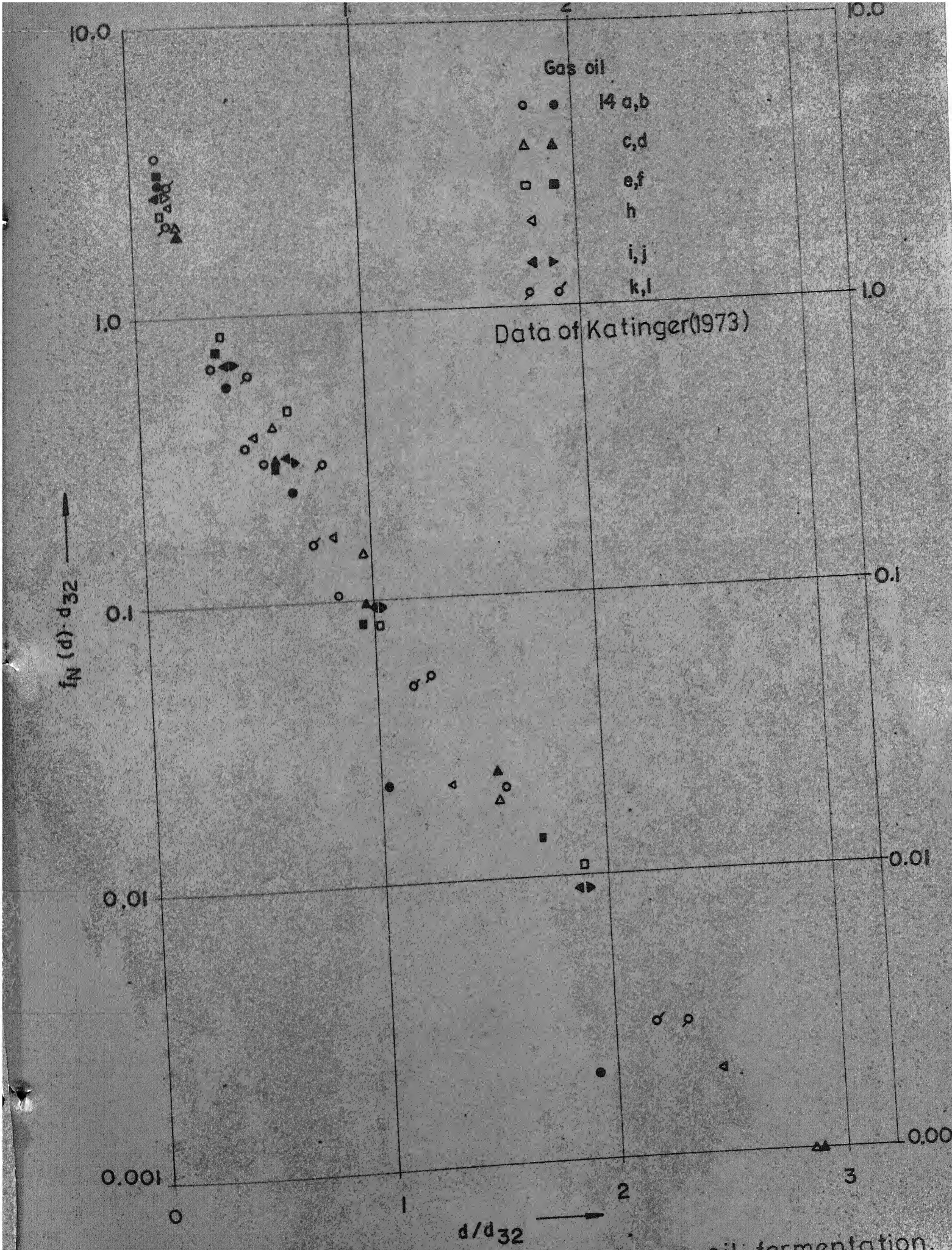

Fig. 2.2.9 - Normalized DSDs observed during gas-oil fermentation.

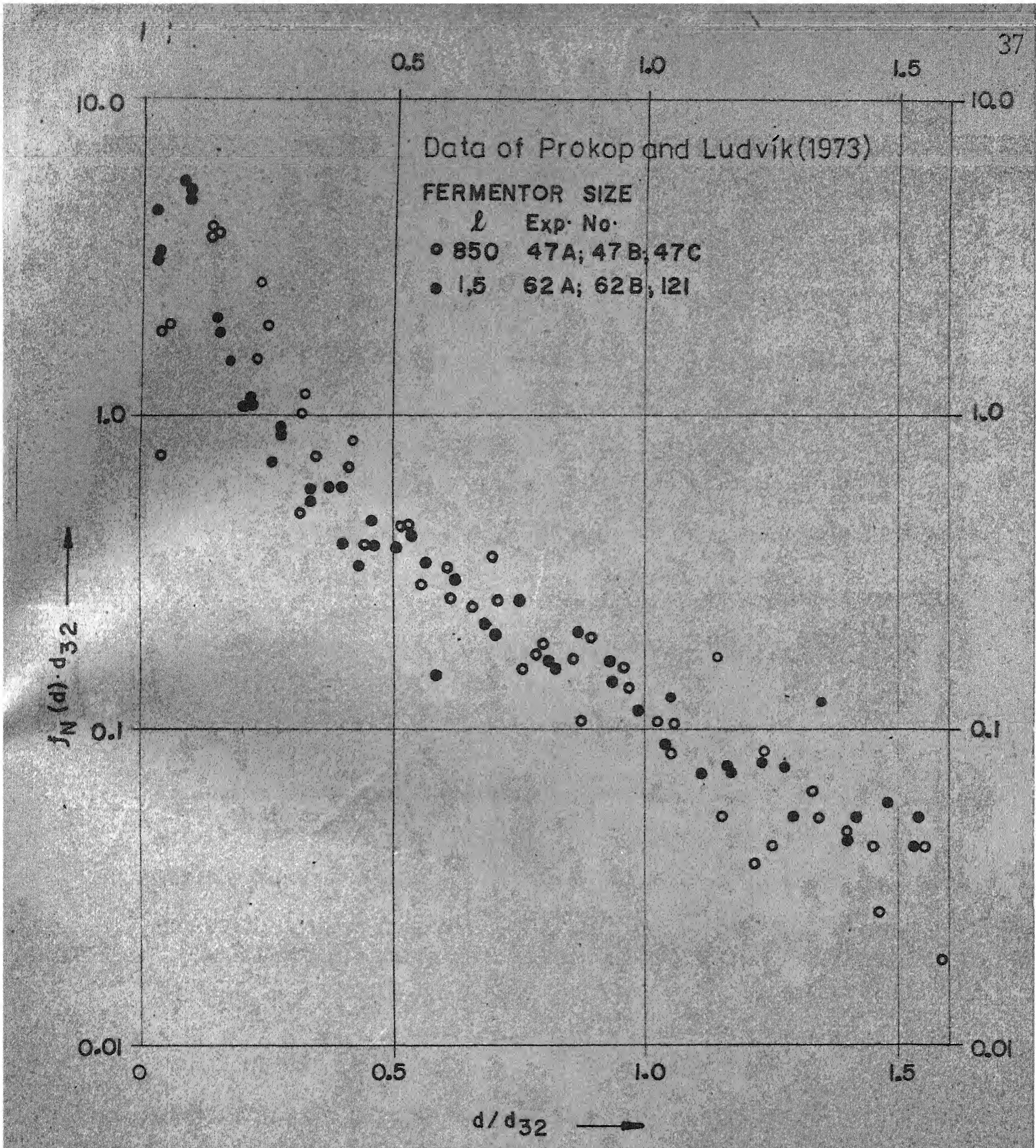

Fig. 2.2.10 - Normalized DSDs in fermentors of different sizes.

suggests that the Sauter-mean diameter can serve as a useful criterion for scale-up of fermentors for single-cell protein production. Recently, Sauter-mean diameter has been reported to be of use in the scale-up of glutamic acid fermentors from n-paraffins (Hattori et al., 1974). This aspect of applicability of Sauter-mean diameter requires further investigation and is recommended for further study.

A polynomial equation of the following nature was found to best fit the normalized drop-size distribution data:

$$\ln \left\{ f_N(d).d_{32} \right\} = a_o + b_1 (d/d_{32}) + b_2 (d/d_{32})^2 \qquad (2.2.1)$$

where $f_N(d)$ is the number density of drops and d_{32} is the Sauter-mean diameter. a_o, b_1 and b_2 are constants and these can be different for different systems. For the data of Prokop and Ludvík (1973) for model gas-oil fermentation in circulation - stirrer (CS) systems, the following constants were obtained at 5% level of significance:

$a_o = 0.58$

$b_1 = -1.79 \qquad -2.05 < b_1 < -1.53$

$b_2 = 0.28 \qquad 0.17 < b_2 < 0.39$

Similarly, for several sets of Katinger's data, including those in Figure 2.2.9 (covering effects of time, dispersed phase fraction, and speed of rotation in non-biological as well as in biological systems on model gas-oil and n-hexadecane) the following constants were obtained:

$a_o = 0.58$

$b_1 = -1.86$ $\qquad -1.96 < b_1 < -1.76$

$b_2 = 0.22$ $\qquad 0.19 < b_2 < 0.26$

Blanch and Einsele's data (Figures 2.2.5, 2.2.7 and 2.2.8) also fit into one equation with the following constants:

$a_o = 0.53$

$b_1 = -1.71$ $\qquad -1.81 < b_1 < -1.50$

$b_2 = 0.10$ $\qquad 0.06 < b_2 < 0.15$

2.2.2 Correlation of Sauter-Mean Diameter:

From the above discussion, it is clear that if the Sauter-mean diameter is known, the distribution of drop-sizes in the hydrocarbon fermentor can be predicted. Therefore, an attempt was made to correlate the Sauter-mean diameter with the experimental conditions.

For the data of Prokop and Ludvík (1973) collected on model gas-oil at constant speed of rotation, the following equation was found to fit the best:

$$d_{32} = 0.002\ (1 + 3.9\ \emptyset) \quad \text{cm.} \qquad (2.2.2)$$

The mean and standard deviation of the percent error [defined as absolute $(d_{32\ \text{predicted}}/d_{32\ \text{experimental}} - 1) \times 100$] were 12.01 and 11.12 respectively. For data on gas-oil,

$$d_{32} = 0.002\ (1 + 2.7\ \emptyset) \quad \text{cm.} \qquad (2.2.3)$$

the mean and standard deviation of the percentage error were 13.54 and 10.47, respectively.

The data of Blanch and Einsele (1973) for n-hexadecane water system mixed by Waldhof agitator (CS), were found to have a very low exponent of Weber number dependence,

$$d_{32} = (\text{constant}).\ We^{-0.10} \qquad (2.2.4)$$

Katinger's data (1973) including distributions of gas-oil or model gas-oil from biological as well as non-biological CS systems were found to conform to the following correlation:

$$d_{32} = (\text{constant}).\ We^{-0.12} \qquad (2.2.5)$$

For all these calculations, σ = 5 dynes/cm. was used for biological systems, although the value of interfacial tension may depend upon the cell density (Prokop et al. 1972; Srivastava et al., 1970). For non-biological system of gas-oil or model gas-oil, σ = 23.0 dynes/cm. was used. The effect of $\emptyset$ could not be evaluated properly.

Attempts to compare these correlations with those reported in the literature did not succeed as most of the previous work has been carried out in pure chemical systems agitated by flat-blade turbines (FBT). Table II-2.1 summarizes the different correlations. In most of these cases, the exponent of Weber number dependence is -0.6 which is significantly different from the ones obtained for the data of Katinger (1973), and of Blanch and Einsele (1973). In order to check the results, fresh sets of experimental data were collected for n-alkanes – water systems

TABLE II-2.1: CORRELATIONS OF SAUTER-MEAN DIAMETER TO MIXING CONDITIONS

Author	Vessel	Turbine	ϕ and N range	Correlation	Remarks
Shinnar and Church (1960)	-	-	-	$d_{32}/D = K\ We^{-0.6}$ $d_{32}/D = K\ We^{-0.375}$	Theoretical considerations for low and high ϕ
Rodger et al.(1956)	Open	6-bladed	ϕ=0.50; 60 ≤ N ≤ 1200	$d_{32}/D = K\ We^{-0.36}$	-
Chen and Middleman (1967)	Open	6-bladed	$0 \leq \phi \leq 0.015$; $80 \leq N \leq 1000$	$d_{32}/D = 0.053\ We^{-0.6}$	-
Sprow (1967)	Open	6-bladed	$0.005 \leq \phi \leq 0.015$; $250 \leq N \leq 2000$	$d_{32}/D = 0.051\ We^{-0.6}$	-
Vermeulen et al.(1955)	Closed	4-bladed	$0.1 \leq \phi \leq 0.4$; $100 \leq N \leq 400$	$d_{32}/D = 0.055(1+3.3\phi)\ We^{-0.6}$	effective density in Weber number
Calderbank (1958)	Open	6-bladed	$0 \leq \phi \leq 0.2$	$d_{32}/D = 0.060(1+9.0\ \phi)We^{-0.6}$	-
		4-bladed	-	$d_{32}/D = 0.060(1+3.75\phi)We^{-0.6}$	-
vanHeuven and Beek (1971)	Closed	6-bladed	$0.03 \leq \phi \leq 0.35$	$d_{32}/D = 0.047(1+2.5\phi)\ We^{-0.6}$	-
Brown and Pitt (1971)	Closed	6-bladed	$0.05 \leq \phi \leq 0.3$ $250 \leq N \leq 400$	$d_{32}/D = 0.051(1+3.14\phi)We^{-0.6}$	-
Giles et al. (1971)	Closed	-	$0.19 \leq \phi \leq 0.50$ $1000 \leq N \leq 2000$	$d_{32} = d_{32}^{\ o}\ (1+36.7\ \phi)$	-
Thornton and Bouyetiotis (1963)	Closed	-	$0.1 \leq \phi \leq 0.5$	$d_{32} = d_{32}^{\ o}\ (1+k\ \phi)$	-
Yoshida and Yamada(1971)	Open	4-bladed	$0.01 \leq \phi \leq 0.3$	$d_{32} \propto \phi^{0.2 - 0.3}$	-
Shiloh et al. (1973)	Closed	6-bladed	$0.002 \leq \phi \leq 0.04$ $320 \leq N \leq 500$	$d_{32} \propto \phi^{0.4 - 0.5}$	-
Weinstein and Treybal (1973)	Closed	6-bladed	$0.125 \leq \phi \leq 0.83$ $150 \leq N \leq 620$	$d_{32} = 10^{c_1+c_2\ \phi}$ $We = 10^{c_3+c_4\ \phi}$	-

mixed by a Waldhof agitator. The detergent stabilization method had been used for the measurement of drop-size distributions. Experiments were conducted at various speeds of rotation and for different dispersed phase fractions. These distributions have been tabulated in Appendix B. The effect of $\emptyset$ and speed of rotation on the Sauter-mean diameter is demonstrated in Table II-2.2. The following correlation was found with σ = 48.1 dynes/cm.

$$d_{32} = 0.0145\ (1 + 1.17\ \emptyset\ )\ We^{-0.27}\ \text{cm.} \qquad (2.2.6)$$

The mean and the standard deviation of the percent error in predictions were 12.0 and 10.36, respectively. Comparisons between the experimentally obtained Sauter-mean diameters and those calculated using Eq. 2.2.6 are shown in Figure 2.2.11. It can be noted that in this case also, the exponent of Sauter-mean diameter dependence is considerably different from the value of -0.6 obtained for the FBT systems. A low value of the exponent could result from the distribution of power for mixing between that consumed for creating turbulence, air-liquid interface in case of open vessels, and for circulation in case of CS systems. Since a substantial axial flow is required (Prokop and Sobotká, 1973) in hydrocarbon fermentors, a greater attention should be devoted to dispersions in aerated systems having a high ratio of axial to radial flow. In future investigations, special care should be taken in designing a mixer and to the presence of

TABLE II-2.2: EFFECT OF VOLUME FRACTION AND SPEED OF ROTATION ON SAUTER-MEAN DIAMETER IN n-PARAFFINS/WATER SYSTEM MIXED BY MEANS OF CIRCULATION STIRRER

Speed of rotation N, rpm	Volume Fraction, Ø				Weber Number, We*
	0.02	0.05	0.10	0.15	
600	30.62	31.12	36.97 37.91	28.42	444.0
800	-	-	-	22.70	789.3
900	22.65	24.04	27.12	20.12	999.0
1200	16.05	21.05	19.82	28.17	1776.0
1500	17.05	20.12	15.00	26.41	2775.0

*based on continuous phase properties

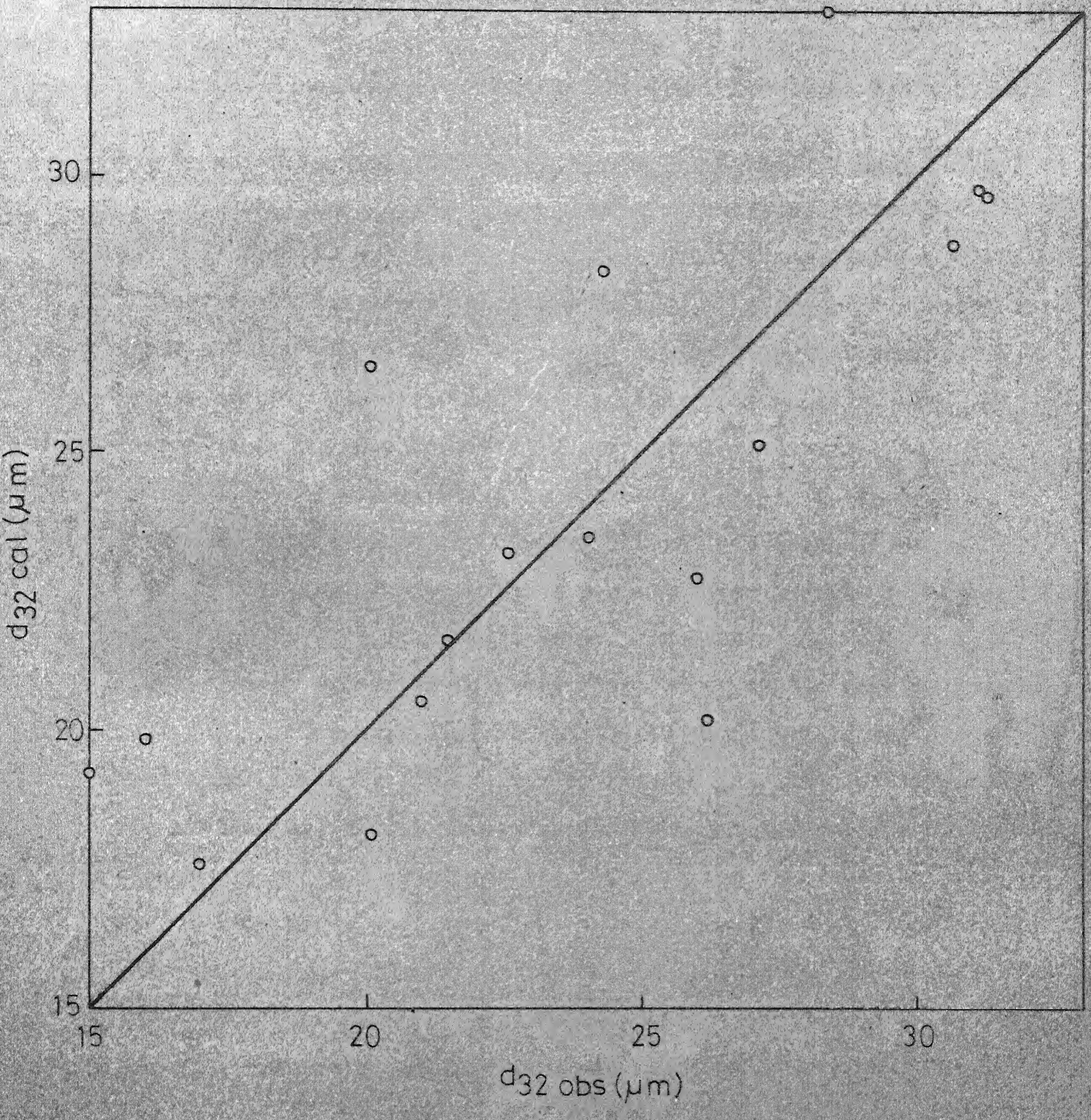

Fig. 2.2.11 - Comparison between observed and predicted Sauter-mean diameters.

air-liquid interface with regards to circulation time and scale-up.

2.2.3 Effect of Cell Density on the Sauter-Mean Diameter:

The study of DSDs in gas-oil fermentors suggests that the cell density and the physiological state of the biomass strongly influence the distribution of drop sizes in hydrocarbon fermentors where all the other variables remain almost invariant during the fermentation. However, from the existing data no conclusive correlation could be derived. Therefore fresh experiments were designed to throw some light upon this aspect of the system behavior. Experiments were conducted for dispersion of 5% v/v of n-alkanes in aqueous medium in a fermentor fitted with a Waldhof agitator. C. lipolytica 4-1, grown in a chemostat, was added to the system in steps. With every step change in the biomass concentration, drop-size distributions were estimated by the detergent stabilization method after 30 minutes of mixing at 1200 rpm. The various distributions have been tabulated in Appendix C. Actual biomass concentration at the time of sampling for distributions was also estimated by the dry weight method. Sauter-mean diameter has been plotted vs. biomass density in Figure 2.2.12. As was expected there is a considerable drop in Sauter-mean diameter at relatively low cell densities, of the order of less than 1 g/l. These results corroborate the observations of Wang and Ochoa (1972) who found that the distributions of droplet diameters in presence of C. intermedia cells were very different from those in absence of

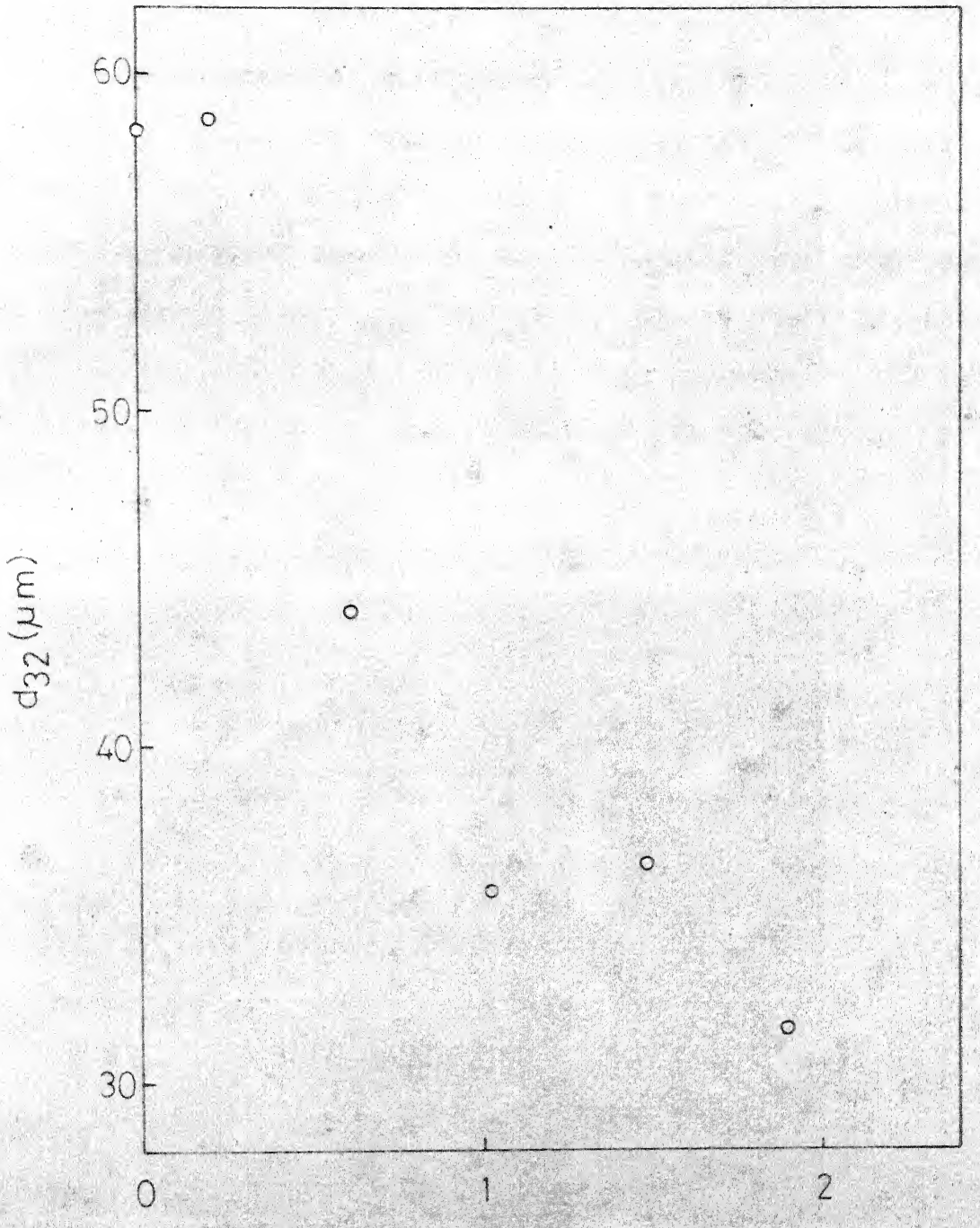

Fig. 2.2.12 - Effect of biomass concentration on Sauter-mean diameter.

of cells. An exponential dependence is suggested by the nature of the data. Other experiments reveal that this effect may be very much influenced by the physiological state of the biomass. For example, there is a tendency for the Sauter-mean diameter, d_{32} , to increase towards the end of the fermentation in spite of the high concentrations of biomass (Prokop and Ludvík, 1973). However, this effect could not be studied extensively and is suggested for future work.

* * *

CHAPTER III

MODEL FOR DROP PHENOMENA

The performance of hydrocarbon fermentors depends upon the extent of dispersion of hydrocarbons in the aqueous medium. A good understanding and characterization of the dispersion phenomena is essential before rational design of such fermentors can be attempted. In this chapter, an attempt towards a reasonable quantitative definition of the agglomerative and break-up processes of the dispersed phase particles, is described. The first part concerns with a coalescence-redispersion (C-R) model for drop-size distributions in an agitated vessel and its predictions. The second part discusses a method of measurement of coalescence-redispersion frequency based upon the C-R model and describes the experimental work carried out in this connection.

3.1 Coalescence-Redispersion (C-R) Model:

Dispersed phase systems have been a subject of investigation by chemical engineers for a long time. However, Curl (1963) was the first to make an analytical study of mixing of the dispersed phase in a liquid-liquid dispersion. This effort was to give a quantitative description to the observations of Rietema (1958) on the effect of dispersed phase mixing on conversion for various orders of chemical reactions occurring exclusively in the dispersed phase drops. Curl's analysis assumed that all

the drops were of identical size and every coalescent interaction between two drops was immediately followed by redispersion of the parent drop back into two equal-sized drops. The net effect, of course, was an exchange of solute between the drops. Since then, several attempts have been made to account for drop-mixing. Erickson *et al.* (1970) have attempted to answer the obvious objection to equal-sized drops by classifying the drop population into size categories derived from a discretized version of the observed size distribution and allowing for interactions between drops of different categories. The authors assumed that two unlike drops when coalesced, immediately redispersed into two drops of the same sizes as those that coalesced; as before the result of coalescence is the exchange of solute material. Obviously such an interaction preserves the size distribution. The assumption of two unlike drops coalescing and redispersing into the same pair except for the exchange of solute is unreasonable, however.

Valentas, Bilous and Amundson (1966) considered both coalescence and redispersion as occurring at finite rates and predicted drop-size distributions which, however, were not compared with the experimental observations. Besides, this framework is somewhat difficult mathematically and is not readily applicable to the study of rate processes such as heat and mass transfer occurring in dispersions.

More recently, Zeitlin and Tavlarides (1972) have simulated the drop-phenomena in an agitated system by dividing

the system into two zones, first the zone of high turbulence where breakage of drops predominates, second the zone of circulation where essentially coalescence takes place. But no adequate information is available about the breakage and the coalescence frequencies which appear in the equations.

The present work aims at developing a coalescence-redispersion model capable of predicting experimentally observed drop-size distributions in batch stirred vessels, in which lies the test of the proposed mechanism of interaction and redispersion. The stipulations further require that the model be sufficiently simple from a mathematical point of view so that it is extendable to the study of chemical and physical rate processes in dispersions. The model features interaction of droplets (distributed according to their volumes) with a certain coalescence frequency and immediate redispersion into two droplets of arbitrary sizes subject to the constraint of mass conservation. The redistribution is assumed to be uniform with respect to the parent drop volume in the statistical sense. The underlying assumption is that the coalescence frequencies are probably of a much smaller order of magnitude than the breakage frequencies so that the breakage may be regarded as instantaneous relative to coalescence.

3.1.1 Theory:

Let us consider a batch vessel containing two immiscible liquids, provided with an agitator which disperses one of the

phases as fine droplets in the other phase. The process involves an almost instantaneous breakdown of the dispersed phase into a large number of droplets leading into a second phase of droplet - phenomena during which breakage and coalescence occur at a much slower rate. It is proposed that soon after the second phase is in progress the total number of drops remains essentially constant with respect to time. The size distribution, however, continues to change as a result of droplet interactions which, it is further proposed, results in an exchange of mass between the (two) interacting drops. The implication is that the drop-interaction is one of exchange of mass rather than coalescence and redispersion.

Let $n(v,t)dv$ represent the number density of droplets with volume between v and v+dv at any time t in the vessel. Let $q(v',v'')$ represent the interaction frequency for the droplet pair of sizes v' and v". Given that the interaction has occurred between the droplets of sizes v' and v", let the probability of a new droplet pair of sizes in the intervals (v'+x, v'+x+dx) and (v"-x, v"-x-dx) be given by $g(v',v''; x)dx$, where x obviously varies between -v' and +v". Outside the interval $[-v', v'']$, g vanishes and

$$\int_{-v'}^{v''} g(v', v''; x)\, dx = 1 \qquad (3.1.1)$$

The population balance equation for $n(v,t)$ is then easily derived

$$\frac{\partial}{\partial t} n(v,t) = \frac{1}{2} \iint_{v'+v'' \geq v} q(v',v'') \left\{ g(v',v'';v-v') + g(v',v'';v''-v) \right\} n(v',t)\, n(v'',t)\, dv'\, dv'' - \int_0^{\infty} q(v,v')\, n(v,t)\, n(v',t)\, dv' \qquad (3.1.2)$$

The first term on the right hand side of Equation (3.1.2) represents the rate of formation of drops of volume v due to interaction of other drops, while the second is the rate of loss of drops of volume v by interaction with drops of other sizes. No rate process like mass transfer, heat transfer or chemical reaction is assumed to occur in the system.

At equilibrium, Equation (3.1.2) reduces to

$$\frac{1}{2} \iint_{v'+v'' \geq v} q(v',v'') \left\{ g(v',v'';v-v') + g(v',v'';v''-v) \right\} n^*(v')\, n^*(v'')\, dv'\, dv'' = \int_0^{\infty} q(v,v')\, n^*(v)\, n^*(v')\, dv' \qquad (3.1.3)$$

where the terms with asterisk represent equilibrium values.

At this stage, it is necessary to introduce specific assumptions concerning the interaction frequency $q(v',v'')$ and the function $g(v',v'';x)$ before any prediction of the equilibrium drop-size distribution is possible. Let us assume the following

type of functional dependence of the interaction frequency upon the sizes of interacting drops:

$$q(v',v'') = w_o (v'+v'')^m \qquad (3.1.4)$$

where w_o and m are constants. When m is taken to be zero, the frequency is constant; a value of m=1/3 represents the interaction frequency proportional to the diameters of the two drops; m = 2/3 implies a dependence upon the surface areas.

Let us further assume that the function g(v',v"; x) is a <u>uniform</u> distribution so that

$$g(v',v'',x) = \frac{1}{v' + v''} \qquad -v' \leq x \leq v''$$

$$= 0 \qquad \text{otherwise} \qquad (3.1.5)$$

With these assumptions, Equation (3.1.3) becomes,

$$\iint_{v'+v'' \geq v} \frac{v'^m \, n^*(v') \, v''^m \, n^*(v'')}{(v'+v'')} \, dv' \, dv''$$

$$= \int_0^\infty v^m n^*(v) \, v'^m n^*(v') \, dv' \qquad (3.1.6)$$

The equilibrium size distribution f*(v) defined by,

$$f^*(v) = \frac{n^*(v)}{\int_0^\infty n^*(v') \, dv'} \qquad (3.1.7)$$

may then be expressed in terms of Equation (3.1.6) in the following form by means of a transformation of variables:

$$\int_v^\infty \frac{dy}{y} \int_0^y (y-x)^m \, x^m \, f^*(y-x) \, f^*(x) \, dx$$

$$= v^m \, f^*(v) \int_0^\infty x^m \, f^*(x) \, dx \qquad (3.1.8)$$

If we define $\varphi^*(v) \equiv v^m \, f^*(v)$, then Equation (3.1.8) becomes,

$$\int_v^\infty \frac{dy}{y} \int_0^y \varphi^*(y-x) \, \varphi^*(x) \, dx = \varphi^*(v) \int_0^\infty \varphi^*(x) \, dx \qquad (3.1.9)$$

which is readily solved by the method of Laplace transforms to obtain,

$$\varphi^*(v) = \alpha \exp\left(- \frac{v}{\beta} \right) \qquad (3.1.10)$$

so that the drop-size distribution emerges as,

$$f^*(v) = \alpha \, v^{-m} \exp\left(- \frac{v}{\beta} \right) . \qquad (3.1.11)$$

The constants α and β are given by

$$\alpha = \frac{\mu_m^*}{\left[\mu_m^* \, \lceil 1 - m \rceil \right]^{1/m}} \qquad m \neq 0$$

$$\beta = \left[\mu_m^* \, \lceil 1 - m \rceil \right]^{1/m} \qquad m \neq 0 \qquad (3.1.12)$$

For the case of $m = 0$, Equation (3.1.11) predicts an <u>exponential</u> distribution for the equilibrium drop-size,

$$f^*(v) = \frac{1}{\mu_1^*} \exp\left(- \frac{v}{\mu_1^*} \right) \qquad (3.1.13)$$

When m = 2/3, μ_m^* represents the average drop surface and average drop diameter for m = 1/3. Equation (3.1.11) with m regarded as fixed is a one-parameter distribution.

The justification for the forms assumed for q(v',v") and g(v',v"; x) lies in the ability of Equation (3.1.11) to describe experimentally observed drop-size distributions.

3.1.2 Comparison with Experimental Data:

Drop-size distributions were measured in Waldhof - agitated n-alkane - water systems using the detergent stabilization method. The data obtained for various conditions of speeds of rotation and dispersed phase fractions have been tabulated in Appendix B.

Experimental data were also obtained from various sources reported in the literature (Shinnar, 1961; Luhning and Sawistowski, 1971; Brown and Pitt, 1972; Prokop and Ludvík, 1973). Data of Shinnar, Luhning and Sawistowski, and Brown and Pitt were collected in flat-blade turbine systems while those of Prokop and Ludvík belonged to the circulation-stirring type. All these data were utilized for verifying the predictions of the coalescence-redispersion (C-R) model and for comparison of the C-R model with other distributions reported in the literature.

In Figures 3.1.1 to 3.1.6 the drop-size distributions have been presented. Figures 3.1.1 show the data of Shinnar for 5% dispersion of shell-wax in hot water for different speeds of

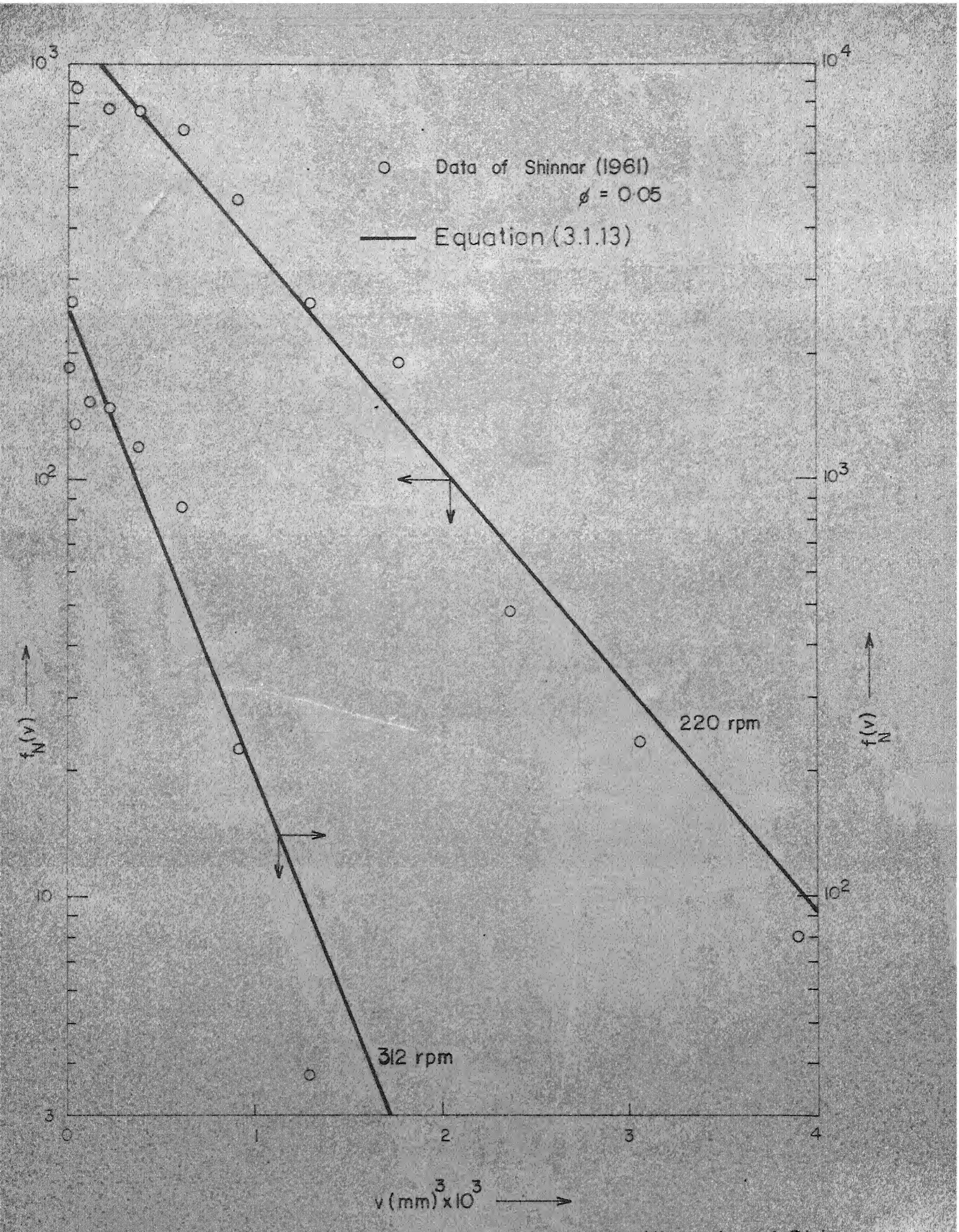

Fig.3.1.1a - Comparison of C-R model predictions with data of Shinnar (1961)

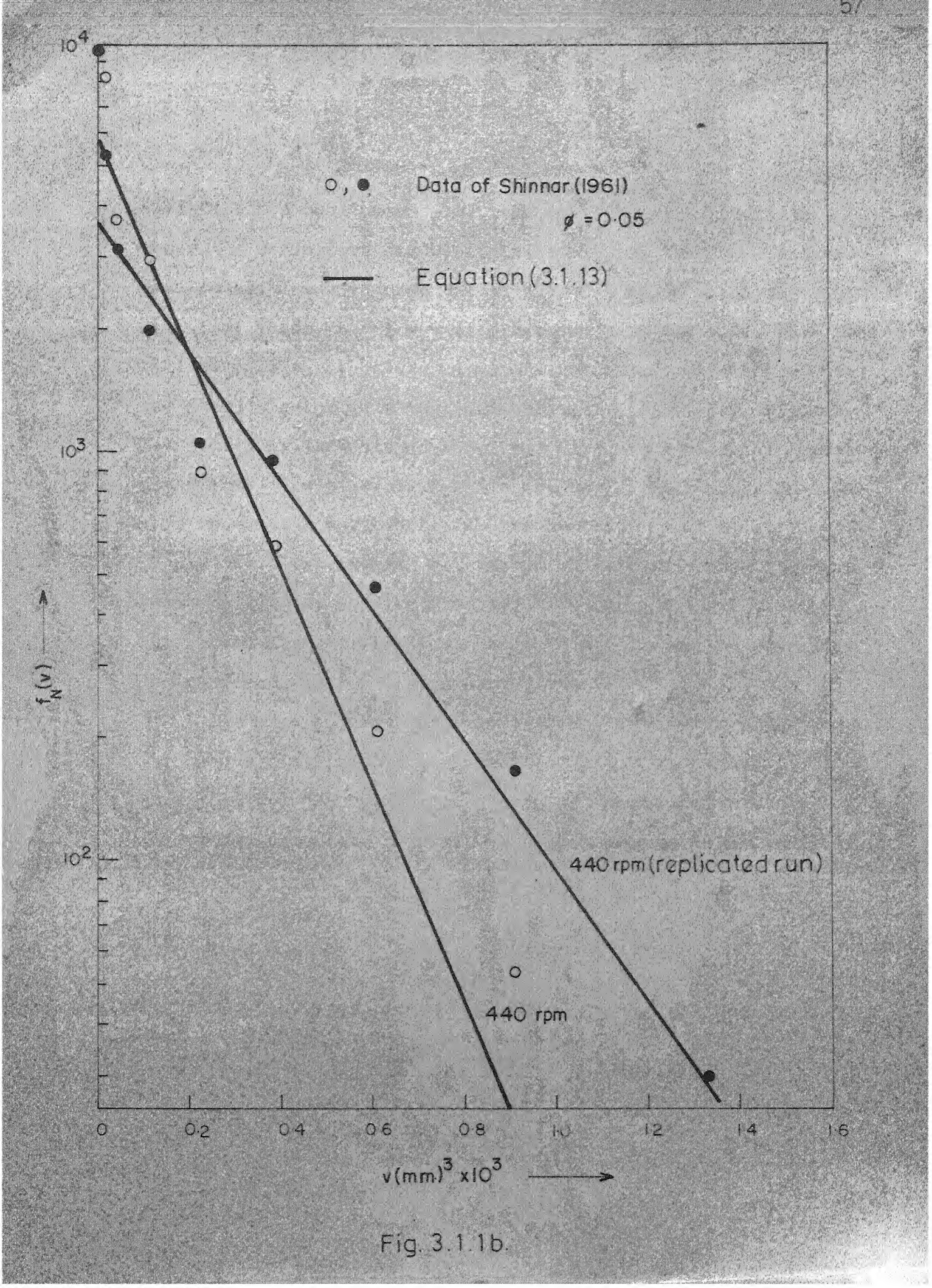
10^4
10^3
10^2
$f_N(v)$
○, ● Data of Shinnar (1961)
$\phi = 0.05$
—— Equation (3.1.13)
440 rpm (replicated run)
440 rpm
0
0·2
0·4
0·6
0·8
1·0
1·2
1·4
1·6
$v(mm)^3 \times 10^3$

Fig. 3.1.1b.

agitation. A continuous line represents Equation (3.1.13) where the average volume was calculated from the experimental data itself. Luhning and Sawistowski's data in which the dispersed phase fraction varied between 0.10 and 0.50, have been plotted in Figures 3.1.2. Again, a continuous line represents the theoretical predictions using Equation (3.1.13).* Figures 3.1.3 display the data of Brown and Pitt for a range of dispersed phase fractions at various agitator speeds. All these data show reasonable agreement with the predictions of Equation (3.1.13). Figure 3.1.4 represents all the above data on a single dimensionless plot. The scatter observed is perhaps not serious considering the diversity of their sources and the errors attendant on measurement of drop-size distributions.

For a more quantitative treatment, a Chi-square test of the goodness of fit was performed. But the test proved too stringent being very sensitive even to sporadic appearances of one or two 'bad data points'. The data were also subjected to a Chi-square test using an empirical model of vanHeuven and Hoevenaar (1968),

$$f_A = \frac{k\,A}{b(k-1)!}\left[\frac{k\,d}{b}\right]^{k-1} \exp\left[-\frac{k\,d}{b}\right] \qquad (3.1.14)$$

where $b = d_{32}$, $k = \dfrac{1}{(1 - d_{21}/d_{32})}$

and one from Gal-Or (1968),

---

*$F(v) = \int_0^v f(v')\,dv'$

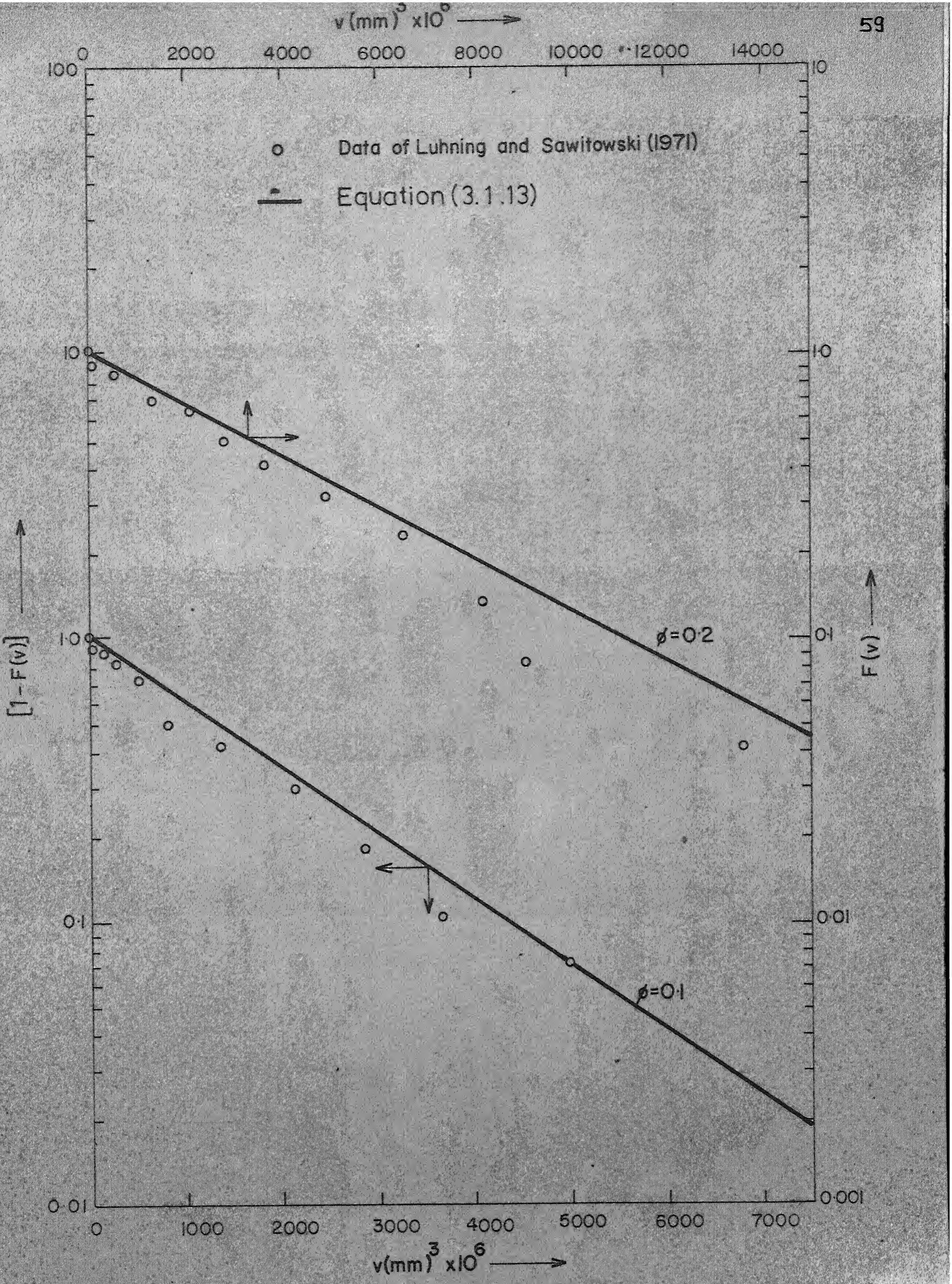

Fig. 3.1.2a - Comparison of C-R model predictions with data of Luhning and Sawistowski (1971).

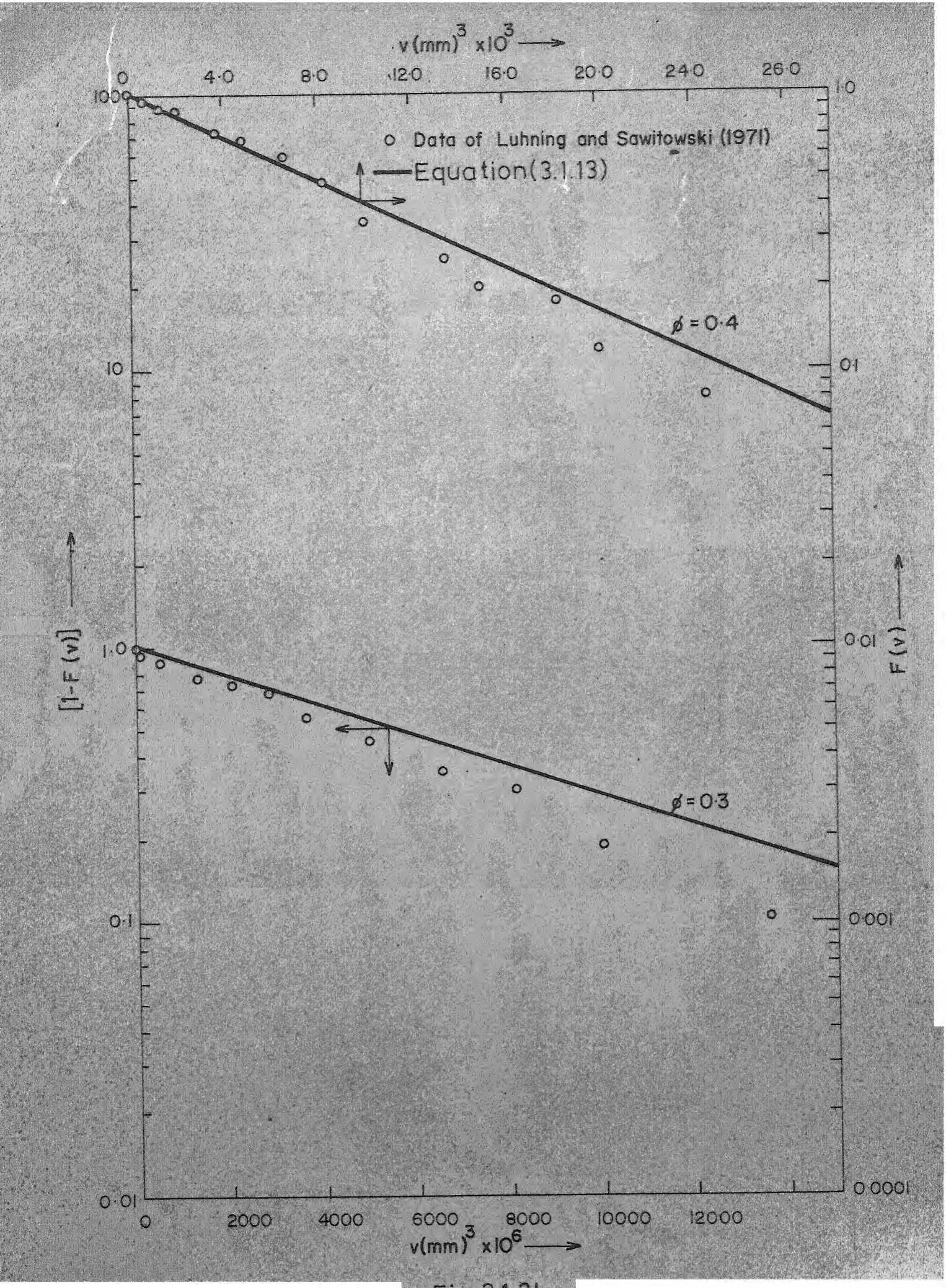
v(mm)³ x10³ →
0
4·0
8·0
12·0
16·0
20·0
24·0
26·0
1·0
100
10
1·0
0·1
0·01
[1-F(v)]
F(v) →
0·01
0·001
0·0001
o Data of Luhning and Sawitowski (1971)
—Equation(3.1.13)
ø = 0·4
ø = 0·3
0
2000
4000
6000
8000
10000
12000
v(mm)³ x10⁶ →

Fig. 3.1.2b.

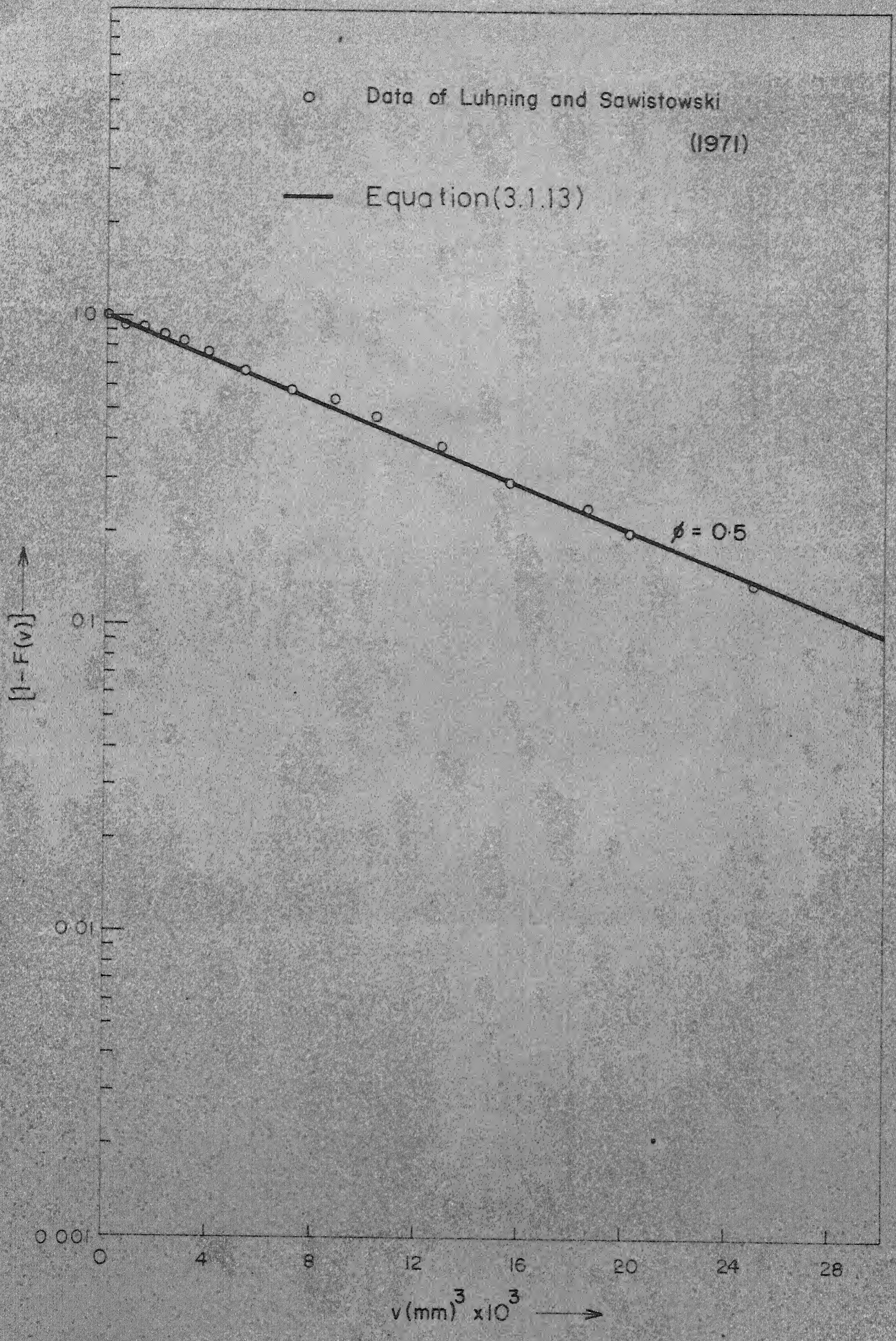
o Data of Luhning and Sawistowski
(1971)
Equation (3.1.13)
ϕ = 0·5
1·0
0·1
0·01
0·001
[1 - F(v)]
0
4
8
12
16
20
24
28
v (mm)³ x10³

Fig. 3.1.2c.

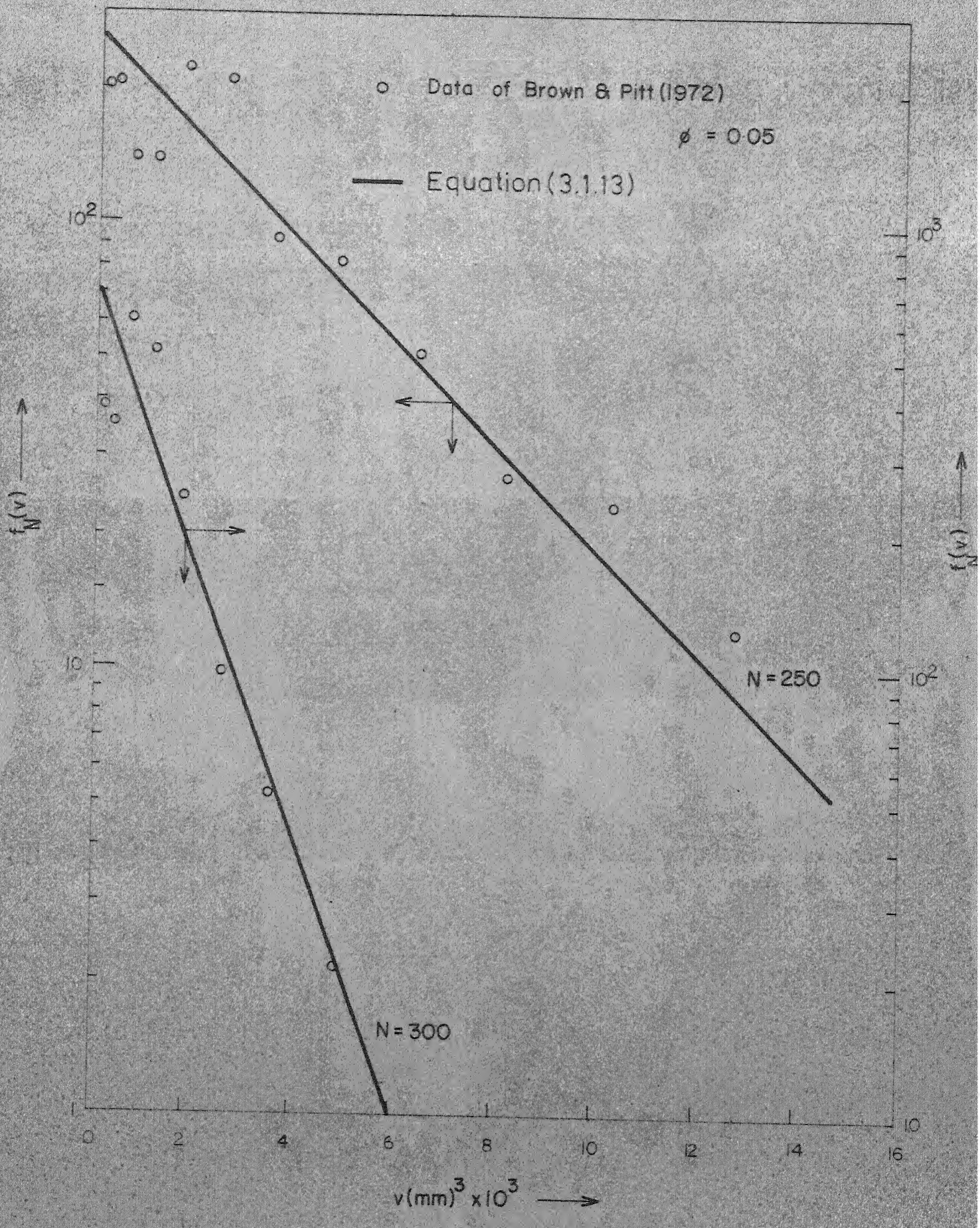

Fig. 3.1.3a - Comparison of C-R model predictions with data of Brown and Pitt (1972)

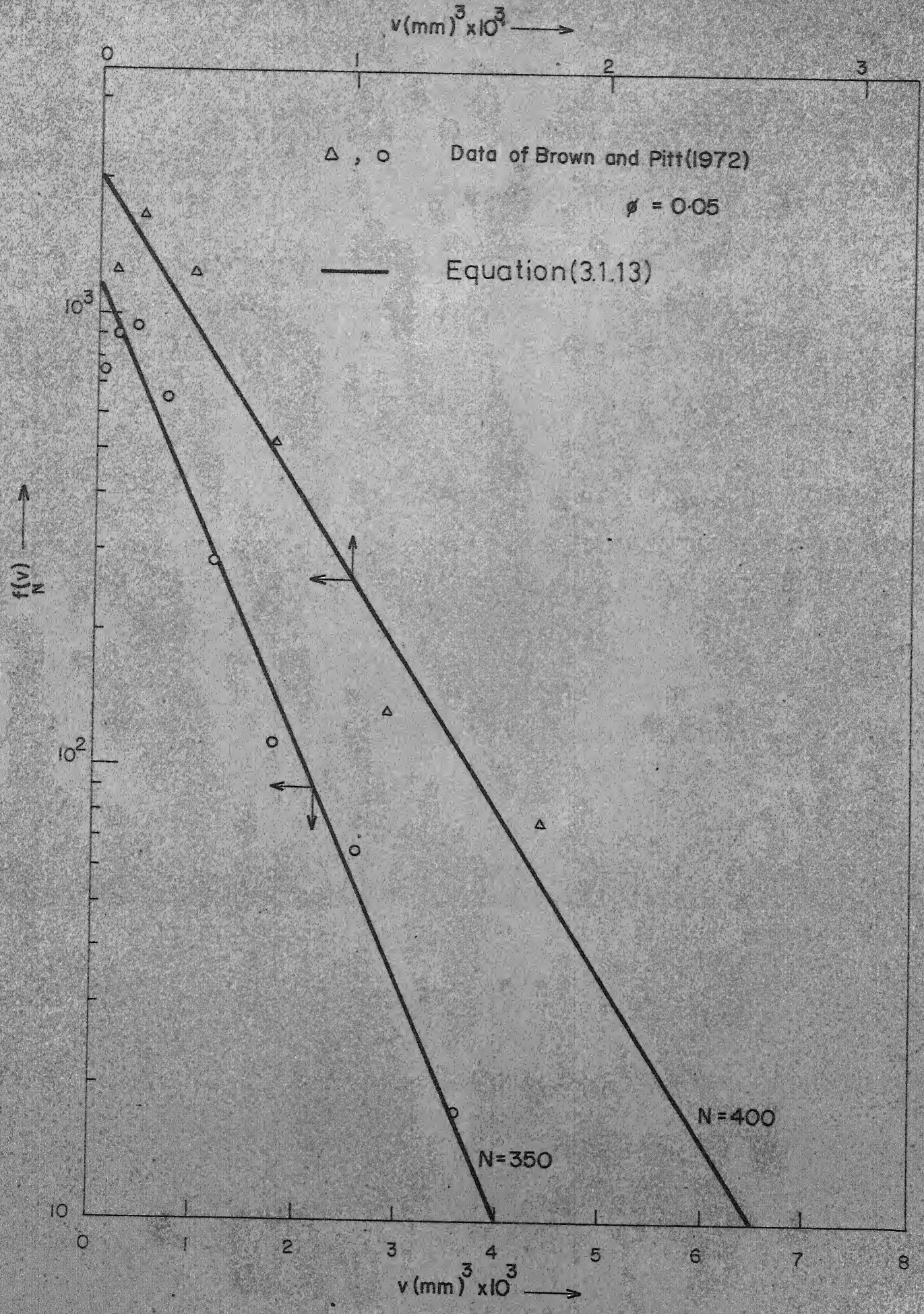
v(mm)³ x10³
0
1
2
3
Δ , o Data of Brown and Pitt(1972)
ø = 0·05
Equation(3.1.13)
10³
10²
10
f(v)/N
N=400
N=350
0
1
2
3
4
5
6
7
8
v(mm)³ x10³

Fig.3.1.3b.

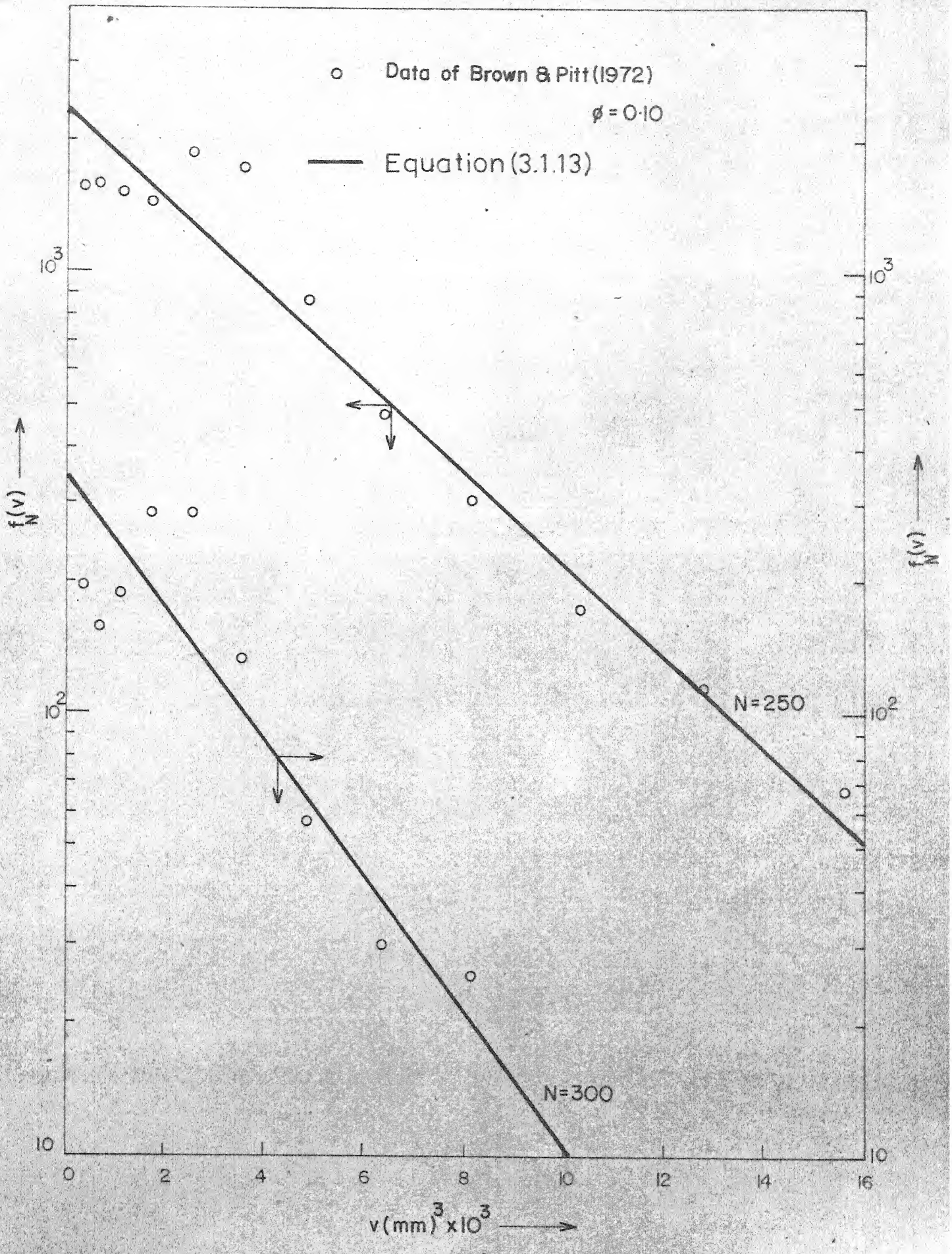
Data of Brown & Pitt (1972)
ϕ = 0·10
Equation (3.1.13)
N=250
N=300
$f(v)_N$
10^3
10^2
10
0
2
4
6
8
10
12
14
16
$v(mm)^3 \times 10^3$

Fig. 3.1.3c.

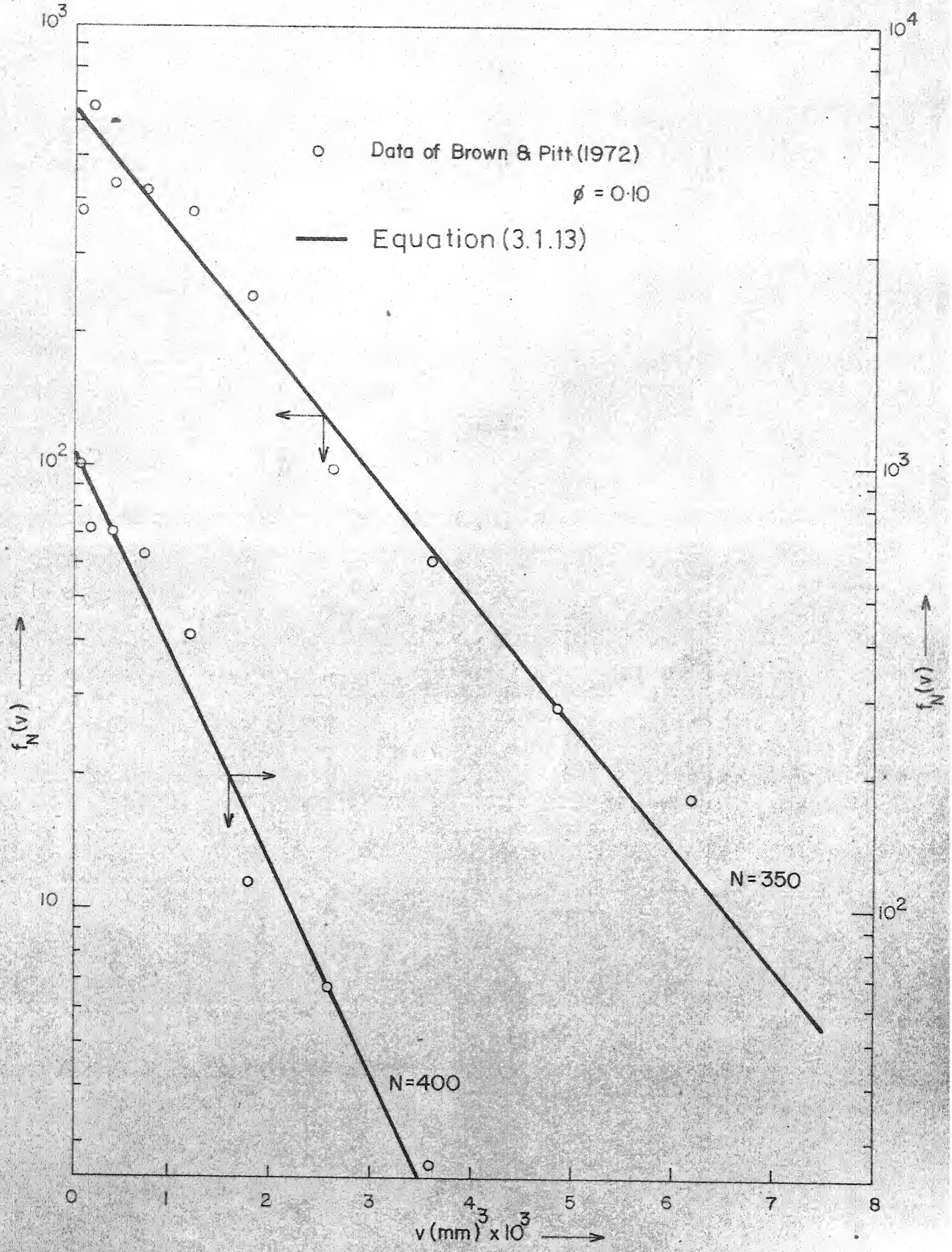
Data of Brown & Pitt (1972)
ϕ = 0·10
Equation (3.1.13)
N=350
N=400
$f_N(v)$
$f_N(v)N$
$v\,(mm)^3 \times 10^3$
10^3
10^4
10^2
10^3
10
10^2
0
1
2
3
4
5
6
7
8

Fig. 3.1.3d.

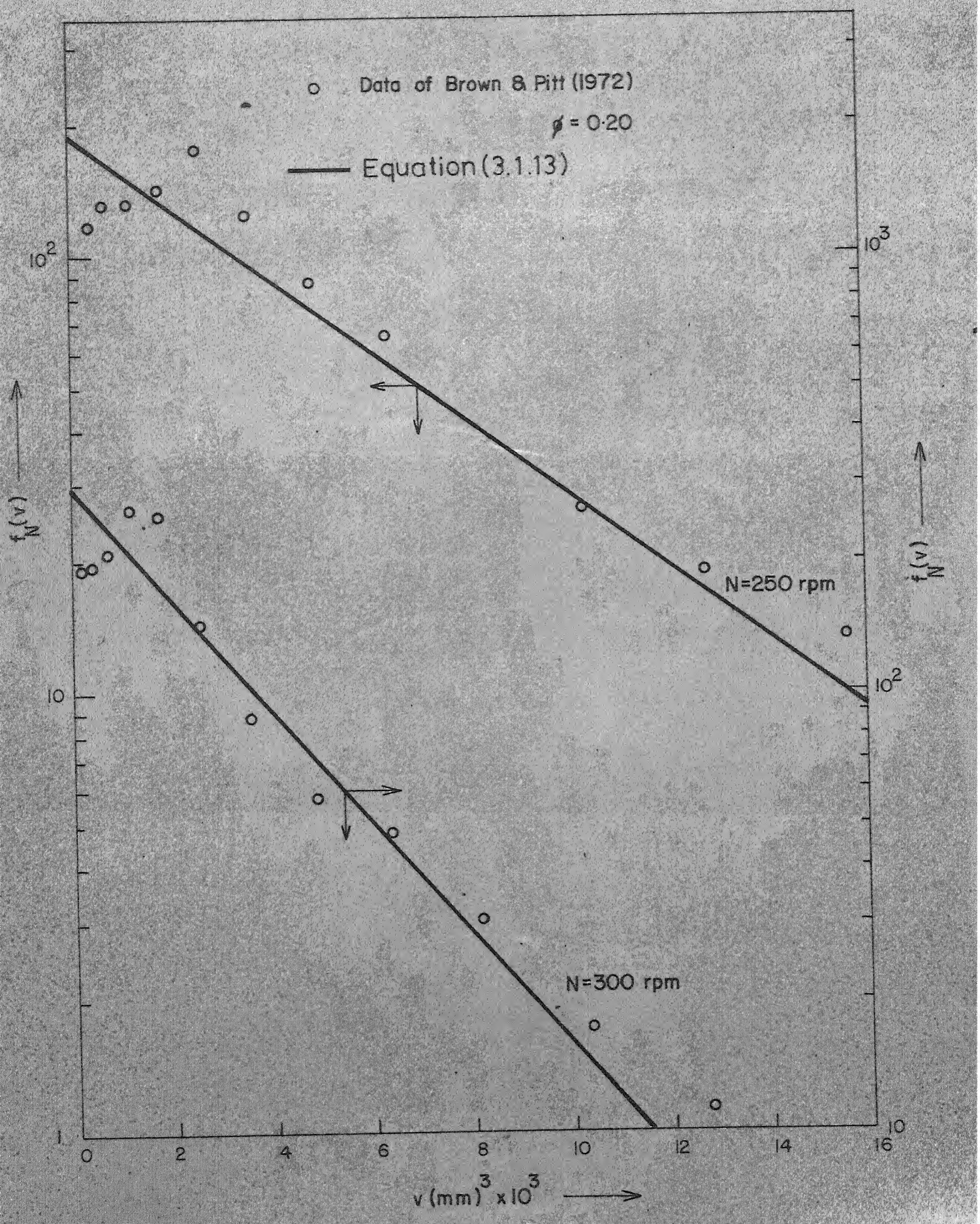
Data of Brown & Pitt (1972)
ϕ = 0·20
Equation (3.1.13)
N=250 rpm
N=300 rpm
$f_N(v)$
$f_N(v)$
$v\,(mm)^3 \times 10^3$
1
10
10^2
10^3
0
2
4
6
8
10
12
14
16

Fig 3.1.3e

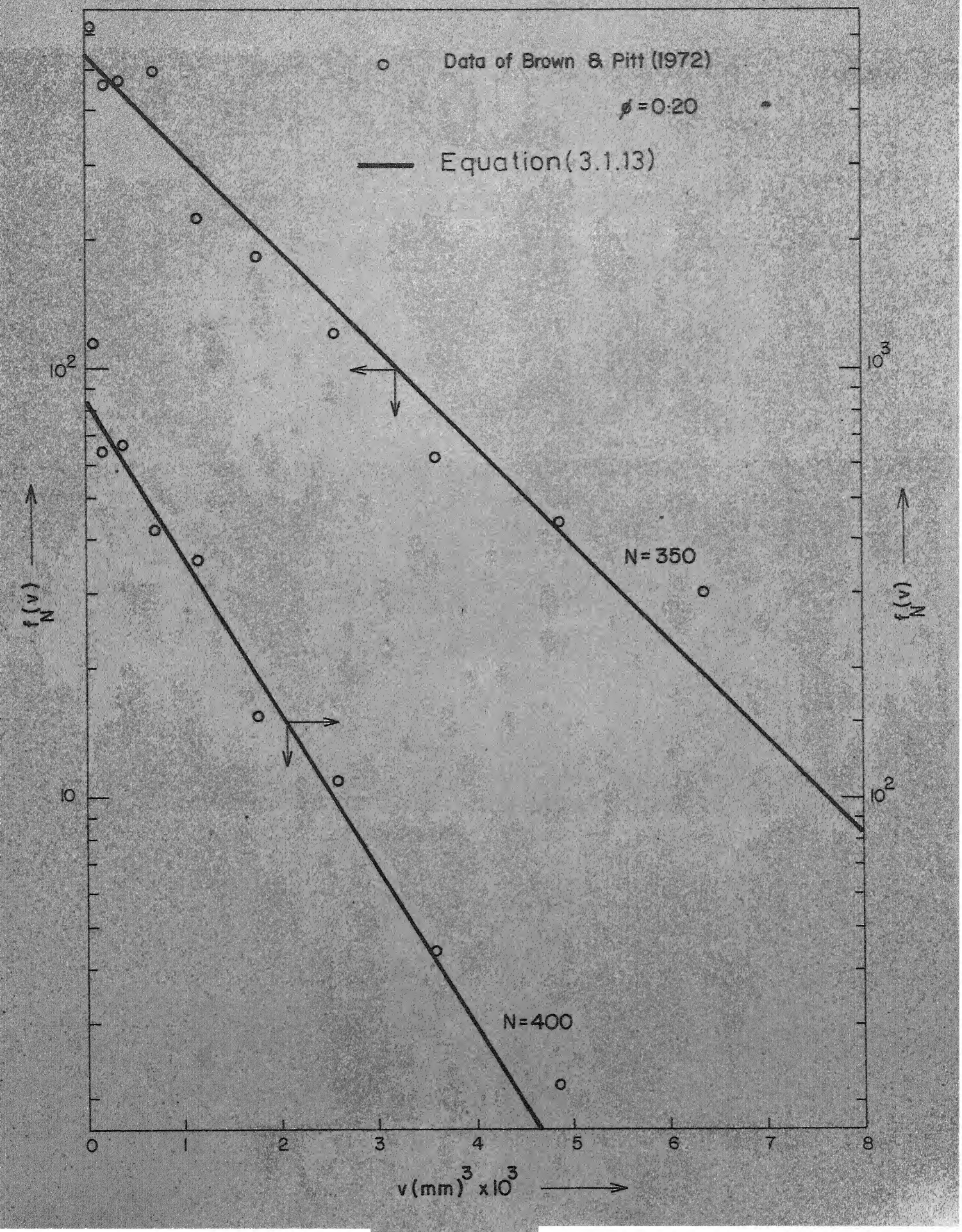
Data of Brown & Pitt (1972)
ϕ = 0·20
Equation (3.1.13)
N = 350
N = 400
f(v)N
f(v)N
v (mm)³ x 10³
10²
10³
10
10²
0
1
2
3
4
5
6
7
8

Fig 3.1.3f

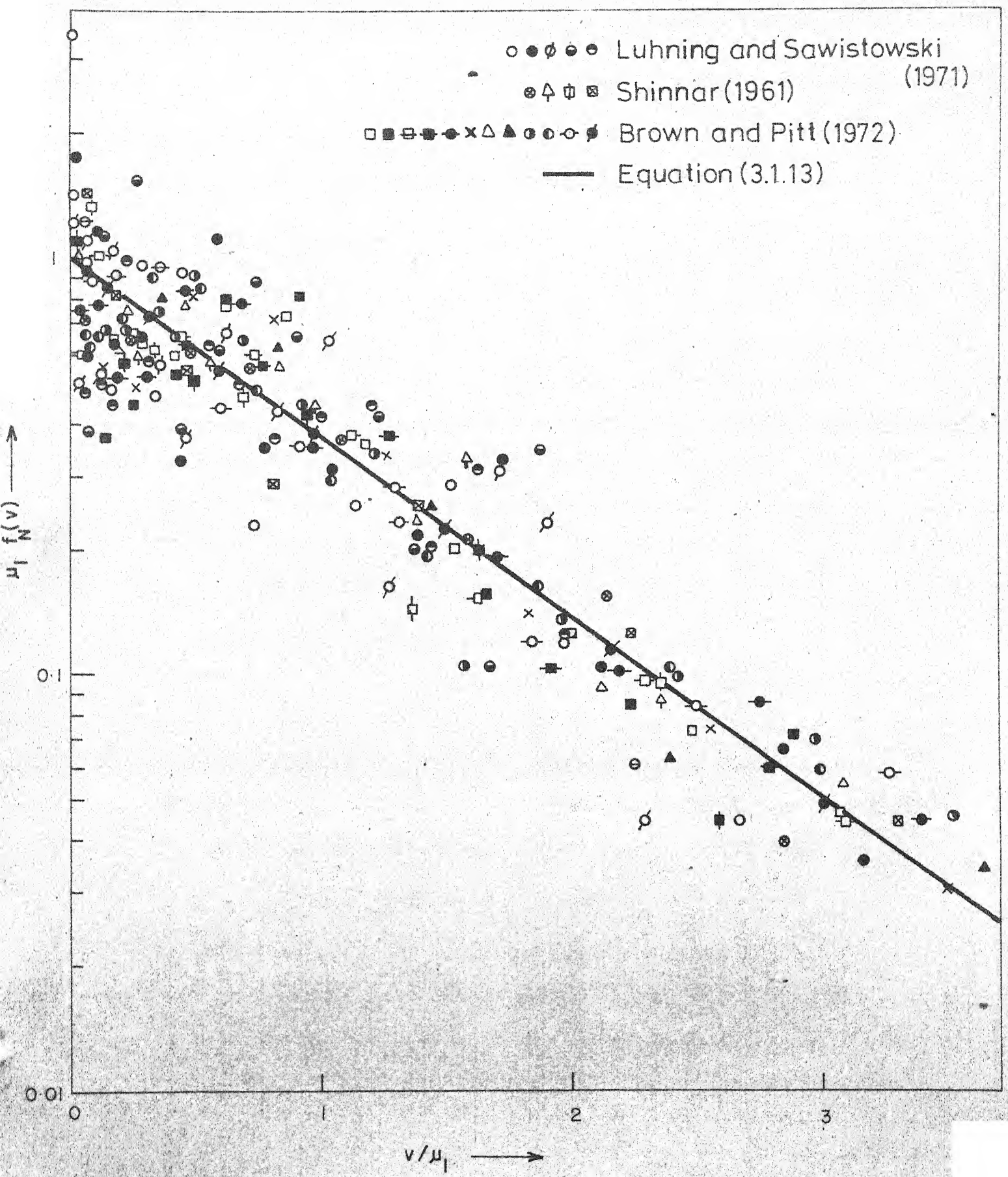

Fig. 3.1.4.-Dimensionless plot of experimentally observed DSD data of various authors.

$$f_n = 4 \left[\frac{\alpha^3}{\pi} \right]^{1/2} d^2 \exp(-\alpha d^2) \qquad (3.1.15)$$

where $\alpha = \left(\frac{16\sqrt{\pi}\, N}{3\,\emptyset} \right)^{2/3}$.

The Chi-square test disqualified these models also for the same reason as mentioned earlier. It was, therefore, felt that it would be expedient to make a relative assessment of the C-R model (Equation 3.1.11 or 3.1.13) with those of vanHeuven and Hoevenaar (Equation 3.1.14) and of Gal-Or (Equation 3.1.15), on their applicability to the data at hand. This assessment was based upon a simple statistical hypothesis-testing procedure described below.

Suppose there are two models A and B whose predictions of a certain experiment are to be relatively assessed with respect to the available experimental observations. Let there be N observations available; we calculate the χ^2 values for the jth experimental set (obtained by summing for the error sources at each point in the set) for both models, A and B, represented by $\chi_A^{j^2}$ and $\chi_B^{j^2}$ respectively. Consider the random variable

$$X = \chi_A^{j^2} - \chi_B^{j^2} \quad .$$

The hypothesis, H, to be tested is taken to be

H : {Model A is either as good as or worse than Model B.}

If p is the probability that the random variable X has a negative sign, then for H to be true $p \leq 1/2$. Let N_- be the number of

negative signs of X out of N observations (or sets of experimental data). Assuming the observations to be independent of one another, the probability of N_- or more negative signs out of N, denoted by P, is given by a Bernoulli distribution as given below.

$$P = \sum_{k=N_-}^{N} \binom{N}{k} p^k (1-p)^{N-k} \qquad (3.1.16)$$

Since $p \leq 1/2$, we must have

$$P \leq \sum_{k=N_-}^{N} \binom{N}{k} \left(\frac{1}{2}\right)^N \equiv P_{max} \qquad (3.1.17)$$

If P_{max} is very small, we infer that the observation made is very improbable under the hypothesis H, on the basis of which we reject the hypothesis and conclude that model A is better than model B; the level of significance at which this inference will be drawn is given by P_{max}.

Calculations were made for different sets of experimental observations. The subscripts used were o for Equation (3.1.13), v for the expression proposed by vanHeuven and Hoevenaar (Equation 3.1.14), and G for that contained in the work of Gal-Or (Equation 3.1.15). Table III-1.1 displays the results of the calculations. It demonstrates the high rating of the exponential distribution (Equation 3.1.13) over that used by Gal-Or. The model appears to be superior to that of vanHeuven and Hoevenaar also.

TABLE III-1.1: COMPARISON BETWEEN MODELS FOR DSD DATA FROM FBT SYSTEMS

Model A	Model B	Total number N	Number of negative signs N-	P_{max}	Percentage level of significance at which model A is better than model B
o	G	24	22	1.79×10^{-5}	0.00179
o	v	24	16	0.076	7.6

For the drop-size distribution data obtained during the present investigation as well as for those of Prokop and Ludvík (1973), Equation (3.1.13) was found to give a better fit than the models of vanHeuven and Hoevenaar (Equation 3.1.14), and of Gal-Or (Equation 3.1.15) which among themselves could not be distinguished (Table III-1.2). However, significant improvement in predictions was observed when the value of m was different from zero in Equation (3.1.11).

TABLE III-1.2: COMPARISON BETWEEN MODELS FOR DSD DATA FROM CS SYSTEMS

Model A	Model B	Total number N	Number of negative signs N_-	P_{max}	Percentage level of significance at which model A is better than model B
v	G	5	3	0.50	50.0
o	G	22	20	0.606×10^{-4}	0.0061
1/3	o	22	21	0.562×10^{-5}	0.562×10^{-3}

As a matter of fact, Equation (3.1.11) with m = 0.3 and m = 0.4 was found to be definitely superior to Equation (3.1.13). Equation (3.1.11) with m >0.4 was found to worsen the predictions. However, no difference could be ascertained between predictions with m=0.3 and those with m = 0.4. Figures 3.1.5 and 3.1.6 show some of the data from Waldhof-agitated systems. Plots of Figure 3.1.5 correspond to data taken by Prokop and Ludvík (1973) during gas-oil fermentation. Data in Figures3.1.6 belong to some conditions from Appendix B. The difference in patterns of these systems which have a well pronounced circulation zone, from those mentioned earlier which were agitated by flat-blade turbines must, however, be noted. It is this circulation zone which manifests itself in terms of higher number frequencies generally obtained experimentally for large drops than predicted.

From the above results, it appears that the droplet interaction mechanism suggested here-in has experimental support in view of satisfactory agreement with data from diverse dispersed systems. The exponential distribution (Equation 3.1.13) describes dispersions mixed by turbine agitators. On the other hand, for systems having a pronounced circulation zone, the model with coalescence frequency dependent upon droplet diameter, produces substantially improved results.

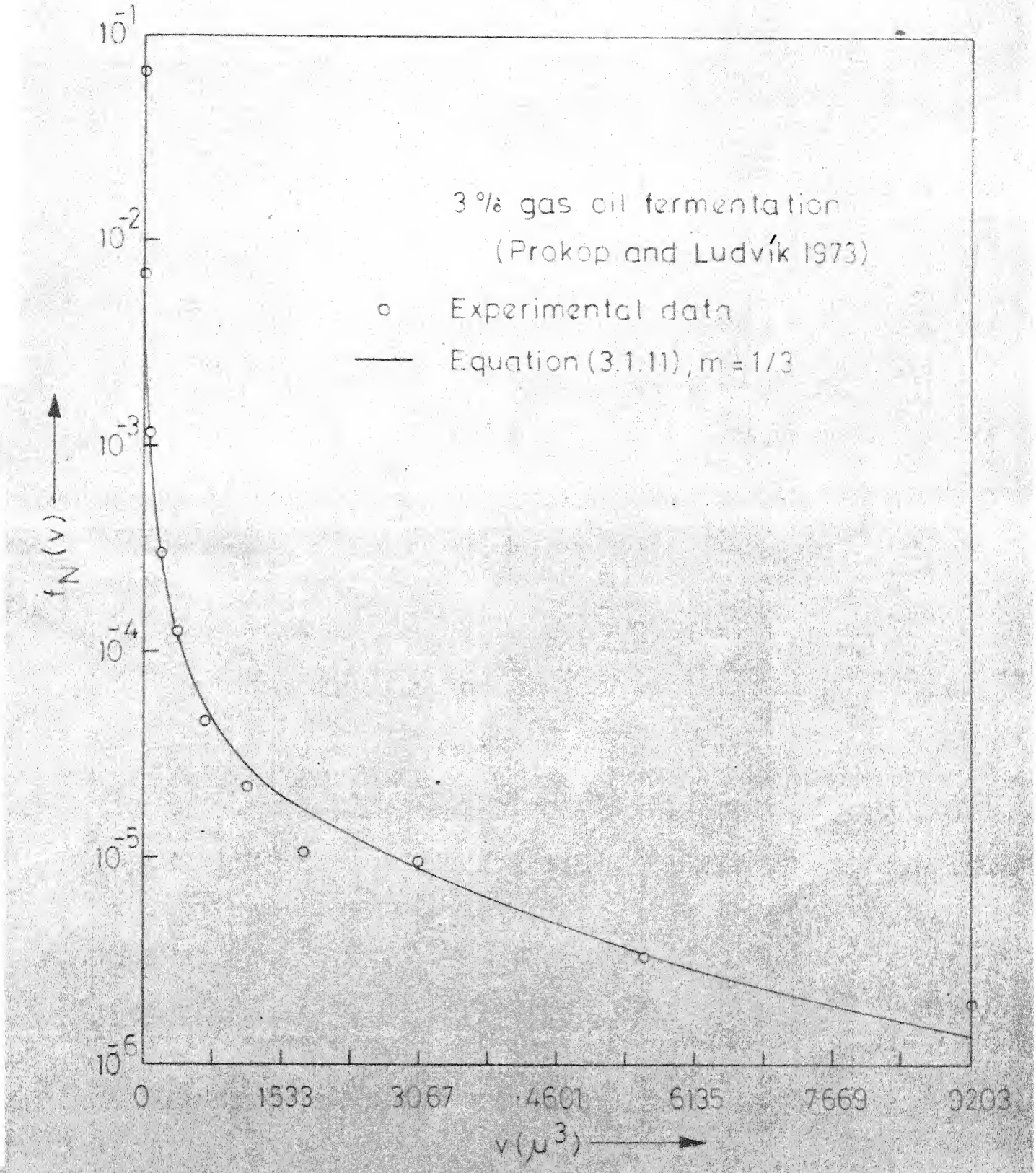

Fig. 3.1.5a - Comparison of C-R model predictions with data of Prokop and Ludvík (1973)

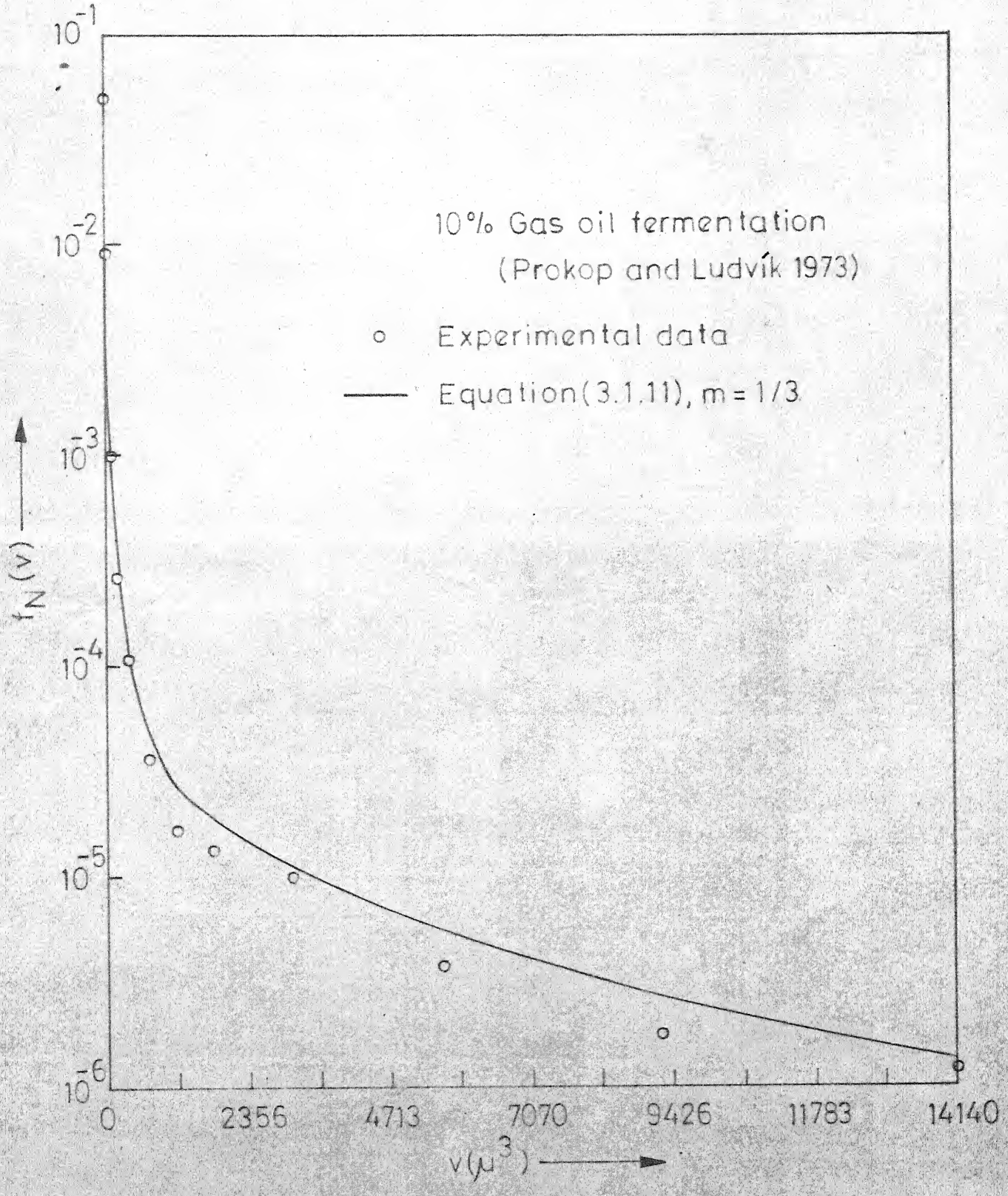
10% Gas oil fermentation
(Prokop and Ludvík 1973)
Experimental data
Equation (3.1.11), m = 1/3
10^{-1}
10^{-2}
10^{-3}
10^{-4}
10^{-5}
10^{-6}
$t_N(v)$
0
2356
4713
7070
9426
11783
14140
$v(\mu^3)$

Fig. 3.1.5 b.

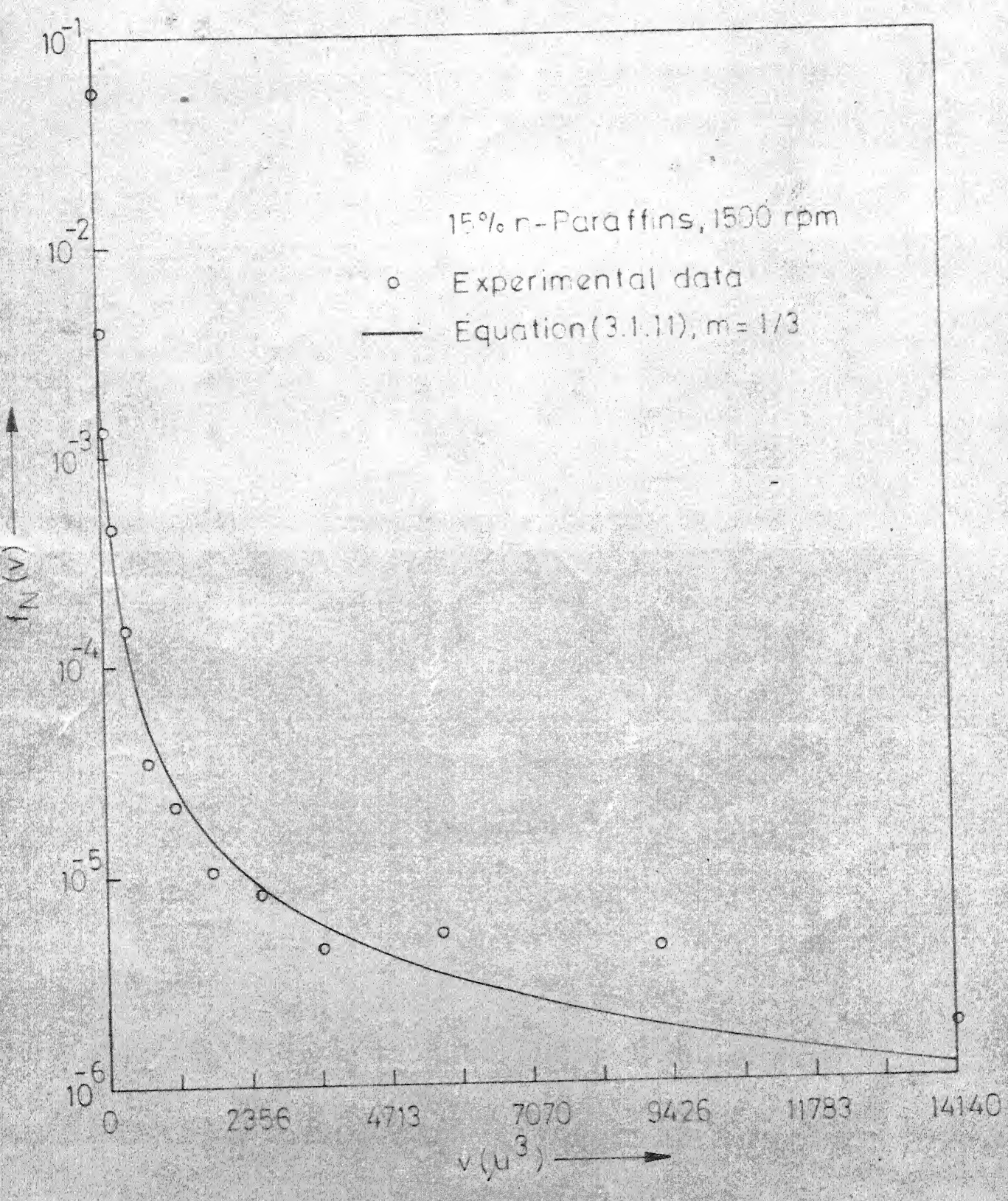

Fig. 3.1.6a - Comparison of C-R model predictions with DSD data from Waldhof agitated n-alkane-water system.

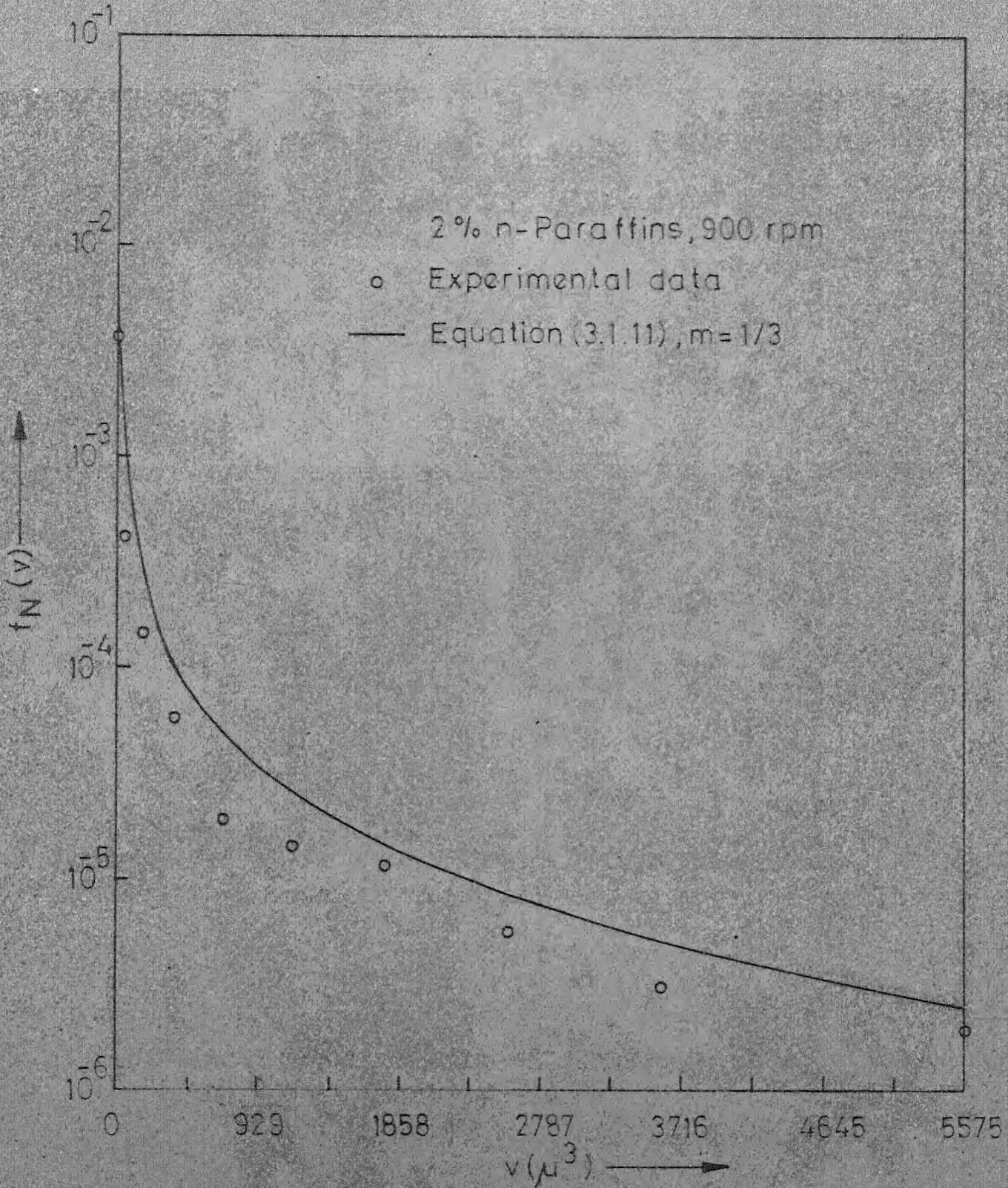
2% n-Paraffins, 900 rpm
Experimental data
Equation (3.1.11), m=1/3
$f_N(v)$
10^{-1}
10^{-2}
10^{-3}
10^{-4}
10^{-5}
10^{-6}
0
929
1858
2787
3716
4645
5575
$v(\mu^3)$

Fig. 3.1.6 b.

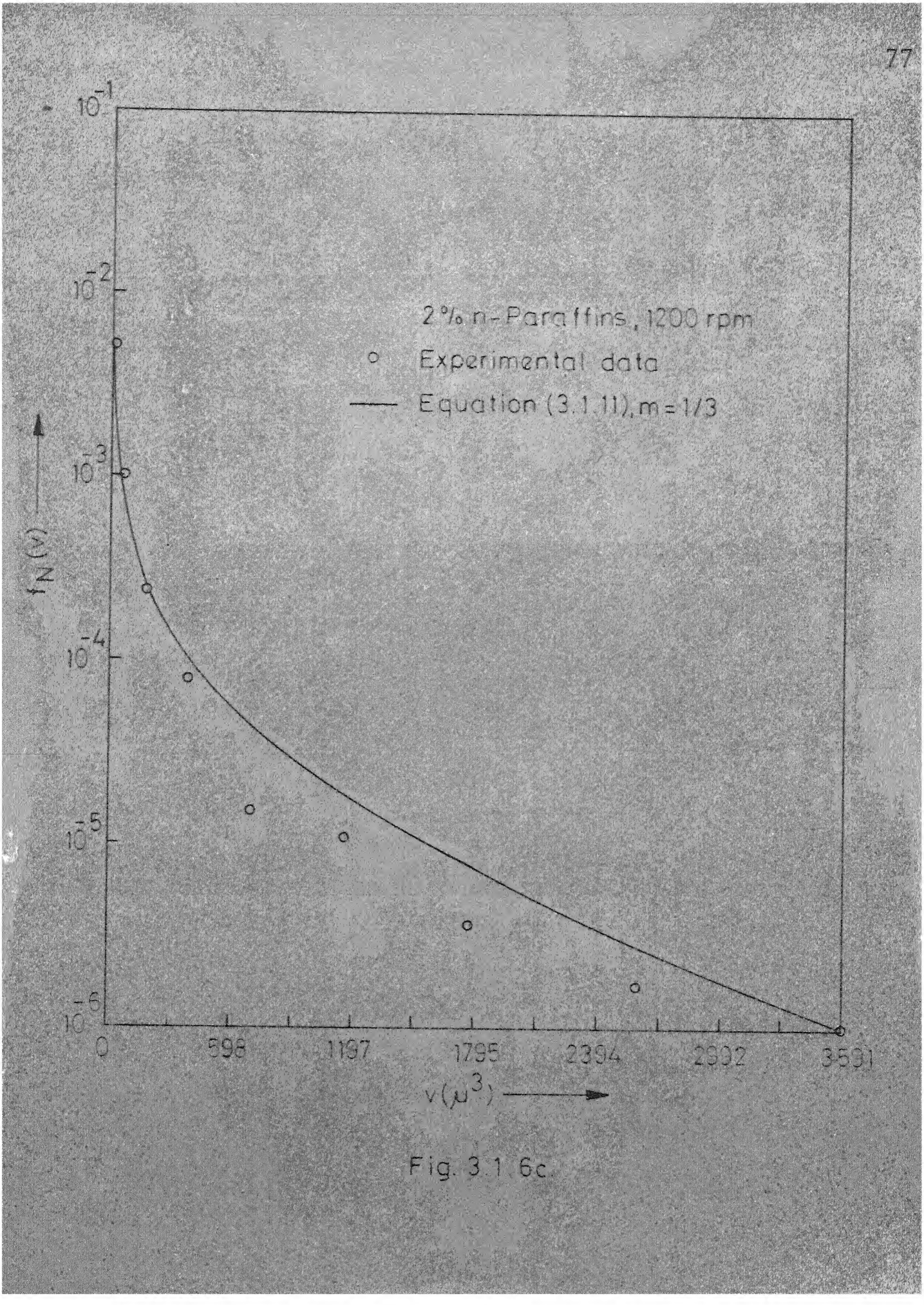
2% n-Paraffins, 1200 rpm
Experimental data
Equation (3.1.11), m = 1/3
$f_N(v)$
10^{-1}
10^{-2}
10^{-3}
10^{-4}
10^{-5}
10^{-6}
0
598
1197
1795
2394
2992
3591
$v(\mu^3)$

Fig. 3.1.6c

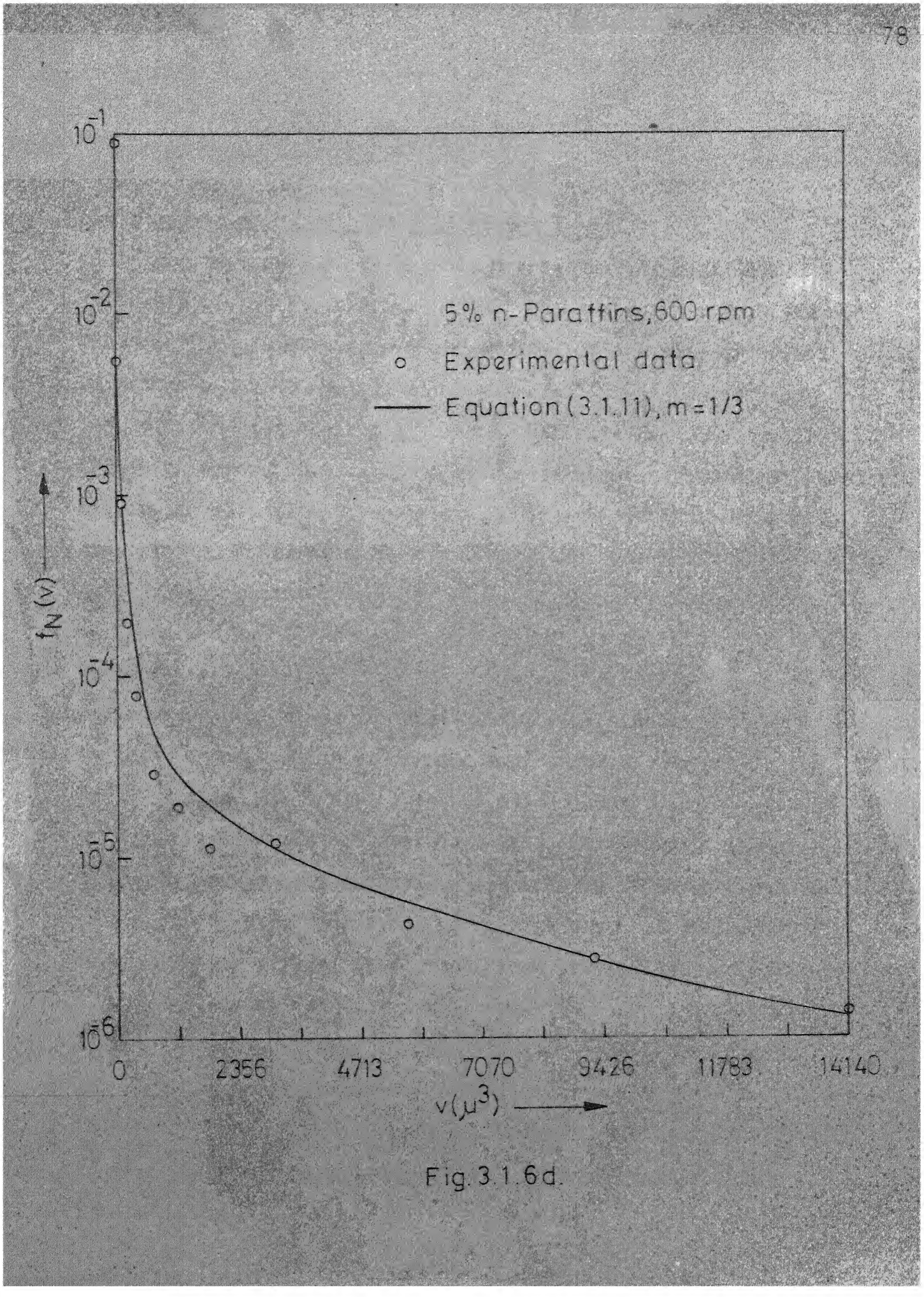
5% n-Paraffins, 600 rpm
Experimental data
Equation (3.1.11), m = 1/3
10^{-1}
10^{-2}
10^{-3}
10^{-4}
10^{-5}
10^{-6}
$f_N(v)$
0
2356
4713
7070
9426
11783
14140
$v(\mu^3)$

Fig. 3.1.6d.

3.2 Measurement of the Interaction Frequency:

The present methods for the measurement of coalescence frequency can be broadly classified into two categories. The first methods involve direct observation of the rate of spread of a tracer due to mixing in the dispersed phase (Madden and Damerell, 1962; Miller et al., 1963; Hillestad and Rushton, 1966). For this purpose, some drops having a continuous-phase-insoluble dye are introduced into an existing dispersion. Alternatively, the existing dispersion may have a chemical which on reacting with another chemical present in the freshly introduced drops, may form a dye. The reaction must, however, be limited to the dispersed phase only. In both the cases, it is essential to add a dye or a chemical to the dispersed phase, and the contamination may result in substantial change in dispersion characteristics. In the second method, the speed of agitation is suddenly reduced to a lower value and the transient response of an optical probe which measures Sauter-mean diameter is noted. The coalescence frequency is calculated from the initial slope of the response curve. (Howarth, 1967; Blanch and Fiechter, 1974). The underlying assumptions are that a step reduction in agitator speed results in a step change in the degree of turbulence, and the new steady state drop-size distribution is achieved by a coalescence-only process. In practice, however, it is very difficult to meet the first assumption as some time invariably lapses

before the turbulence decays to the new value, and the second assumption will be valid only for a very specific kind of dispersion. Moreover, the use of an optical probe for measuring the dispersion characteristics in biological systems is also controversial because of the interfering presence of microbial cells and air-bubbles.

The C-R model proposed in section 3.1 suggests a method of measuring the interaction frequency. The method does not require addition of any chemical to the system and thus avoids any deliberate contamination. Another strong point for the method is that the basic model satisfactorily predicts the experimentally observed DSDs in diverse systems. Either a batch or a steady state continuous system can be employed. In the case of batch vessels, the method requires measurement of unsteady state DSDs at various times from the start of the agitation. According to the model predictions, a semi-log plot of $(\mu_2 - 2\mu_1^2)$ vs time should yield a straight line. From the slope of this straight line, the coalescence or interaction frequency can be calculated.

3.2.1 Theory:

For the unsteady state case in a stirred batch vessel, Equation (3.1.8) may be written as,

$$\frac{\partial}{\partial t} n(v,t) = w_o \iint_{v'+v'' \geq v}^{\infty} \frac{v'^m \, n(v',t) \; v''^m \, n(v'',t)}{(v' + v'')} \, dv' \, dv''$$

$$- w_o \, v^m \, n(v,t) \int_o^{\infty} v'^m \, n(v',t) \, dv' \qquad (3.2.1)$$

Since the total number of drops in the vessel is assumed to be constant during the secondary phase,

$$\frac{\partial}{\partial t} f(v,t) = w_o \, N \iint_{v'+v'' \geq v}^{\infty} \frac{v'^m \, f(v',t) \; v''^m \, f(v'',t)}{(v' + v'')} \, dv' \, dv''$$

$$- w_o \, v^m \, N \, f(v,t) \int_o^{\infty} v'^m \, f(v',t) \, dv' \qquad (3.2.2)$$

where $n(v,t) = N. \; f(v,t)$.

The moment equations may be generated to obtain,

$$\frac{d}{dt} \mu_o = 0 \qquad (3.2.3)$$

$$\frac{d}{dt} \mu_1 = 0 \qquad (3.2.4)$$

$$\frac{d}{dt} \mu_2 = w_o \, N \left[\frac{2}{3} \, \mu_{m+1}^{\,2} - \frac{1}{3} \, \mu_m \, \mu_{m+2} \right] \qquad (3.2.5)$$

Equation (3.2.3) is a reflection of the assumption of constant number of droplets in the secondary phase while Equation (3.2.4) is a statement of mass conservation. Equation (3.2.5) and those of higher moments are an unclosed set when m is not zero.

However, for m = 0 (i.e. constant coalescence frequency), one obtains,

$$\frac{d\mu_2}{dt} = -\frac{w_o N}{3} (\mu_2 - 2\mu_1^2) \qquad (3.2.6)$$

which is easily solved resulting in,

$$\mu_2 = 2\mu_1^2 + (\text{constant}).\ \exp\left(-\frac{w_o N}{3} t\right) \qquad (3.2.7)$$

so that a semi-log plot of $(\mu_2 - 2\mu_1^2)$ vs time should yield a straight line of slope $(-w_o N/3)$. It would, of course, be necessary to test the constancy of μ_o and μ_1.

Defining the coalescence frequency, w, as the number of volumes of dispersed phase that undergo mixing in unit time,

$$w = w_o N.$$

Hence, Equation (3.2.7) may be written as

$$\mu_2 = 2\mu_1^2 + (\text{constant}).\ \exp\left(-\frac{w}{3} t\right) \qquad (3.2.8)$$

Alternatively, the steady state solution of the continuous flow equation may be shown to be,

$$w = \frac{3\tilde{\mu}_1}{\phi\theta} \cdot \frac{(\mu_{2f} - \tilde{\mu}_2)}{(2\tilde{\mu}_{m+1}^2 - \tilde{\mu}_m\tilde{\mu}_{m+2})} \qquad (3.2.9)$$

where μ_{2f} is the second moment of the feed droplet size distribution.

3.2.2 Experimental Work and Results:

Transient state DSDs in n-alkane - water system in a vessel fitted with a Waldhof-agitator were measured using the

detergent stabilization method. Samples were drawn from the region of intense mixing at various times from the start of the agitation. Care was taken so as not to change the system volume appreciably due to repeated sampling. In case large number of samples were desired, the experiment was repeated under exactly similar conditions. Since it requires the calculation of second moments of drop-volume distributions, the experiments were carried out under carefully controlled conditions and with high precision. In spite of all the care, some samples had still to be discarded because some coalescence took place before the dispersion could be mixed well with the detergent. Experiments were performed for various levels of speed of rotation and dispersed phase fraction. The various DSDs measured are tabulated in Appendix D.

In Table III-2.1 are listed the first moments of DSDs for some experimental conditions. After an initial breakdown of drops for about 9-12 minutes, the first moment becomes almost steady (as predicted by Equation 3.2.4) with a fluctuation of $\pm$ 30% from the mean. It is within the limits of reproducibility of our experiments which is obvious if we recall that the Sauter-mean diameter in our replicated experiments fluctuates within $\pm$10.0%.

Moments of the unsteady state DSDs were calculated and $(\mu_2 - 2\mu_1^2)$ were plotted vs time on semi-log plots. Figures 3.2.1 show the plots for various experimental conditions. From

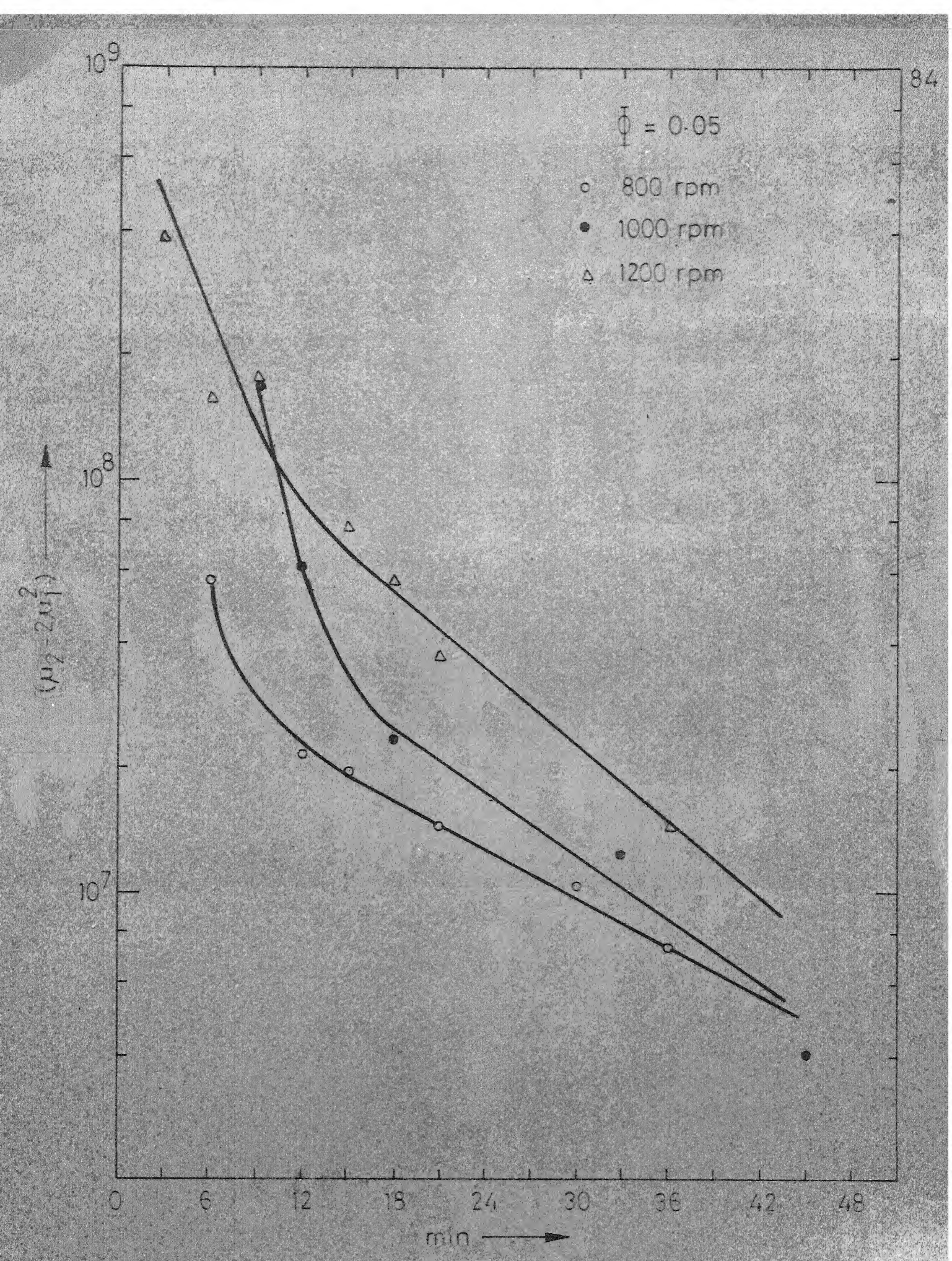

g 3.2.1a - Variation of the moments of transient state DSDs with time.

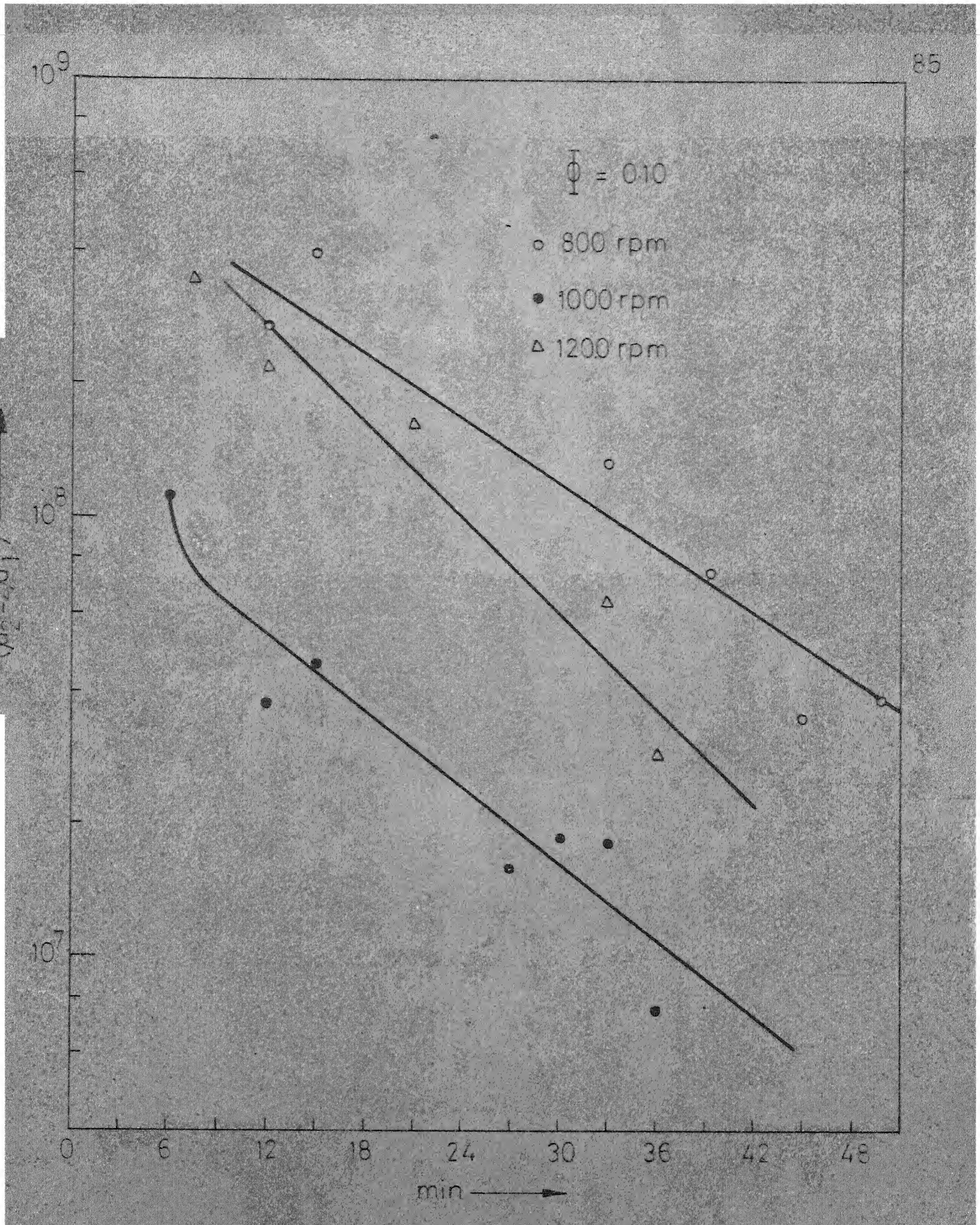
10^9
10^8
10^7
$(\mu_2^2 - 2\mu_1^2)$
Φ = 0.10
800 rpm
1000 rpm
1200 rpm
0
6
12
18
24
30
36
42
48
min

Fig. 3.2.1b.

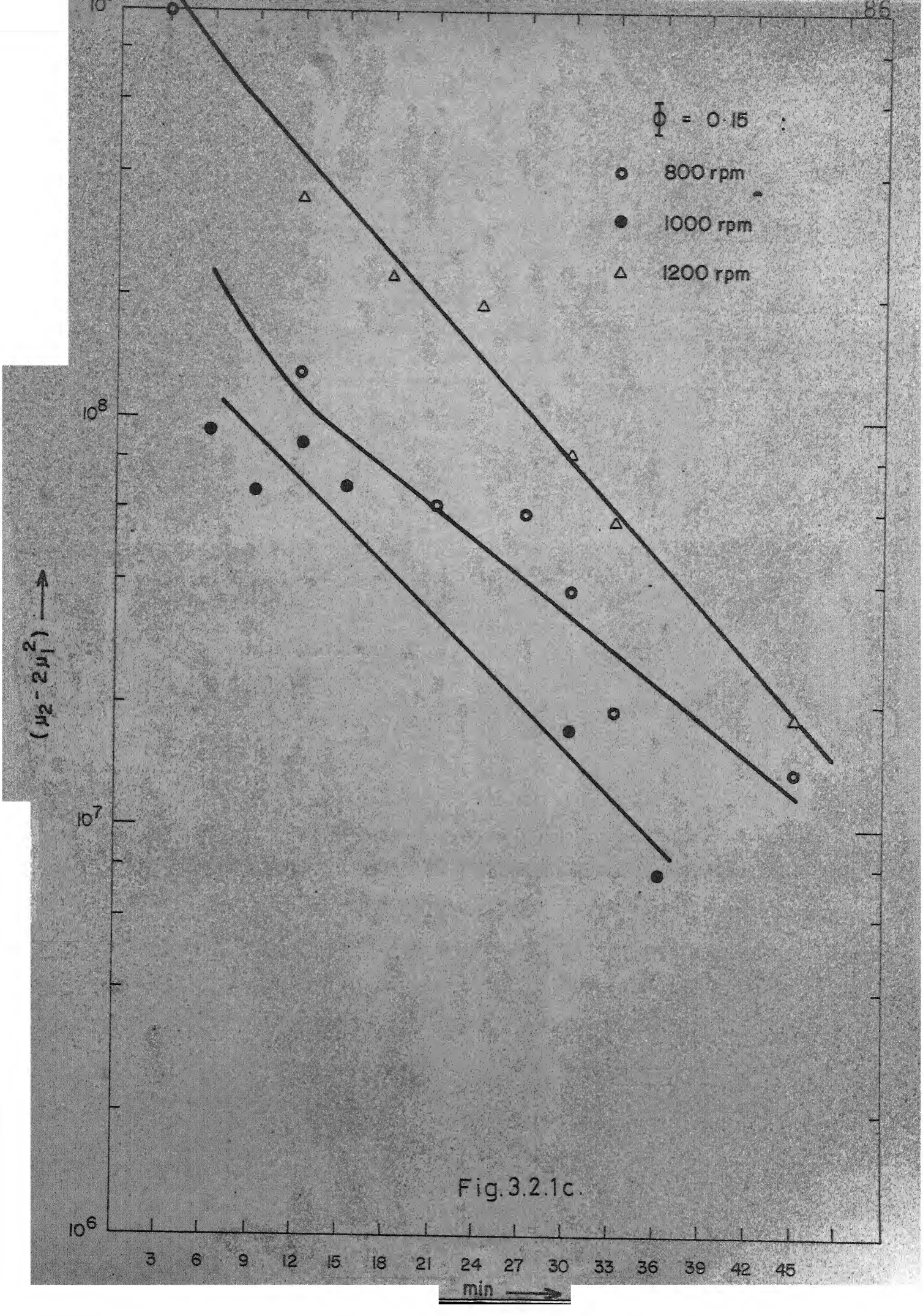
Φ = 0·15 :
800 rpm
1000 rpm
1200 rpm
10^8
10^7
10^6
$(\mu_2 - 2\mu_1^2)$ ⟶
3 6 9 12 15 18 21 24 27 30 33 36 39 42 45
min ⟶

Fig. 3.2.1c.

TABLE III-2.1: FIRST MOMENTS OF DROP-VOLUME DISTRIBUTIONS FROM SOME EXPERIMENTAL RUNS

time (min.)	First moment (micron^3)		
	15% n-P 800 rpm	15% n-P 1200 rpm	5% n-P 1200 rpm
3	13206	9102	8205
6	8458	6108	5312
9	5436	2791	-
12	4324	-	2469
15	2603	1150	-
18	1986	-	2627
21	-	1474	2060
24	1671	-	-
27	2253	2005	2080
30	2374	-	1354
33	1648	1670	-

the slopes of these straight lines, values of coalescence frequencies (defined as number of dispersed phase volumes that undergo mixing in unit time) were calculated using Equation (3.2.8). The results have been plotted in Figures 3.2.2 and 3.2.3. Figure 3.2.2 shows that a linear relation exists between w and the speed of rotation at constant ϕ. Similarly, Figure 3.2.3 indicates a linear dependence of w upon ϕ.

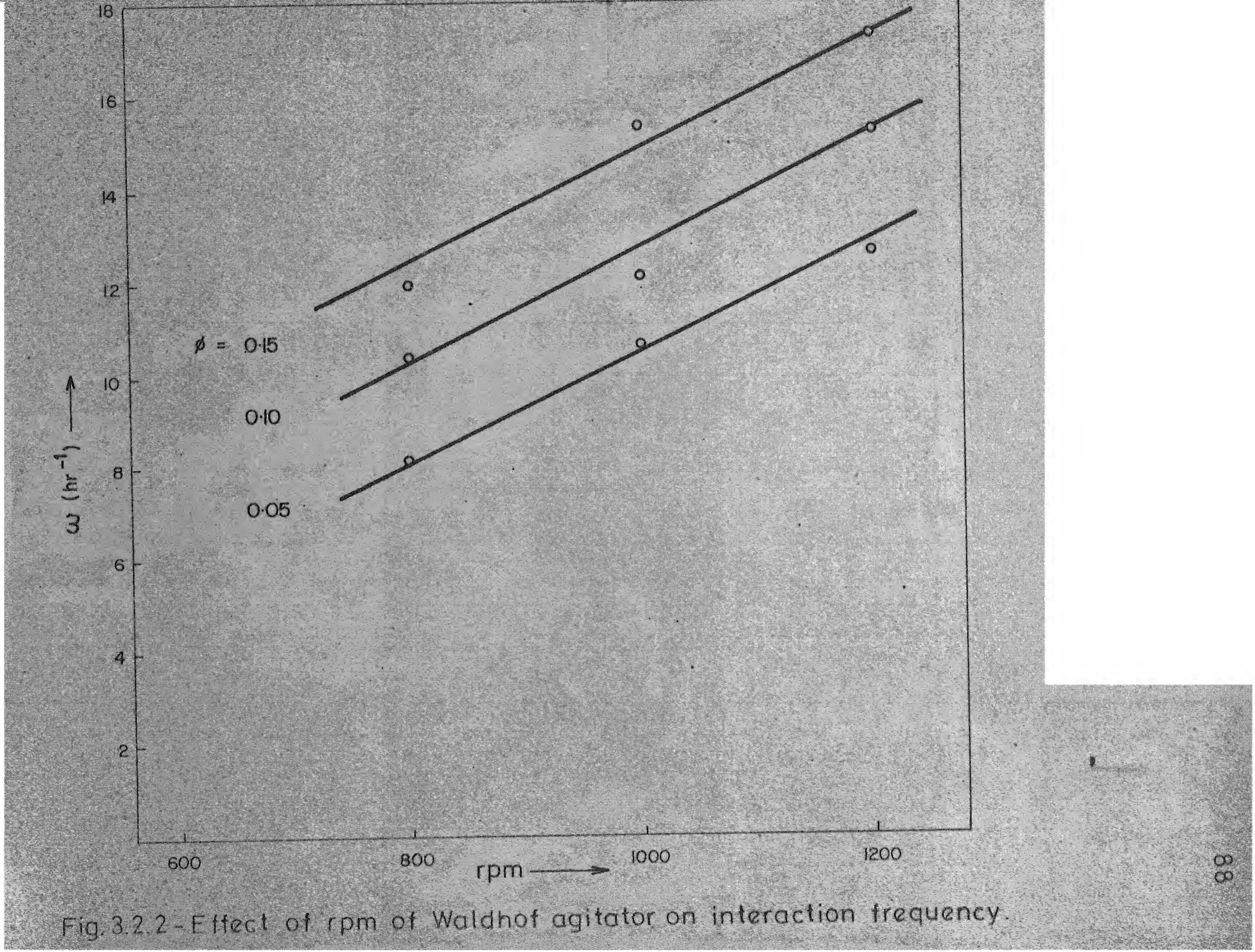

Fig. 3.2.2 - Effect of rpm of Waldhof agitator on interaction frequency.

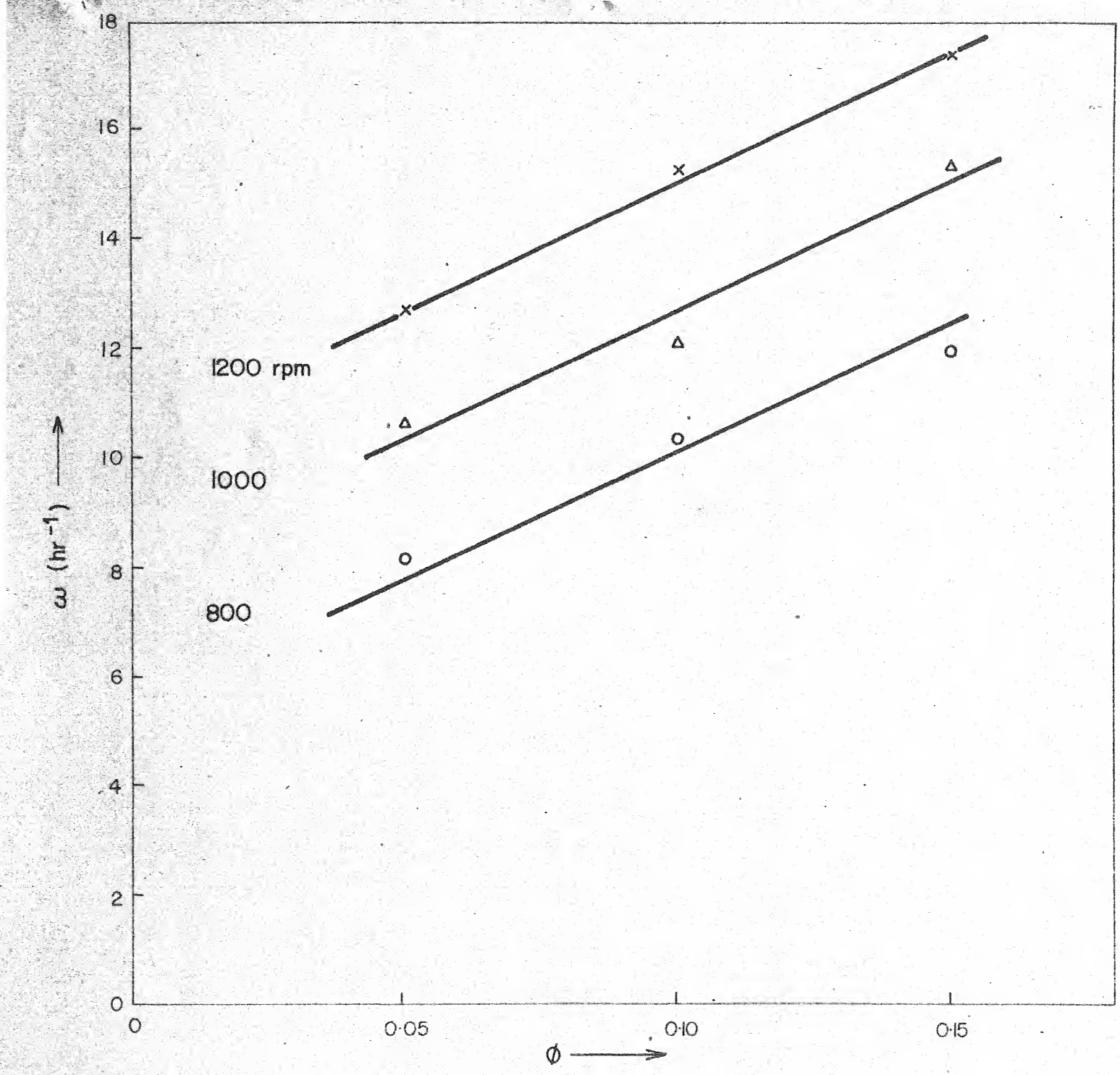

Fig. 3.2.3 - Effect of dispersed phase fraction on interaction frequency.

3.2.3 Discussion:

In the present investigation, coalescence frequency has been measured in n-alkane - water systems mixed by a Waldhof - agitator. Most of the previous work in the measurement of coalescence frequencies in dispersed systems has been carried out in those agitated by flat-blade turbines (FBT). This has been summarized in a review article by Shah et al.(1972 b). These two systems have widely different characteristics. The dispersions mixed by Waldhof-agitators are characterized by marked zones of high turbulence and of circulation, and are therefore referred to as circulation-stirring systems (CS). The qualitative observation for FBT systems that w increases with mixing velocity and with dispersed phase ratio, holds true in CS systems also. Based upon the reported data, it can be concluded that for FBT systems, coalescence frequency is proportional to the powers of N ranging from 1.5 to 3.3, and of $\emptyset$ ranging from 0.5 to 1.1. But as is clear from Figure 3.2.2, w in CS systems varies linearly with N. This could be because in CS systems a significant fraction of energy supplied is utilized in creation of circulation currents. It has already been reported in Chapter II, section 2.2 that in such systems the Sauter-mean diameter is inversely proportional to the 0.1 - 0.3 power of the Weber number as against a 0.6 power for FBT systems. Thus a rather weak dependence of coalescence frequency upon the speed of rotation is in accordance with other observations on CS systems.

However, a careful study of the energy distribution for the creation of turbulence, interfacial area, circulation currents, and air-bubbles is desired before any generalization can be drawn.

In the present investigation, experiments have been performed in batch agitated vessels and, therefore, only constant coalescence frequency could be calculated. But the assumption of the constant coalescence frequency could be done away with if the experiments were carried out in continuous flow stirred tank vessels (CFSTV). In that case it will be necessary to feed the CFSTV with finely dispersed dispersion and Equation (3.2.9) can be used to calculate the interaction frequency provided the input and output DSDs are known.

* * *

CHAPTER IV

SIMULATION OF HYDROCARBON FERMENTATION

In the present chapter, an attempt has been made to predict the performance of hydrocarbon fermentors using a Monte-Carlo simulation method developed by Shah (1974). Both the gas-oil and the n-alkane fermentations have been studied. The drop-phenomena have been modelled by the coalescence - redispersion mechanism described in Chapter III. Significance of dispersed phase mixing and the importance of the nature of drop-interactions has been demonstrated. The contribution of growth in the continuous-phase towards overall growth is also investigated.

4.1 Introduction:

A number of attempts have been reported in literature to represent substrate-limited growth in hydrocarbon fermentors by mathematical models. These models involve various assumptions regarding drop-size distributions and their interactions. Erickson and coworkers (1969a,b,c) proposed models for growth on a single droplet. Extensions to real case fermentations were made assuming complete mixing. These models, however, present an over-simplified picture of the actual phenomena and were found inadequate to predict the effects of inoculum size and dispersed phase fraction as observed experimentally

for gas-oil fermentations (Prokop et al., 1971). The model for gas-oil fermentation was modified by Erickson et al. (1970) who took into account the presence of drop-size distribution (DSD) and the dynamics of adsorption and desorption of cells between the interface and the continuous phase. Dispersed phase mixing due to drop interactions was accounted for by a mass transfer coefficient term. The interactions proposed were of such a nature so as to preserve the initial drop-size distribution which was taken to be the same as that experimentally observed in pure chemical systems having lean dispersions (Chen and Middleman, 1967). The model is applicable only to those systems for which the dispersed phase consists of hydrocarbons dissolved in an inert medium. Since it lacks the capability to predict the evolution of the drop-size distribution, the predicted growth performance is strongly influenced by the initial DSD. Moreover, the interactions assumed are not realistic.

More recently, Stamatoudis and Tavlarides (1973) have simulated the drop-phenomena in hydrocarbon fermentors using a Monte-Carlo method developed by Zeitlin and Tavlarides (1972). The biomass growth model is the same as that used by Erickson et al. (1970) with a slight modification to account for reduction in contact surface area between cell and hydrocarbon drop due to rigidity of cell surface. Different breakage and coalescence frequencies have been considered in

different parts of the fermentor. The growth patterns for the extreme cases of complete mixing and complete segregation of dispersed phase drops have been worked out. However, the calculations of growth for intermediate cases of mixing between drops could not be carried out due to the excessive computation times involved.

In the present investigation, substrate-limited growth on gas-oil and on n-alkanes has been considered. That is, the oxygen concentration in the vessel is maintained above a critical level throughout. It is assumed that the presence of air bubbles does not in any way affect the drop-phenomena and the growth. Growth of biomass takes place both in the continuous phase as well as on the interface between the hydrocarbon and aqueous media. Monod's model has been used for representing growth in the various phases. In the continuous phase (i.e. aqueous phase), the specific growth rate of the biomass is given by,

$$\mu_c = \mu_{max} \frac{S'}{k_{s'} + S'} \qquad (4.1.1)$$

where μ_{max} is the maximum specific growth rate of the microorganism on the given substrate; $k_{s'}$ is the Michaelis-Menten type of constant (or saturation constant), and S' is the dissolved hydrocarbon concentration in the aqueous phase.

The specific growth rate of the cell on n-alkane droplets is assumed to be,

$$\mu_d = \mu_{max} \qquad (4.1.2)$$

For gas-oil fermentation, the specific growth rate of

cells on the interface is assumed to be,

$$\mu_d = \mu_{max} \frac{S}{k_s + S} \qquad (4.1.3)$$

where S is the concentration of the consumable substrate in the dispersed phase drops, and k_s is the saturation constant.

In n-alkane fermentation, the dispersed phase itself is the consumable substrate. Hence, the dispersed phase fraction changes considerably during the course of fermentation which may be carried out until all the dispersed phase is consumed. On the other hand, only a small fraction of gas-oil constitutes the consumable substrate. Therefore, changes of dispersed phase fraction in gas-oil fermentation are rather small and can be ignored if the concentration of the consumable substrate in gas-oil is not very high (Erickson et al., 1969a). It has been assumed in this investigation that the volume of a gas-oil drop does not change because of substrate consumption.

The exchange of biomass between the continuous phase and the interface is assumed to be controlled by Langmuir's adsorption/ desorption dynamics. Thus, the biomass growth model is the same as that used by Humphrey and Erickson (1972).

The details of the growth equations and the methodology of simulation are given in Appendices E and F, respectively.

4.2 Simulation of Drop-Phenomena Without Growth:

The drop phenomena were represented by the coalescence-redispersion model proposed in Chapter III. Any two drops can

coalesce with equal probability and the coalesced drop redisperses immediately into two drops of arbitrary sizes. Computer simulation experiments were conducted for different initial drop size distributions (Exponential, Uniform, and Dirac-delta) and for different values of the coalescence-redispersion frequency (CRF). The results have been plotted in Figures 4.2.1 - 4.2.4 and compared with the analytical solutions of 'population balance equations' (Equation 3.1.13) which have also been presented in these figures.

Figure 4.2.1 shows the results for exponential initial distribution. Cumulative size distributions at zero and at one hour of simulation have been plotted. A continuous line shows the analytical solution of the population balance equation at equilibrium. In the computer simulation experiment, the distribution of drop sizes does not change with time because the analytical solution itself is an exponential distribution. Results of uniform initial distribution have been presented in Figure 4.2.2. The distribution changes to the exponential form (the analytical solution) with the lapse of time. Similarly, also for a Dirac-delta initial distribution, the final distribution becomes exponential (Figures 4.2.3 and 4.2.4).

In all the cases, an equilibrium of drop sizes is achieved within one hour of the start of the simulation experiment. The actual time for achieving the equilibrium DSD, of course, depends upon the value of the CRF employed for the

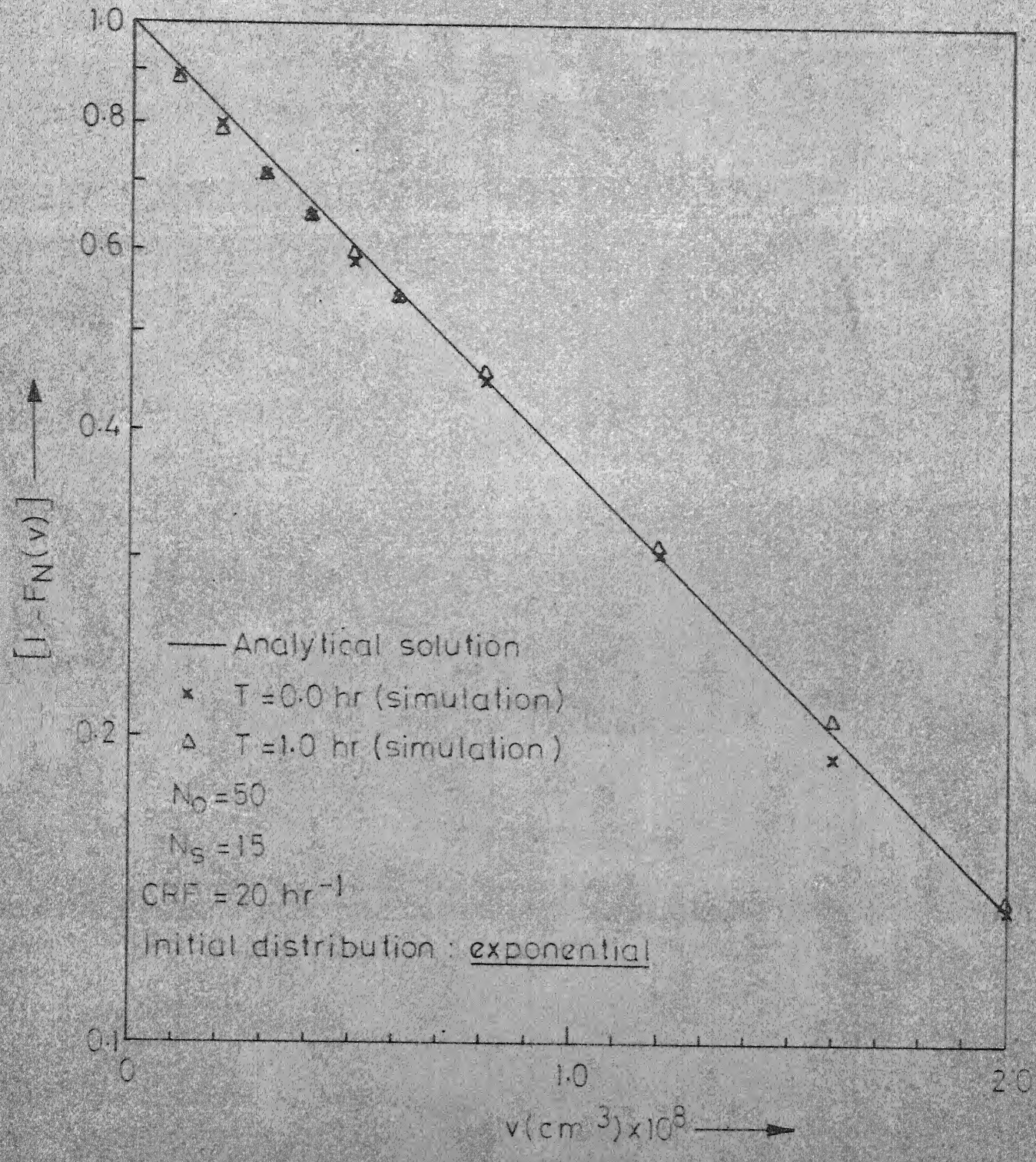

Fig 4.2.1-Cumulative DSDs obtained by computer simulation without growth

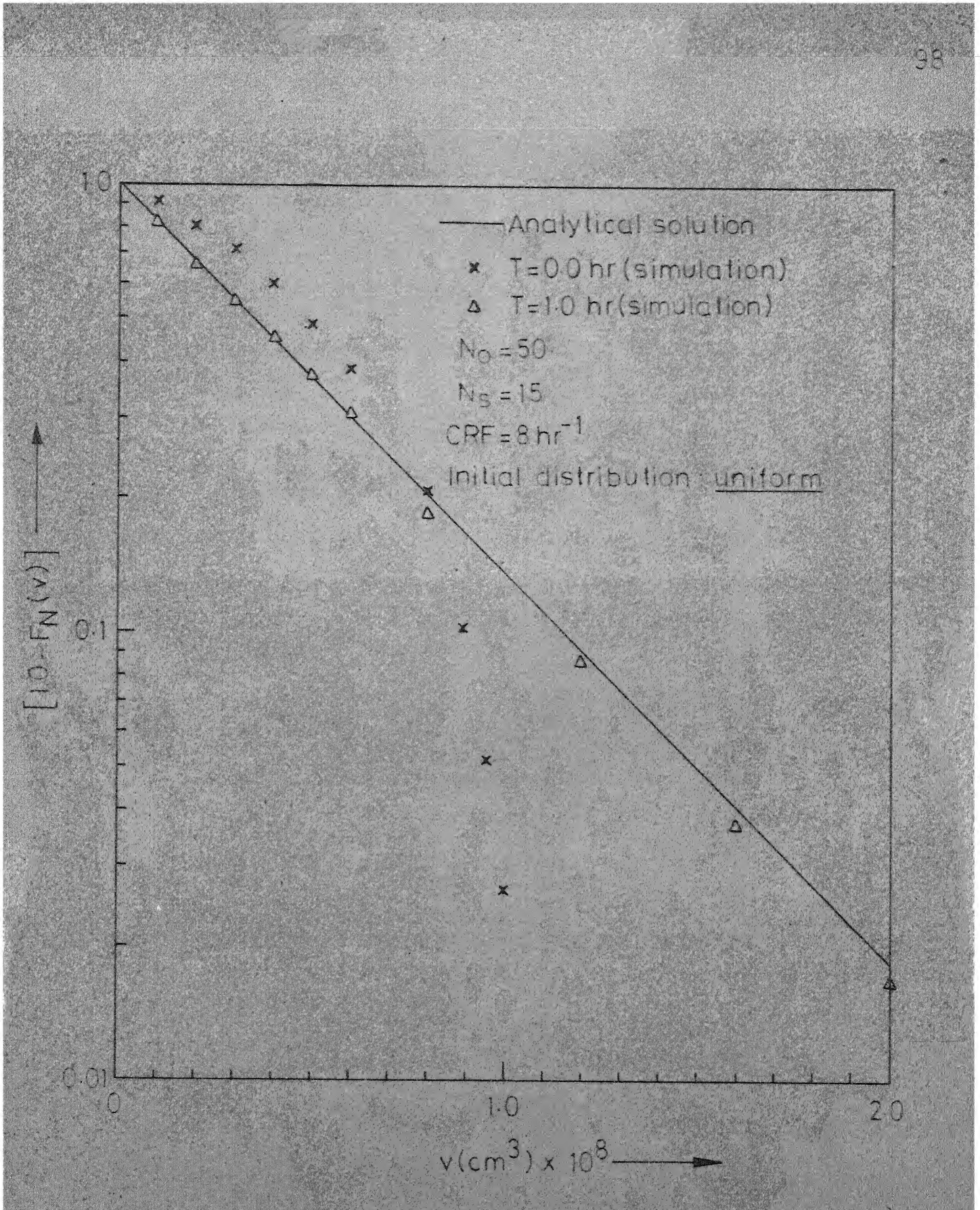

Fig. 4.2.2 - Cumulative DSDs obtained by computer simulation without growth.

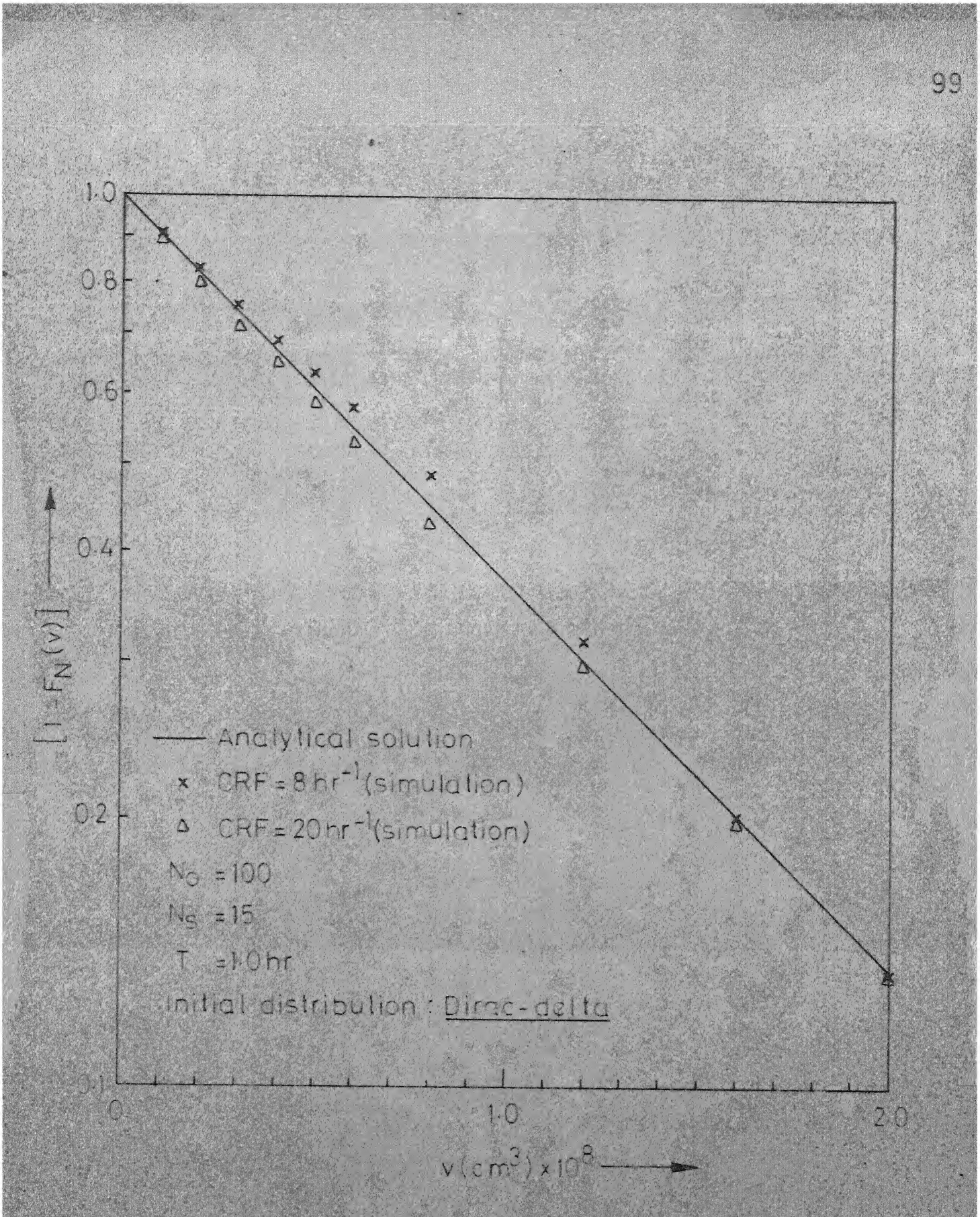

Fig. 4.2.3 - Cumulative DSDs obtained by computer simulation without growth

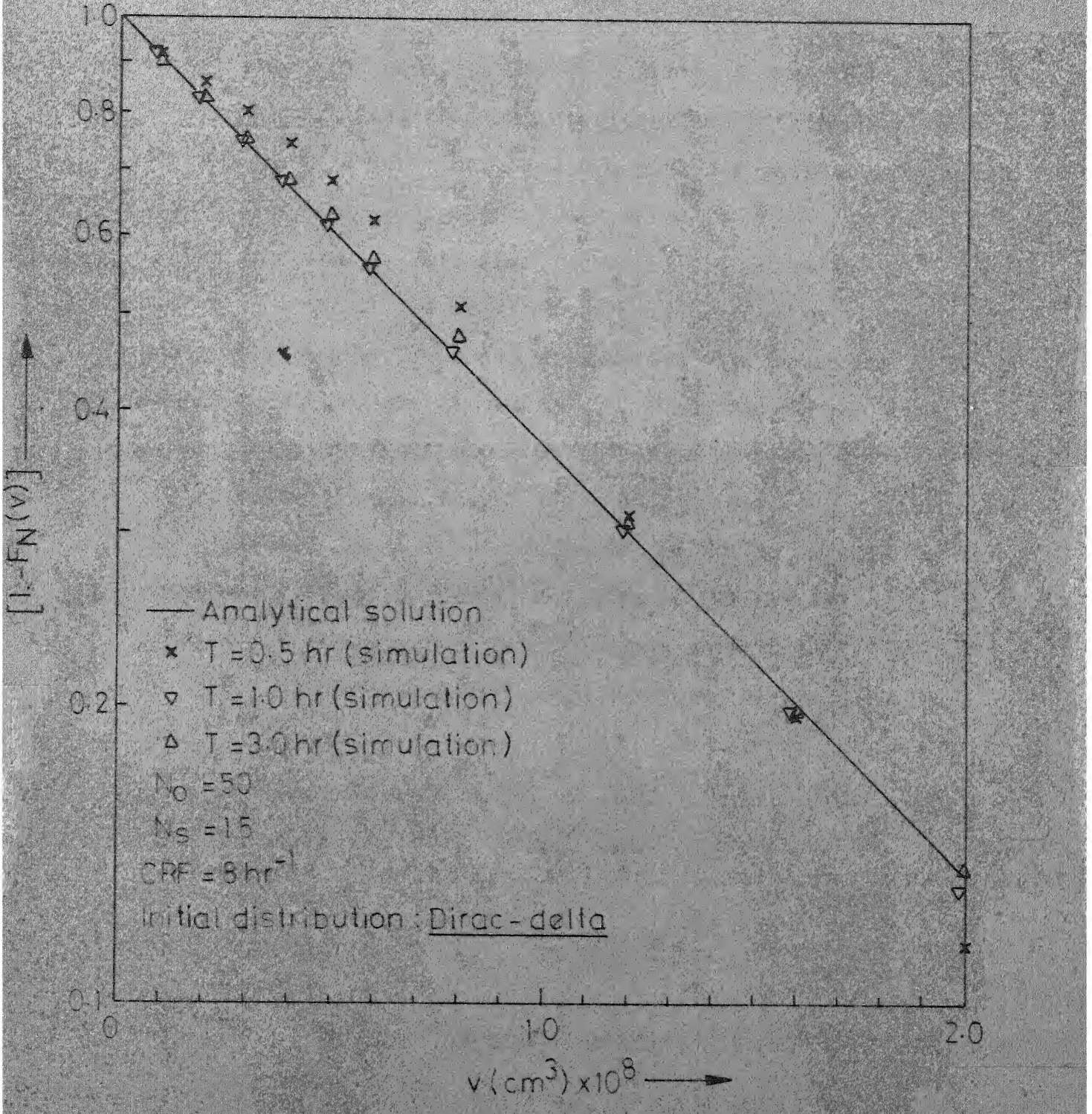

Fig. 4. 2. 4 - Cumulative DSDs obtained by computer simulation without growth.

experiment. For example, for an experiment with CRF = 20 hr^{-1}, an exponential distribution is established within 30 minutes whereas about double the time is needed for another experiment with CRF = 8 hr^{-1} (Figure 4.2.4).

In order to determine the size of the system and the number of simulations required to produce results within acceptable bounds, computer experiments were performed with the number of drops equal to 10, 20, 50, and 100. For all the experiments, 95% confidence bands became narrower as the number of drops was increased, and also when the number of simulations was increased for a fixed number of drops. As an illustration, reference is made to Table IV-2.1 where percent deviations at $F_N(v) = 0.5$ are recorded for different conditions of the number of drops and the number of simulations for Dirac-delta initial DSD.

TABLE IV-2.1A: VARIATION OF PER CENT DEVIATION WITH N_o AND N_s

Number of drops, N_o	Percent deviation at $F_N(v)=0.5$ for $N_s = 15$
10	±11.0
20	± 7.0
50	± 4.0
100	± 2.4

TABLE IV-2.1B: VARIATION OF PER CENT DEVIATION WITH N_o AND N_s

Number of simulations N_s	Per cent deivation at $F_N(v)=0.5$ for N_o = 20
5	± 17.0
10	± 8.0
15	± 7.0
20	± 4.0

The computer time, on the other hand, increased almost linearly with the number of simulations and exponentially with the number of drops. Later, while simulating drop-phenomena with growth, it was observed that the deviations for biomass concentration were affected also by the nature of initial drop-size distribution. For example, for the case of Dirac-delta initial DSD, these deviations were within ± 1.0 per cent when N_o and N_s were 10 and 15 respectively, whereas for the other two initial DSDs double the number of drops were necessary. For N_o=10 and N_s=15, simulation of drop-phenomena with growth required one minute of computer (IBM 7044/1401) time for one hour of simulated fermentation. For all the subsequent simulations, N_s was kept at 15 and N_o was either 10 or 20 depending upon initial DSD.

4.3 Simulation of Drop-Phenomena with Growth:

Here the properties of the particles change continuously during each IQ and this change is governed by the growth equations

given in Appendix E, as against simulation without growth where properties of the particles do not change except when a random event occurs.

During each IQ, these equations were solved simultaneously using Euler's method which was found to be as efficient as a Hammings Runge-Kutta predictor-corrector method because in general, the IQ is very small. However, the solution of equations for substrate concentration in the continuous phase (Equation E.14 and E.23) required an extremely small step-size. For instance, for a step size as small as 10^{-5} hr., the solution resulted in negative substrate concentrations in the continuous phase. Later, an analytical solution of Equation E.14 considering all the other variables constant for a very small time interval revealed that the substrate concentration approaches a steady state value very fast, this interval depending upon the value of constant a_5. (For real case fermentations, a_5 is of the order of 10^7.) The above problem can be tackled either by using a smaller value of this parameter (Erickson et al., 1970) or by assuming a quasi-steady state for the continuous-phase substrate-concentration. (Algebraic equations E.16 and E.25 to be used instead of differential equations E.14 and E.23, respectively). Using a smaller value of this parameter is equivalent to increased solubility of hydrocarbons in the continuous phase and results in more overall growth rate than can be expected in actual fermentations. (Growth

from 1g/l to 14 g/l in 10 hours for $a_5 = 10^3$ as compared to 1 g/l to 10 g/l when $a_5 = 10^7$.)

4.3.1. Effect of Segregations in Dispersed Phase:

As has been pointed out by Humphrey and Erickson (1972), two types of segregations are possible. There could be substrate concentration differences among drops (possible only with gas-oil drops) and cell population differences from drop to drop. Differences in substrate concentration arise due to different rates of mass transfer from interfaces of drops of various sizes and due to different rates of substrate consumption from these drops. Substrate concentration differences between drops, in turn, cause differences in biomass growth rates on the surface of drops, leading to cell population differences. The phenomena of coalescence and redispersion of drops, and the adsorption/desorption of microbial cells at the interface tend to reduce the degree of segregation.

In order to study the effect of dispersed phase segregations, growth performances of gas-oil and n-alkane fermentations were simulated for the extreme cases of complete mixing and complete segregation between drops. These have been presented in Figures 4.3.1 - 4.3.4 for two different initial drop-size distributions (uniform and exponential). In any particular figure, growth performances for the extreme cases are significantly different from each other. For example, for the case

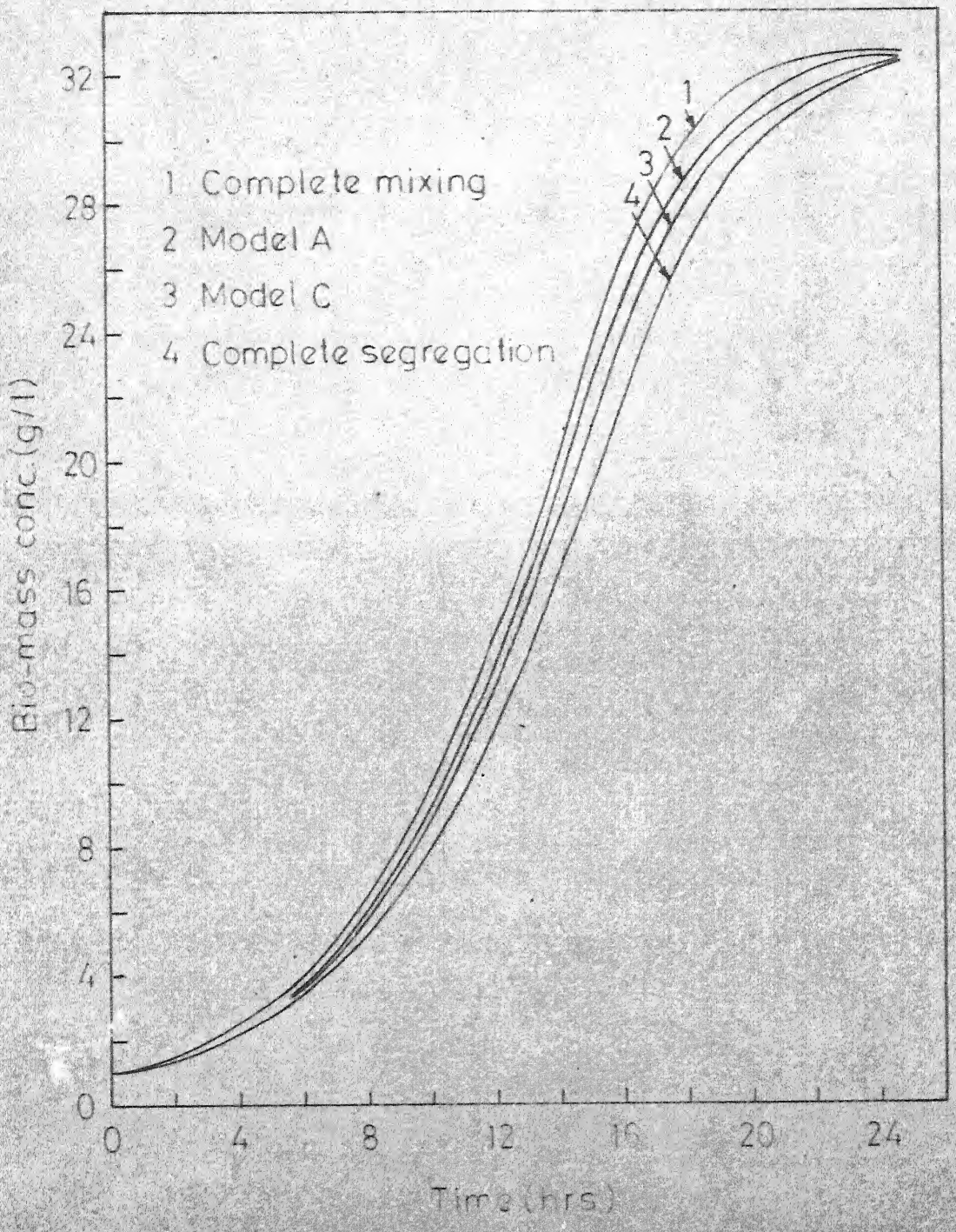

Fig. 4.3.1 - n-Alkane fermentation, uniform initial DSD.

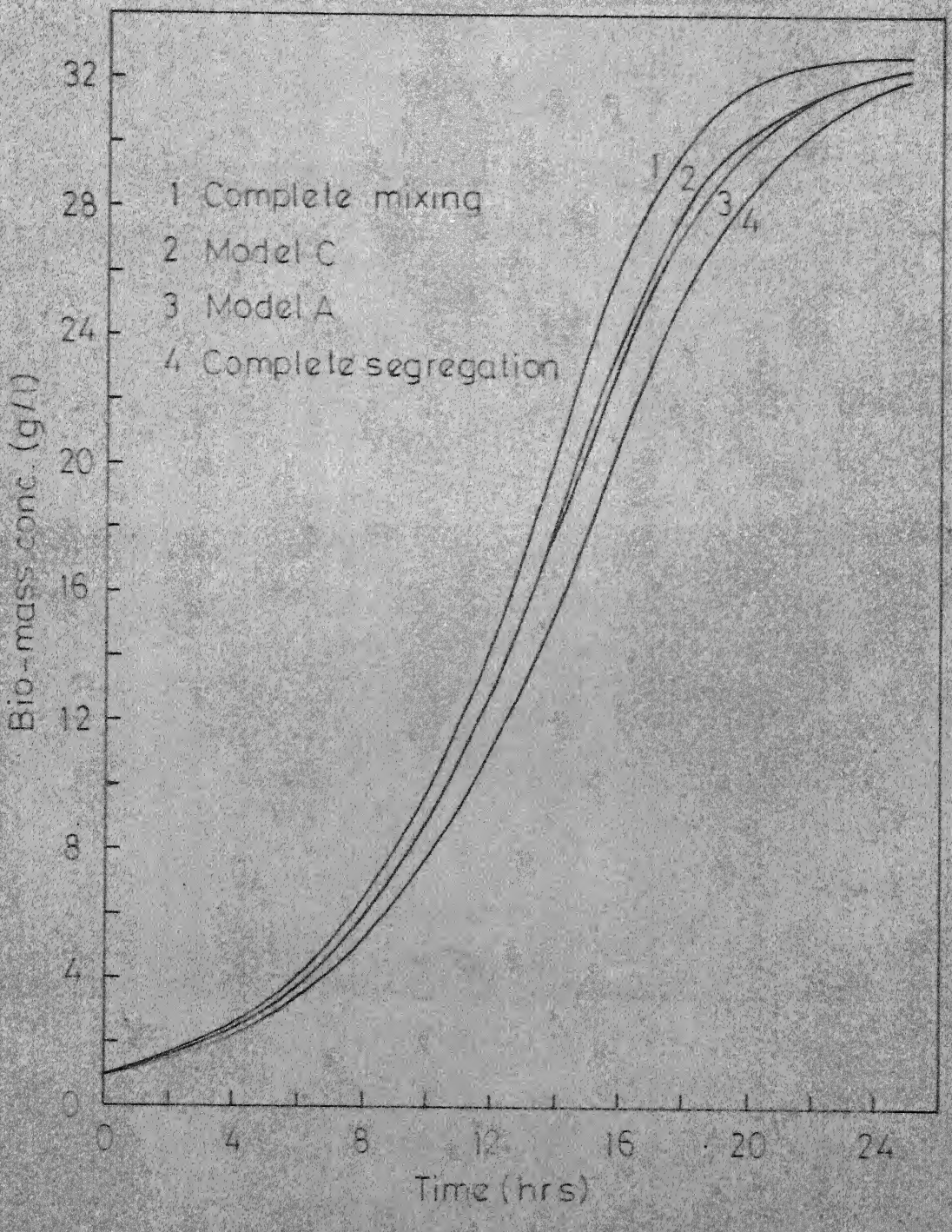

Fig. 4.3.2 - n - Alkane fermentation, experimental initial DSD

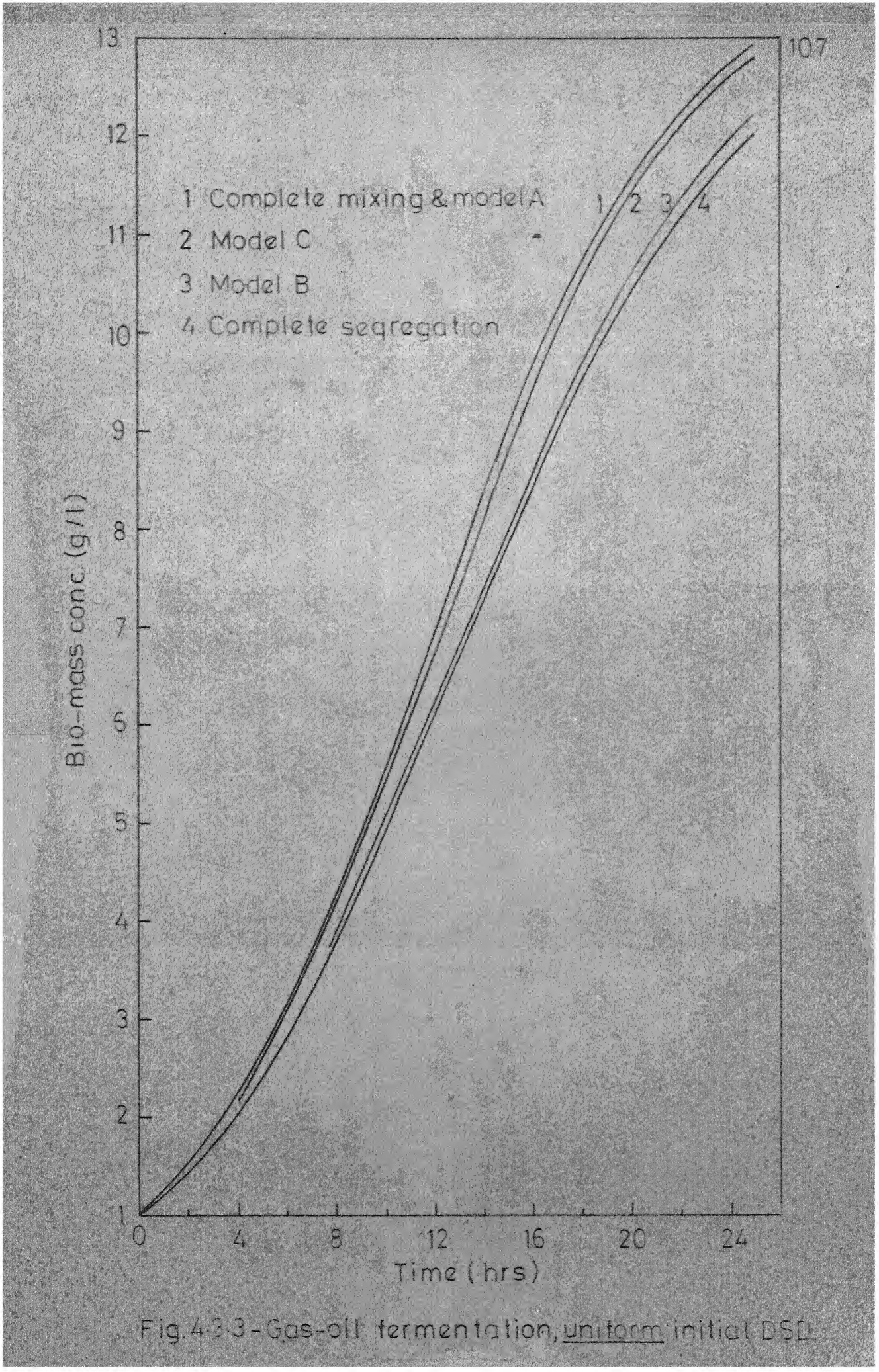

Fig. 4·3·3 - Gas-oil fermentation, uniform initial DSD

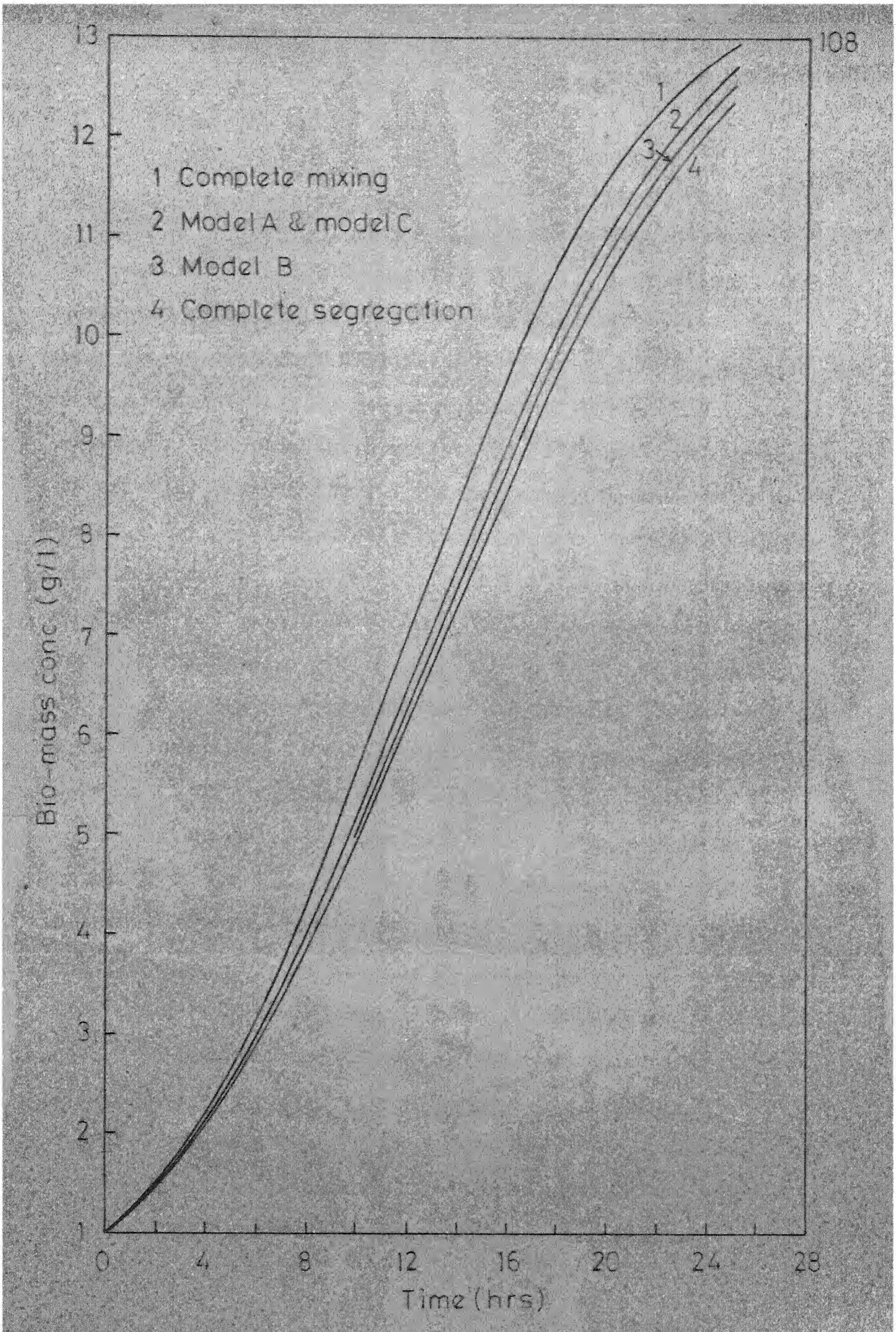

Fig. 4.3.4 - Gas-oil fermentation, exponential initial DSD.

of uniform initial DSD in gas-oil fermentation, as much as 97.5 per cent fermentation is completed for complete mixing between dispersed phase drops, while for the case of complete segregation only 90 per cent fermentation is over in 24 hours. In terms of fermentation time required to convert 95 per cent consumable substrate into biomass, a difference of as much as 7 hrs. can be expected between the two cases. Also, these extreme cases envelop the growth curves for intermediate degrees of mixing discussed below. This establishes that the drop-interactions are important and cannot as such be neglected while attempting to predict the biomass growth performance in these fermentors.

In order to determine the significance of the nature of drop-interactions, the following three types of coalescence-redispersion (C-R) processes have been considered:

A. Any two drops can coalesce and the coalesced drop breaks into two drops of the same sizes as those coalesced. The C-R event results in homogenization of substrate concentration and the biomass concentration on the interface of the drops. This model of drop-interactions can be considered as a modification of Curl's model (1963) and in fact reduces to the original model of Curl for the case of Dirac-delta initial DSD. Since the drop-phenomena do not result in creation of new drops, drop-interactions can be realized in the simulation algorithm discussed in Appendix F, by simply generating the representative sequence $T_1, u_1; T_2, u_2; T_3, u_3; \ldots$.

B. The breakage of the coalesced drop is similar to that in A but the C-R event does not affect the individual biomass concentrations on the interface. The substrate mixing is represented by a mass-transfer coefficient term as proposed by Erickson et al.(1970). However, this model of interactions is applicable only to gas-oil fermentation. For n-alkane fermentation, this model is equivalent to the case of complete segregation of hydrocarbon droplets. Realization of this model of interactions can be carried out easily by addition of a term

$$\left[\sum_{j=1}^{N_o} k_c \frac{v_j}{V_d} (S_j - S_i) \right]$$

in Equation E.17 (Appendix E).

C. Two drops coalesce and the coalesced drop breaks into two drops of arbitrary sizes. The C-R event results in uniform biomass and substrate concentrations in the two drops (same as that in A). This model of interactions has been discussed in detail in Chapter III.

These models differ from each other in the nature of the drop-phenomena and the results of the interaction. A schematic representation of the three models is as follows:

Model A :

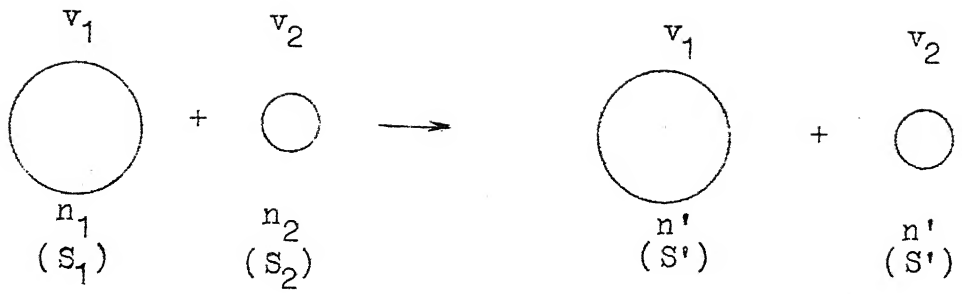

$$n' = \frac{n_1 A_1 + n_2 A_2}{A_1 + A_2}$$

$$S' = \frac{S_1 v_1 + S_2 v_2}{v_1 + v_2}$$

Model B :

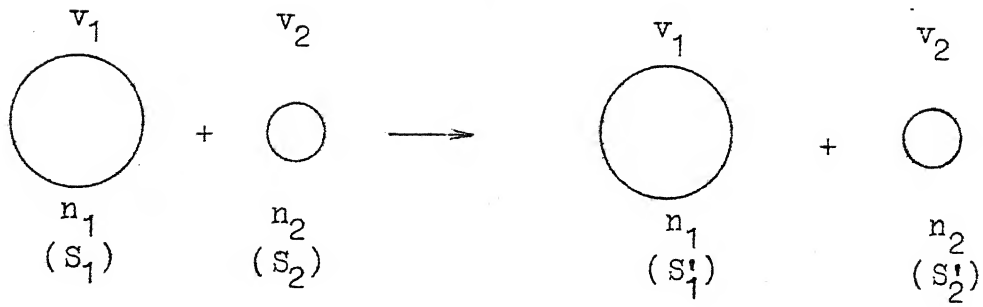

Model C :

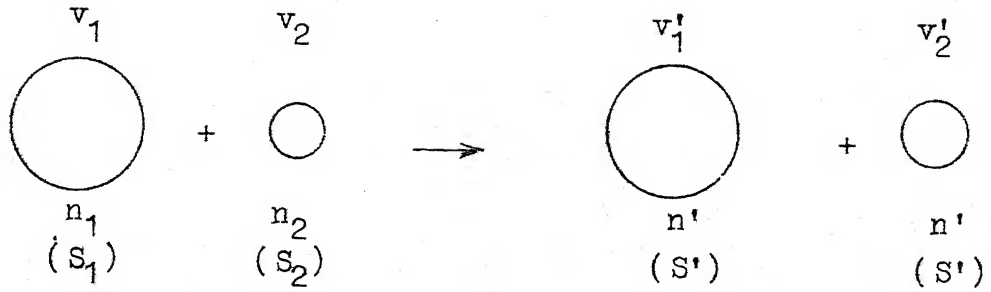

$$v_1' + v_2' = v_1 + v_2$$

$$n' = \frac{n_1 A_1 + n_2 A_2}{A_1' + A_2'}$$

$$S' = \frac{S_1 v_1 + S_2 v_2}{v_1' + v_2'}$$

Computer simulation experiments were carried out for both the gas-oil and the n-alkane fermentations. The value of the coalescence-redispersion frequency (CRF) was chosen to be 10-20 $hr.^{-1}$. (of the same order of magnitude as that experimentally observed in n-alkane -water-Waldhof-agitator systems. Reference: Chapter III). These results have also been presented in Figures 4.3.1 - 4.3.4.

Choice of initial DSD is crucial for models A and B as this strongly influences the predicted growth performance. This is not the case with model C where an equilibrium DSD sets-in in the early phases of growth during which the growth is small. It is only obvious to expect the final growth in actual fermentations to be unaffected by the initial distribution of drop-sizes, since the growth takes place over a period of time incomparably larger than that required to establish equilibrium DSD. When equilibrium DSD (i.e. exponential distribution) is used as initial DSD for model A and Model B, all the models assume the same dynamic equilibrium DSD during gas-oil fermentation because the sizes of the gas-oil drops have been considered not to change

due to substrate consumption. Therefore, any difference in the predicted growth performance of gas-oil fermentors will be a result of different degrees of substrate and biomass segregations in case of various interaction models. Interactions proposed in model B do not cause mixing of biomass on the interfaces of the interacting drops and a high degree of biomass segregation is expected. Substrate concentration in drops at different times of growth shows the same trend and, this is why, the predicted growth curve for the model B lies nearer to that for the case of complete segregation between drops (Figure 4.3.4).

Model B represents an attempt to take into account the effect of dispersed phase mixing by incorporating an additional term in the growth equations and, thus, making the problem amenable to relatively simple numerical solution. Model A and Model C are more realistic realizations of inter-droplet mixing and the drop-phenomena, but cannot be easily subjected to numerical solutions. The difference between models A and C lies in the redispersion mechanism of coalesced droplets. Thus model C has the merit of being able to predict drop-size distributions, whereas model A preserves arbitrary drop-size distributions. The differences between predictions of transport and kinetic phenomena in dispersions based on models A and C would therefore be expected to be due to (i) the role played by the initial size distribution and the transient period of evolution to the equilibrium drop-size

distribution and (ii) the role of the redispersion mechanism in distributing the various component species among the droplets. The first factor becomes unimportant in dealing with processes such as fermentation which are indeed slow in relation to the time scale during which equilibrium drop-size distributions are attained. The redispersion mechanism is therefore the only factor contributing to any differences in fermentation rates predicted by models A and C.

The present simulations indicate little difference between models A and C when the equilibrium drop-size distribution is substituted into model A (Figures 4.3.2 and 4.3.4). Thus the new redispersion mechanism appears to have contributed little to the prediction of fermentation rates in the present context, which could not have been asserted a priori. No difference in fermentation rates can be predicted by the two models unless substantial differences occur in their predictions of the distribution of substrate and biomass concentrations among the drop population; furthermore large differences in fermentation rates are likely to arise if biomass and substrate concentration ranges are such that the growth rate is very sensitive to either one or both of them.

From the preceding discussion, it should be clear that model A cannot always be relied upon to give the right results. Besides, it must be recalled that model C can be used to obtain coalescence frequencies from transient batch or steady state

continuous systems of stirred dispersions. Computer time requirements for model A and Model C are comparable when initial DSDs are same. In a computer simulation experiment, larger number of drops and/or a large number of simulations are required when the starting DSD has also to be randomly generated. From this point of view, model C consumes significantly less computer time as all the simulations may be started with a deterministic DSD without affecting the growth performance. Model C, in this sense, is a significant improvement over model A.

The results presented herein establish the importance of not only drop-interactions, but also the nature of interactions in predicting the performance of these fermentors accurately. Therefore, in further work, model C has been utilized to simulate growth performance in intermediate cases of mixing. The fact that model C and model A with equilibrium DSD predict similar biomass growth performance, makes one aware of a new emphasis in the areas of interest for further research in hydrocarbon fermentation. For improvements in predictions of growth in these fermentors, it will now be desirable to explore the physicochemical and physiological aspects like adsorption and desorption of microbial cells on the hydrocarbon - media interface, and the mode of uptake of hydrocarbons by the microorganisms.

4.3.2 Distribution of Drop-Sizes:

DSDs during the course of computer simulation of gas-oil and n-alkane fermentations were also noted down. Since the sizes of the gas-oil drops have been assumed not to change due to substrate consumption (section 4.1), the distribution of the sizes of the gas-oil drops obtained in computer simulation of drop-phenomena with biomass growth are the same as those obtained without growth. On the other hand, the sizes of the n-alkane drops decrease with time due to consumption of substrate and the DSD becomes finer as the simulation proceeds. However, since the time constant for the process of achieving equilibrium DSD due to drop-phenomena is much smaller (of the order of fraction of an hour) than that for substrate consumption (of the order of hours), DSDs in n-alkane fermentations also show a tendency to preserve shape. It is evident from Figure 4.3.5 where normalized plots of DSDs from a computer simulation experiment of n-alkane fermentation have been presented. It may be noted that the similar tendencies for self preservation of DSD have also been pointed out in section 2.2.1 (Chapter II) for experimentally observed DSDs in gas-oil and n-alkane fermentations.

4.3.3 Effect of Growth in Continuous Phase:

Figures 4.3.6 and 4.3.7 show the effect of mass transfer parameter (a_2) in simulation of n-alkane and gas-oil fermentations, respectively. The value of this parameter, decides the extent of

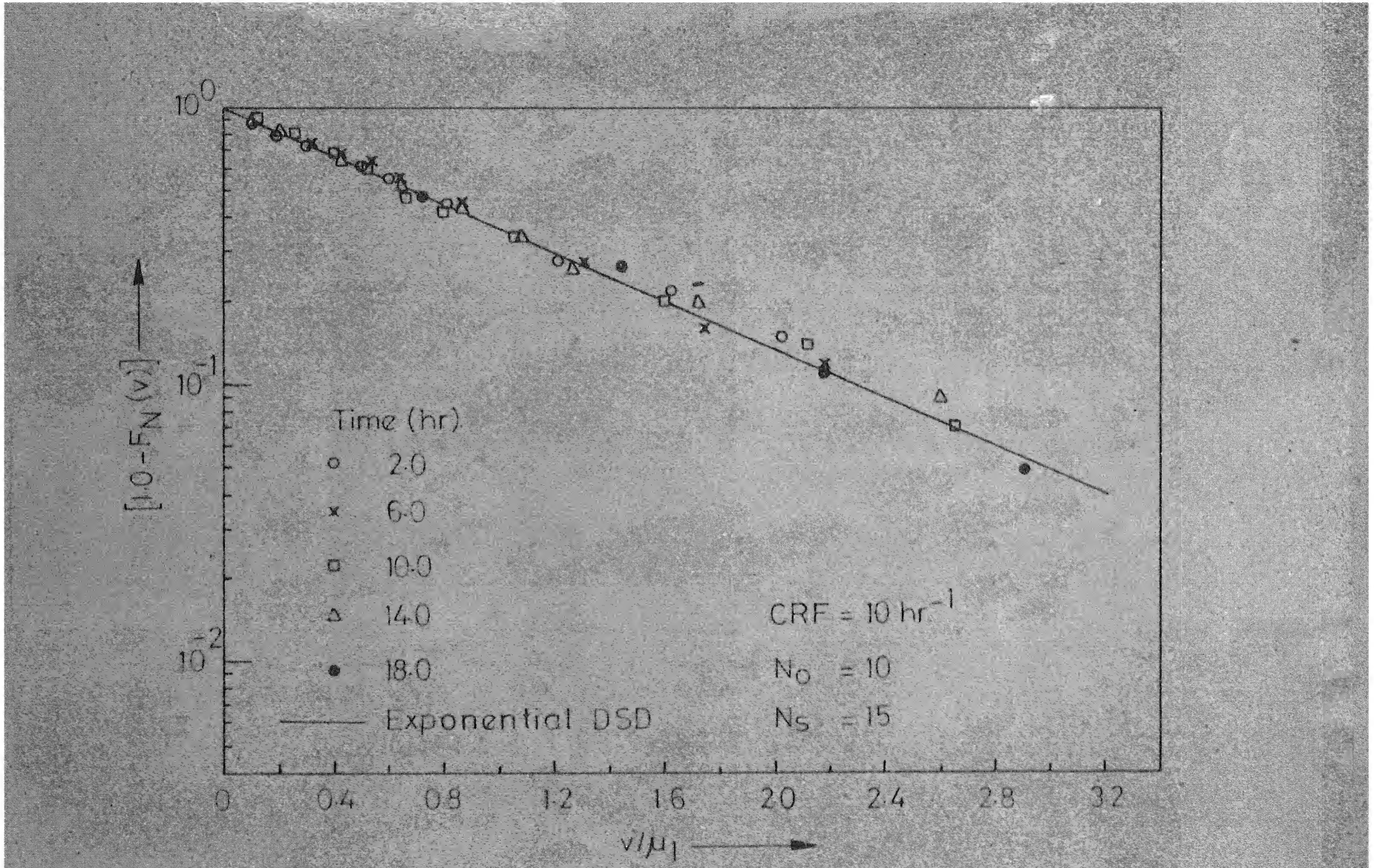

Fig. 4.3.5 - Normalized DSDs obtained in computer simulation of n-alkane fermentation

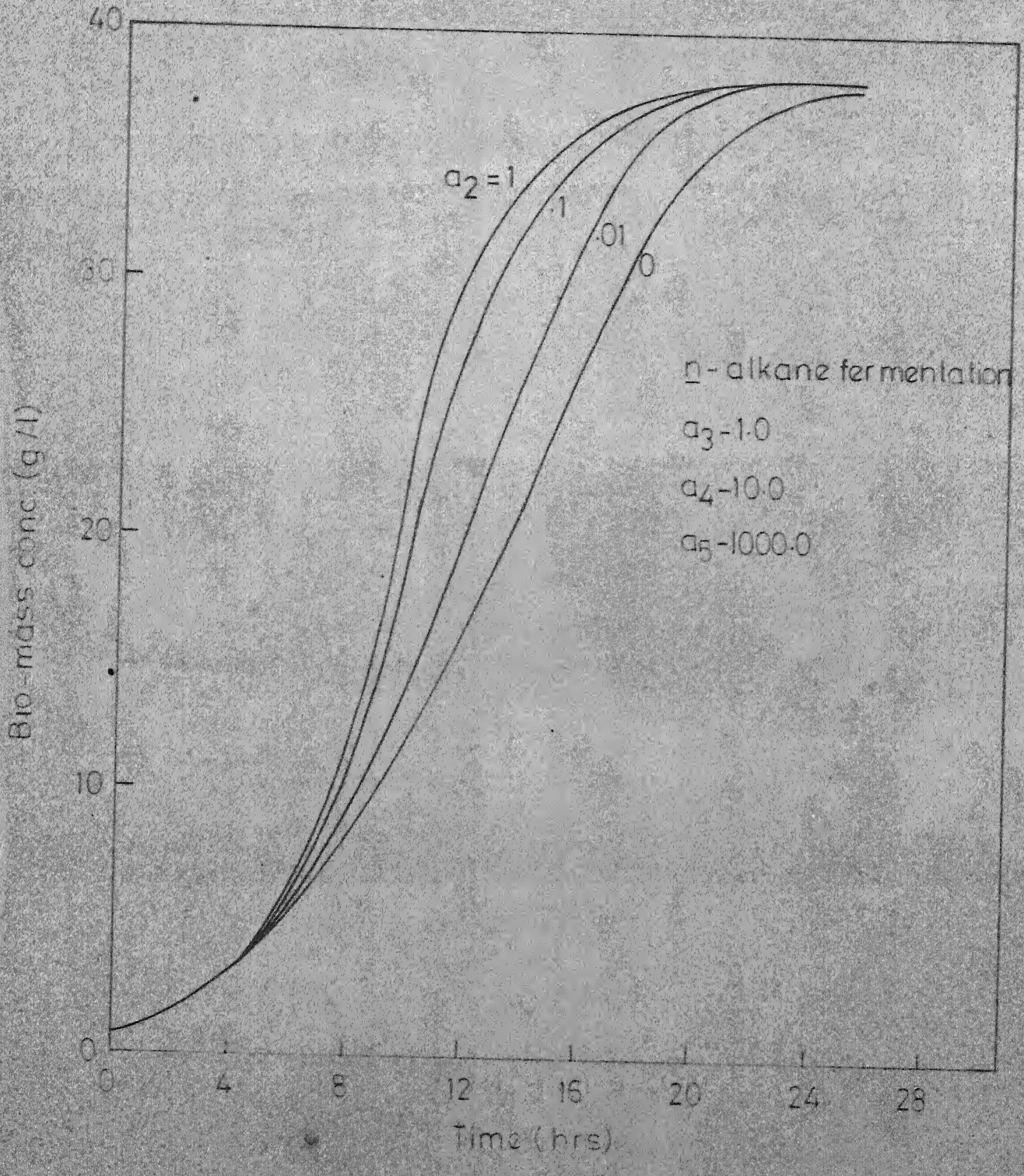

Fig 4.3.6 - Effect of mass transfer parameter a_2.

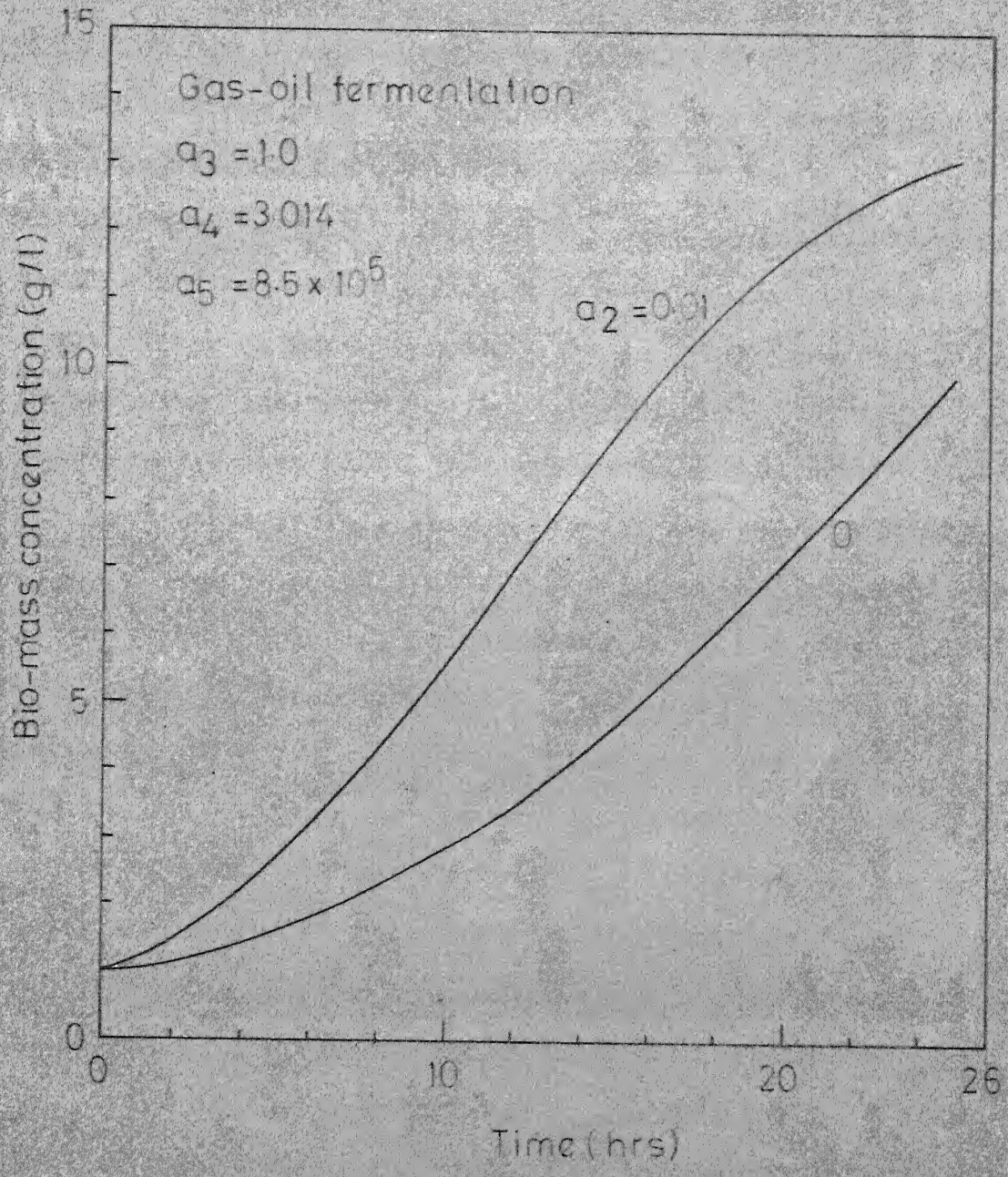

Fig. 4.3.7- Effect of mass transfer parameter a_2

growth in the continuous phase. A value of $a_2 = 0.0$ when the initial substrate concentration in the continuous phase is also zero, represents the case of no growth in the continuous phase. On the other hand, a very high value of a_2 implies that the continuous phase is almost saturated with the substrate all the time. These figures show that the growth in the continuous phase reduces the time required for fermentation considerably. However, Figure 4.3.6 also shows that the contribution of continuous phase growth towards overall growth in n-alkane fermentation for the cases of practical interest (for which value of parameter a_2 is of the order of 10^{-3}, corresponding to $k_m = 9$ cm/hr.) is not very significant. But, for gas-oil fermentations where the value of parameter a_2 for $k_m = 9$ cm/hr. is of the order of 10^{-2}, very significant differences are manifested between the two growth curves with and without continuous phase growth. For example, in order to consume 80 per cent of the consumable C-substrate from gas-oil, as much as 8-9 hr. difference in fermentation times can be expected in presence and in absence of continuous phase growth. Thus it seems that for the values of parameter a_2 corresponding to industrial hydrocarbon fermentations, contributions of continuous phase growth towards overall growth is not as important in n-alkane fermentation as in gas-oil fermentation. This fact is further supported by the effect of adsorption parameter a_4 on the growth predictions of the two fermentations. These are presented in Figures 4.3.8 and 4.3.9. For gas-oil fermentation, due to

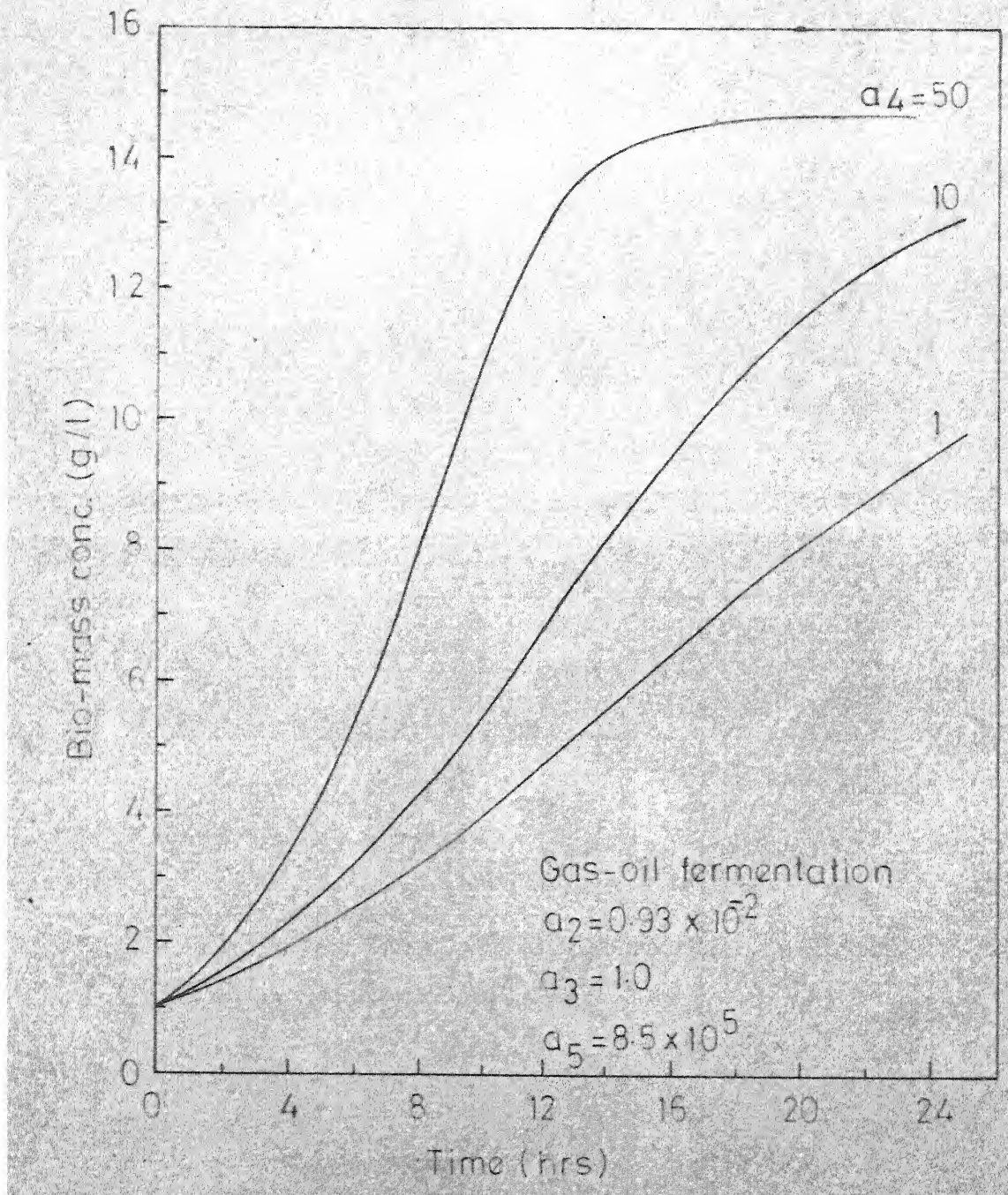

Fig 4.3.8 - Effect of adsorption parameter a_4

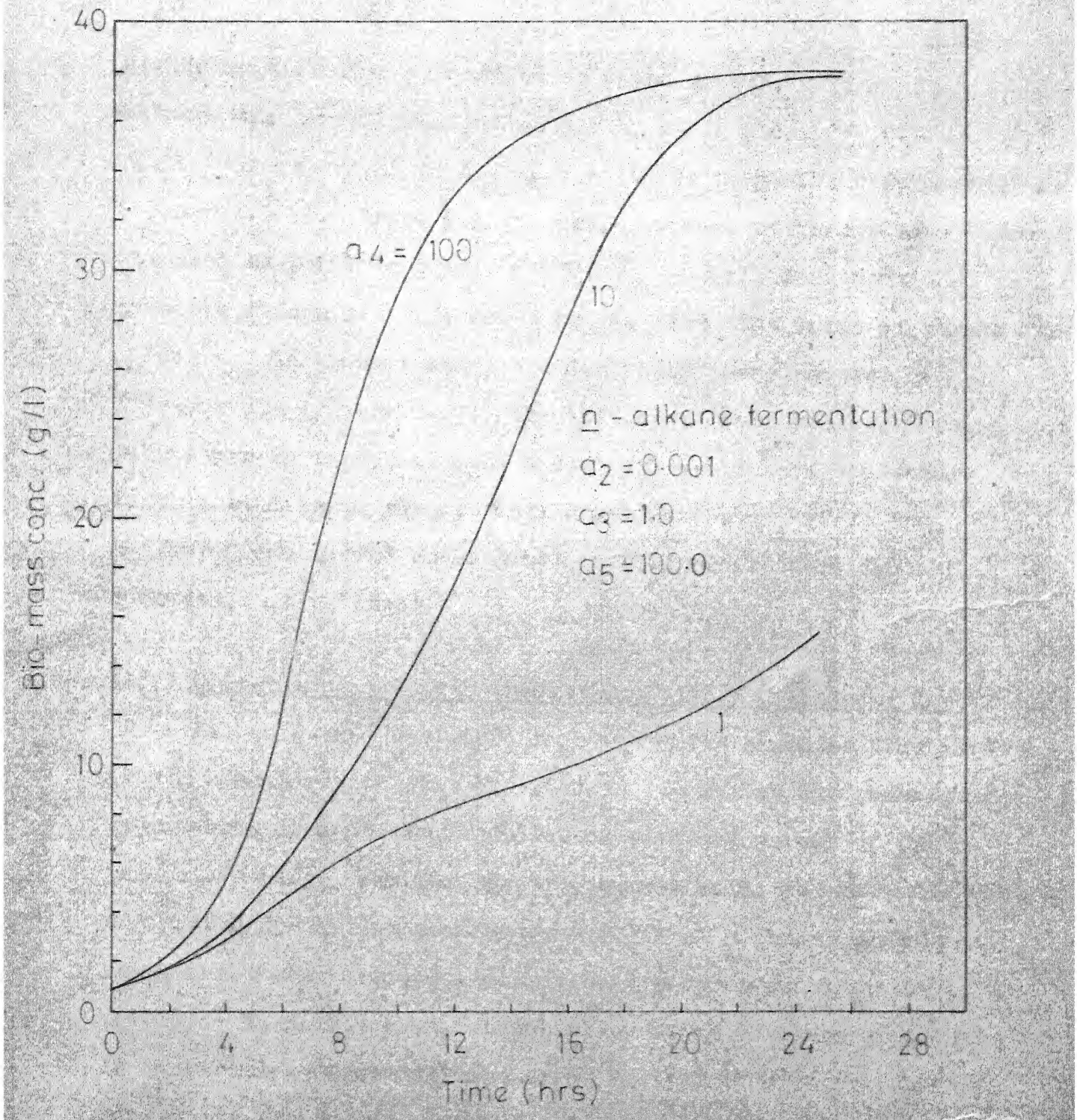

Fig.4.39- Effect of adsorption parameter a_4.

higher contribution of continuous phase growth, differences between the growth predictions for a_4 = 1.0 and a_4 = 10.0 are small (Figure 4.3.8) as compared to those in n-alkane fermentation (Figure 4.3.9). These results are, however, different from those obtained by Erickson et al. (1970) for gas-oil fermentations. A possible reason for this could be the fact that value of parameters a_k and $a_{k'}$ in present study are 1.0 while those adopted by Erickson et al. were 0.01. The effect of small values of these parameters is to magnify the contributions of both the phases. Further studies in this direction are necessary before the contribution of continuous phase growth can be ascertained for all conditions of interest.

4.3.4 Comparison of Growth Predictions with Experimental Data:

It was deemed desirable to compare the computer simulated growth behavior with that observed in laboratory experiments of hydrocarbon fermentation. Choice of suitable values of the parameters (e.g., maximum specific growth rate, saturation constants, adsorption/desorption constants, etc.) that would adequately represent the experimental conditions, posed a considerable problem. No direct experimental measurement of these parameters in hydrocarbon fermentation systems has yet been reported; even solubility of long-chain hydrocarbons in water is a matter of controversy (McAuliffe, 1969; Yoshida and Yamane, 1971; Bell, 1973; Goma, et al. , 1973; Bajpai and Prokop, 1974).

Shah et al. (1972a) estimated the parameters by minimizing the sum of error squares between the predicted and experimentally observed growth data in gas-oil fermentors. Stamatoudis and Tavlarides (1973) also adjusted the parameter values so as to fit the predicted performance into experimental data. Even though the experimental data utilized by the above groups of workers are the same, considerably different values of the parameters were obtained. For example, maximum specific growth rate, μ_{max} reported in the first case is 0.75 as compared to a value of 0.25 in the second case; k_a (as well as k_d) values are also different by two orders of magnitude. After a considerable deliberation, the following parameter values were chosen:

$$\mu_{max} = 0.70 \text{ hr}^{-1}$$

$$k_a = 0.166 \text{ liter}_{CP}/(\text{hr.}, \text{g. cell}_{DW})$$

$$k_d = 0.61 \text{ hr}^{-1}$$

$$k_s = 16.6 \text{ g/liter}_{DP}$$

$$k_{s'} = 3.07 \times 10^{-6} \text{ g/liter}_{CP}$$

$$Seq' = 4.9 \times 10^{-7} \text{ g/liter}_{CP}$$

$$n_{\infty} = 8.16 \times 10^{-6} \text{ g cell dry wt./cm}^2 \text{ DP}$$

These terms have been explained in Appendix E. It may be noted that these values are same as those obtained by Shah et al. (1972a) for one of their models, with a minor adjustment in the value of μ_{max}. Growth data obtained by computer simulation are plotted in Figures 4.3.10 and 4.3.11. Average volume of gas-oil drops

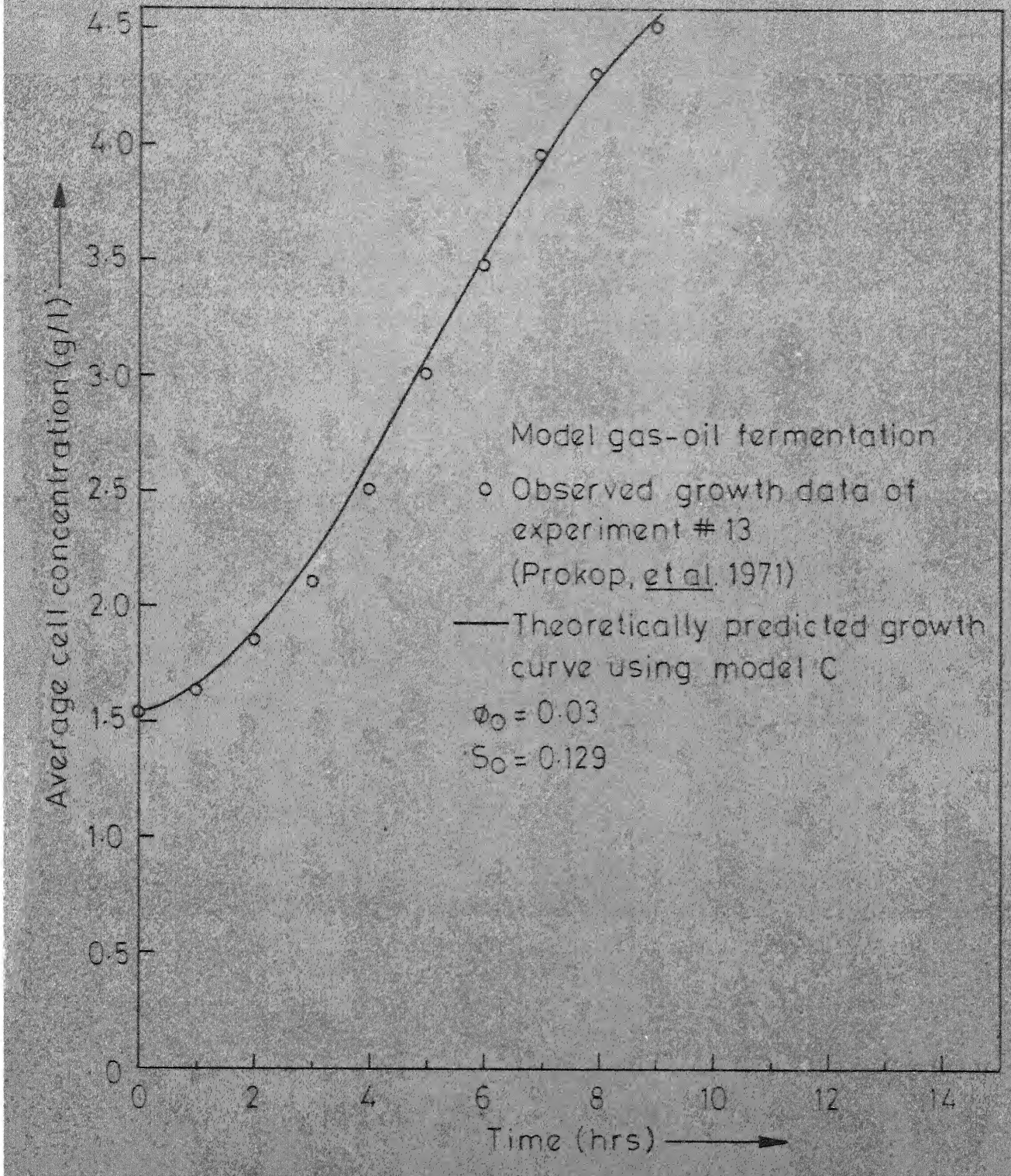

Fig 4.3.10 - Comparison of predicted and experimentally observed growth curves.

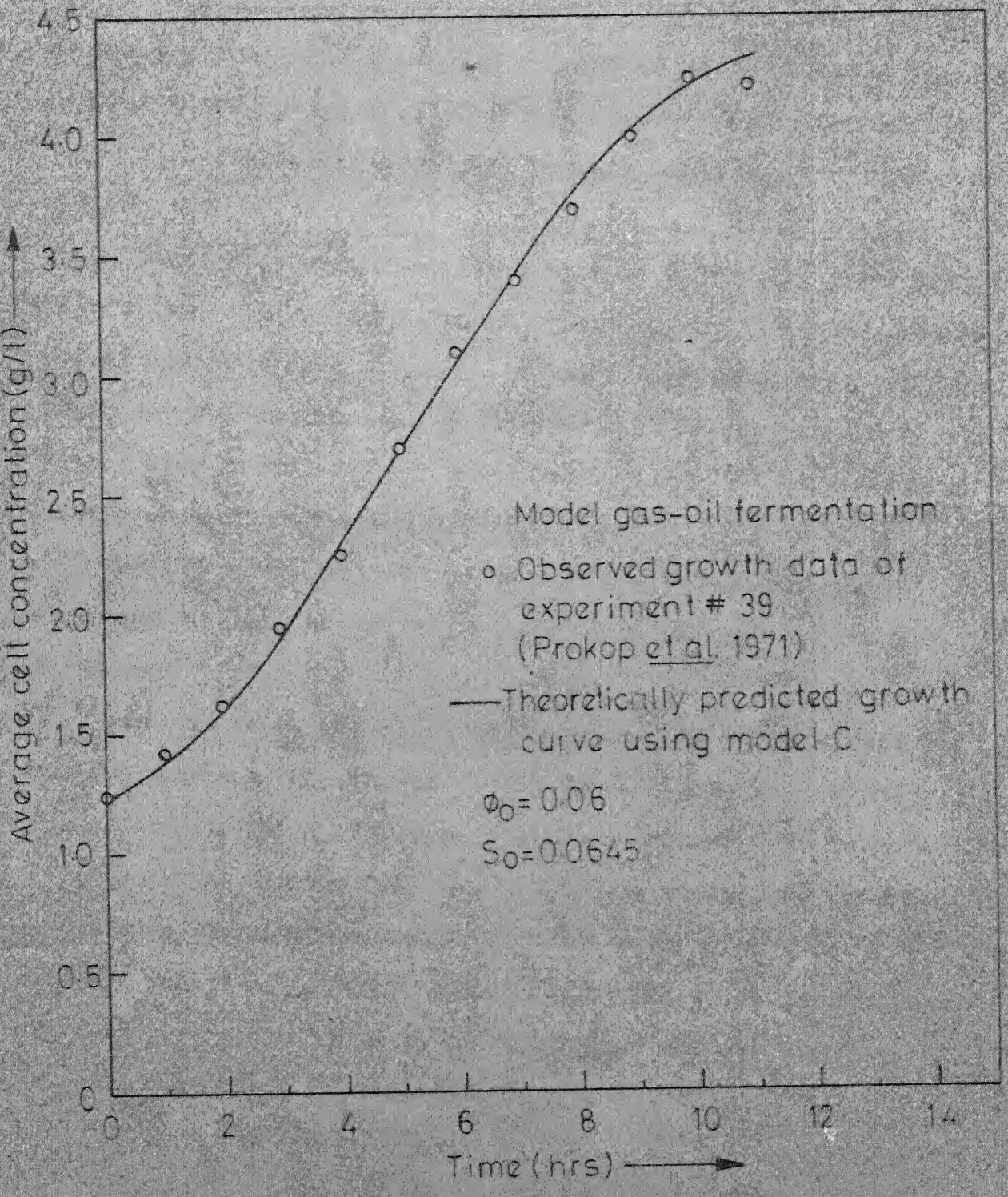

Fig.4.311 - Comparison of predicted and experimentally observed growth curves.

at the start of simulation was calculated using DSD data observed by Prokop and coworkers (1971, 1972) for the experimental conditions. There is a reasonable agreement between predicted and experimental results.

However, a word of caution must be introduced regarding the values of parameters chosen. This set is in no way unique and it may be possible to find a better set of values. In fact, parameter values obtained in this manner normally show a significant bias towards the model chosen and may not represent the actual values for the system, which must be determined by independent measurements. Extensive studies, both theoretical and experimental, are needed to achieve this and are recommended for future work.

In the above pages, an investigation into the effects of various factors upon the growth in gas-oil and in n-alkane fermentors has been reported. The coalescence-redispersion model (discussed in Chapter III) is a realistic representation of drop-phenomena, which is necessary to predict the performance of these vessels accurately. This model is expected to perform better than those previously proposed because of the experimental support various components of the model enjoy.

* * *

CHAPTER V

CONCLUSIONS AND RECOMMENDATIONS

A coalescence-redispersion (C-R) model has been proposed for the drop-interactions in stirred liquid-liquid dispersions. It is a simplified representation of the complex drop-phenomena taking place in such systems and yields an analytical solution for the case of equilibrium drop-size distribution (DSD) in batch vessels. Its capability to represent a large number of experimentally observed DSD data obtained from diverse sources (including those taken during the present investigation), gives credence to the mode of interactions proposed in this study. The model predicts a single parameter expression for equilibrium DSD in stirred vessels. This parameter can be correlated to the experimental variables and, then, the DSD corresponding to the experimental conditions can be theoretically predicted.

Experimental measurement of DSDs in n-alkane-water-Waldhof agitated systems, have been carried out using a detergent stabilization method (DM) developed in this study. This method was found to be especially suitable for studies in biological systems and is relatively simple.

DSDs observed in fermentation systems, have been found to be self preserving in nature. Sauter-mean diameter, the normalizing parameter, takes into account the effect of dispersed phase

fraction, speed of rotation and state of fermentor broth. It when correlated with experimental conditions, revealed that the circulation stirring systems behave in a way different from the flat-blade turbine systems. This fact was also corroborated by the correlations of C-R frequency with the experimental conditions.

A new method for the measurement of coalescence-redispersion frequency has been proposed, based upon the C-R model. Constant coalescence frequency has been measured by carrying out studies in batch stirred vessels and has been correlated to the experimental conditions. However, size dependent C-R frequency can also be measured by using a continuous flow stirred tank vessel (CFSTV), and is recommended for further work. Use of CFSTV will make the measurement quite easy as only two distribution-samples, those of incoming and outgoing streams in steady state operation, need to be taken as compared to many distributions which must be measured while working with batch vessels. Moreover, replicate samples can also be taken with as much ease.

An attempt to simulate the performance of hydrocarbon fermentors using the C-R model along with a model for growth of biomass in the system, was made using a Monte-Carlo simulation procedure. The importance of the extent and the nature of drop-interactions, and contribution of continuous-phase growth towards overall growth have been investigated. The simulation confirms the self preserving nature of DSDs, observed experimentally

in hydrocarbon fermentors. The computer time required for the simulations was also within reasonable limits. This simulation procedure can be easily extended to determine the optimum strategy for the operation of batch hydrocarbon fermentors. It would, however, require additional information regarding the cost of raw materials and the proteins, operating costs, and the recovery costs of single cell proteins and the residual n-alkanes.

Although this investigation throws some light upon the nature of drop-size distributions in hydrocarbon fermentors, further studies (both theoretical as well as experimental) are desirable to determine the kinetic importance of various sizes of drops. It has already been advocated in literature that the submicroscopic drops which could be aggregates of dispersed phase molecules play a crucial role in deciding the mode of uptake of hydrocarbons by the microbial cells. This brings us also to the question of solubility of hydrocarbons in aqueous phase about which many conflicting data have been reported. Theoretical studies supported by experimental work in this field, are needed to explain the diversity of such experimental findings.

Lastly, the knowledge regarding distribution of biomass between the interface and the continuous phase, is a major missing link in modelling of hydrocarbon fermentors. So far, it has been tackled only by hypothesizing the phenomena. A fundamental investigation in to the nature of interactions between cell surface and hydrocarbons, and cells and aqueous phase is desirable.

* * *

REFERENCES

Aiba, S., V. Moritz, J. Someya, and K.L. Haung, J. Ferment. Technol., 47, 203 (1969)a.

Aiba, S., K.L. Haung, V. Moritz, and J. Someya, J. Ferment. Technol., 47, 211 (1969)b.

Bajpai, R.K.,and A. Prokop, Biotechnology and Bioeng., 16, 1557 (1974).

Bayens, C.A., Ph.D. Dissertation, The John Hopkins Univ., U.S.A., 1967.

Bell, G.H., Chem. Phys. Lipids, 10, 1 (1973).

Blanch, H.W., and A. Einsele, Biotechnol. Bioeng., 15, 861 (1973).

Blanch, H.W., and A. Fiechter, Biotechnol. Bioeng., 16, 539 (1974).

Brown, D.E., and K. Pitt, Proc. Chemeca 70, Melbourne and Sidney, p.83, (1971).

Brown, D.E., and K. Pitt, Chem. Eng. Sci., 27, 577 (1972).

Calderbank, P.H., Trans. Inst. Chem.Eng., 36, 443 (1958).

Chen, H.T., and S. Middleman, AIChE Journal, 13, 989 (1967).

Curl, R.L., AIChE Journal, 9, 175 (1963).

Erickson, L.E., A.E. Humphrey, and A. Prokop, Biotechnol. Bioeng., 11, 449 (1969)a.

Erickson, L.E., and A.E. Humphrey, Biotechnol. Bioeng., 11, 467 (1969)b.

Erickson, L.E., and A.E. Humphrey, Biotechnol. Bioeng., 11, 489 (1969)c.

Erickson, L.E., L.T. Fan, P.S. Shah, and M.S.K. Chen, Biotechnol. Bioeng., 12, 713 (1970).

Gal-Or, B., Int. J. Heat Mass Transfer, 11, 551 (1968).

Giles, J.W., C. Hanson, and J.G. Marsland, in 'Solvent Extraction', Proc. Internat. Solvent Extr. Conf., ISEC. 71, The Hague, 19-23 April 1971; Vol. 1, Soc. Chem. Industry, London, p. 70, (1971).

Goma, G., A. Parcilleux, and G. Durand, Arch. Mikrobiol, 88, 97 (1973).

Hillestad, J.G., and J.H. Rushton, Paper presented at AIChE Columbus meeting (1966).

Hattori, K., S. Yakoo, and O. Imada, J.Ferment. Technol., 52, 132 (1974) (Jap.).

Howarth, W.J., AIChE Journal, 13, 1007 (1967).

Humphrey, A.E., and L.E. Erickson, J. Appl. Chem. and Biotechnol., 4, 125 (1972).

Iyengar, M.S., and J.N. Baruah, British Chem.Eng., 13(5), 684 (1968).

Katinger, H.W.D., A. Nobis, and J. Meyrath, Experientia, 26, 565 (1970).

Katinger, H.W.D., in "Advances in Microbial Engineering", Proc. 1st. Internat. Yeast Symp., Marianske Lazne, August 28- Sept. 1, 1972, Czechoslovakia, (B. Sikyta, A. Prokop, and M. Novak, Eds.), Biotechnol. Bioeng. Symp., No. 4, pt. 1, p. 485, 1973, J. Wiley, New York.

Kintner, R.C., T.J. Horton, R.E. Graumann, and S. Ambekor, Can. J. Chem.Eng., 39, 235 (1961).

Luhning, R.W., and H. Sawistowski, Proc. Int. Solvent Extr. Conf., 873-887, (1971); Ed. J.C. Gregory, Soc. Chem. Ind., London,England.

Madden, A.J., and G.L. Damerell, AIChE Journal, 8, 233 (1962).

Madden, A.J., and B.J. McCoy, Chem. Eng. Sci., 19, 506 (1964).

McAuliffe, C., Science, 163, 478 (1969).

Miller, R.S., J.H. Ralph, R.L. Curl, and G.D. Towell, AIChE Journal, 9, 196 (1963).

Mlynek, Y., and W. Resnick, AIChE Journal, 18, 122 (1972).

Morgan, P.W., "Condensation Polymers: By Interfacial and Solution Methods", Interscience Publications, New York, 1965.

Moo-Young, M., T. Shimizu, and D.A. Whitworth, Biotechnol.Bioeng., 13, 741 (1971)a.

Moo-Young, M., and T. Shimizu, Biotechnol. Bioeng. 13, 761 (1971)b.

Podlech, P.A.S., and W. Borzani, Biotechnol. Bioeng., 14, 43 (1972).

Prokop, A., L.E. Erickson, and O. Povedes-Lopez, Biotechnol. Bioeng., 13, 241 (1971).

Prokop, A., M. Ludvík, and L.E. Erickson, Biotechnol. Bioeng.,14, 587 (1972).

Prokop, A., and M. Sobotká, Paper presented in 'Internat. Conf. on SCP', 29-31 May, 1973, Cambridge, Mass.

Prokop, A. and M. Ludvík, in "Advances in Microbial Engineering", Proc. 1st. Internat., Yeast Symp., Marianske Lazne, August 28-Sept.1, 1972, Czechoslovakia (B. Sikyta, A. Prokop, and M. Novak, Eds.), Biotechnol. Bioeng. Symp., No. 4, pt.1, p. 349, 1973, J. Wiley, New York.

Rietema, K., "Chemical Reaction Engineering Meeting, Europ. Federation Chem. Eng. 12th Amsterdam", Chem.Eng.Sci., 8, 103 (1958).

Rodger, W.A., V.G. Trice, Jr., and J.H. Rushton, Chem. Eng.Progr., 52, 515 (1956).

Scott, L.S., W.B. Hayes, and C.D. Holland, AIChE Journal, 4, 346 (1958).

Shah, B.H., Ph.D. Thesis, "A Simulative and Analytical Study of Particulate Systems", IIT-Kanpur, India, 1974.

Shah, P.S., L.T. Fan, I.C. Kuo, and L.E. Erickson, Adv. in Applied Microbiology, 15, 367 (1972); publishers: Academic Press Inc., New York and London.b

Shah, P.S., L.E. Erickson, and L.T. Fan, Biotechnol. Bioeng., 14, 533 (1972) a.

Shiloh, K., S.Sideman, and W. Resnick, Can. J.Chem. Eng., 51, 542 (1973).

Shinnar, R., and J.M. Church, Ind. Eng. Chem., 52, 235 (1960).

Shinnar, R., J. Fluid Mech., 10, 259 (1961).

Sprow, F.B., Chem. Eng. Sci., 22, 435 (1967).

Srivastava, S.P., H.D.Singh, J.N. Baruah, P.V.Krishna, and M.S. Iyengar, J. Appl. Chem., 20, 105 (1970).

Stamatoudis, M., and L.L. Tavlarides, Paper presented at the 75th Nat. Meet. Amer. Inst. Chem. Engrs., June 3-6, 1973, Detroit, Mich., Paper No. 24C.

Thornton, J.D., and B.A. Bouyatiotis, Ind. Chemist., 39, 298 (1963).

Valentas, K.J., O. Bilous, and N.R. Amundson, Ind. Eng. Chem. Fundamentals, 5, 271 (1966).

vanHeuven, J.W., and J.C. Hoevenaar, Proc. 4th Int. Symp. on Reaction Engineering, Bruxelles, September, 1968.

vanHeuven, J.W., and W.J. Beek, in 'Solvent Extraction', Proc. Internat. Solvent. Extr. Conf., ISEC 71, The Hague, 19-23 April 1971; Vol.1, Soc. Chem. Industry, London, p.70, 1971.

Vermeulen, T., G.M. Williams, and G.E.Lenglois, Chem. Eng.Progr. 51, 85 (1955).

Vilenchich, R., and W. Akhtar, Process Biochemistry, 6(2),41 (1971).

Wang, D.I.C., and A. Ochoa, Biotechnol. Bioeng., 14, 345 (1972).

Ward, J.P., Ph.D. Dissertation, Oregon State University, Carvallis 1964 .

Weinstein, B. and R.E. Treybal, AIChE Journal, 19, 304 (1973).

Yoshida, F., and T. Yamada, J. Ferment. Technol. 49, 235 (1971).

Yoshida, F., and T. Yamane, Biotechnol. Bioeng., 13, 691 (1971).

Zeitlin, M. and L.L. Tavlarides, Can.J.Chem. Eng., 50, 207 (1972).

APPENDIX A

DROP-SIZE DISTRIBUTIONS MEASURED USING DETERGENT METHOD (DM), GELATIN METHOD (GM), AND ENCAPSULATION METHOD (EM) OF STABILIZATION OF DISPERSION SAMPLES

TABLE A-1: DISPERSION SAMPLED DURING CONTINUOUS CULTIVATION OF C.LIPOLYTICA ON GAS-OIL

Experiment No.1

Dispersed phase fraction : 0.10
Type of agitator : Waldhof
Speed of rotation : 1000 rpm
Biomass concentration : not noted

Sl. No.	Size Category (μm)	Number of Drops Observed		
		DM (immediately after sampling)	DM (1 hr after sampling)	GM
1	2-4	661	943	479
2	4-6	218	459	197
3	6-8	104	235	68
4	8-12	89	201	94
5	12-16	60	86	84
6	16-20	44	59	70
7	20-24	41	48	62
8	24-32	68	81	93
9	32-40	25	35	44
10	40-48	17	22	38
	Total	1327	2169	1247

TABLE A-2: DISPERSION OF n-ALKANES IN DISTILLED WATER

Experiment No.3

Dispersed phase fraction : 0.04
Type of agitator : Six-bladed turbine
Speed of rotation : 700 rpm
Concentration of Sabocoyl chloride in dispersed phase : 0.5% v/v

Sl. No.	Size Category (μm)	Number of Drops Observed	
		DM	EM
1	0-2	134	139
2	2-4	242	222
3	4-6	257	295
4	6-8	182	287
5	8-10	205	240
6	10-12	156	184
7	12-14	135	134
8	14-16	89	76
9	16-20	138	98
10	20-24	77	42
11	24-28	32	25
12	28-32	12	3
13	32-40	16	6
	Total	1675	1751

TABLE A-3: DISPERSION OF GAS-OIL IN DISTILLED WATER

Experiment No. 6

Dispersed phase fraction : 0.08
Type of agitator : six-bladed turbine
Speed of rotation : 1000 rpm
Concentration of Sabacoyl chloride in dispersed phase : 1% v/v

Sl. No.	Size Category (μm)	Number of Drops Observed	
		DM	EM
1	0-2	1030	785
2	2-4	275	272
3	4-6	141	174
4	6-8	62	70
5	8-10	38	16
6	10-12	26	8
7	12-16	39	11
8	16-20	12	8
9	20-24	10	3
10	24-32	5	1
11	32-48	8	1
12	48-64	1	1
	Total	1647	1350

TABLE A-4: DISPERSION SAMPLED DURING BATCH CULTIVATION OF C. LIPOLYTICA ON GAS-OIL

Experiment No. 7

Dispersed phase fraction : 0.05
Type of agitator : Waldhof
Speed of rotation : 1000 rpm
Biomass concentration : 1 g/l dry weight

Sl. No.	Size Category (μ m)	Number of Drops Observed	
		DM	GM
1	4-6	190	273
2	6-8	66	125
3	8-10	40	107
4	10-12	30	66
5	12-16	41	69
6	16-20	23	56
7	20-24	22	32
8	24-28	13	30
9	28-32	6	15
10	32-40	21	29
11	40-48	13	16
12	48-56	5	14
13	56-64	1	7
14	64-72	2	3
15	72-80	0	3
	Total	473	845

TABLE A-5: DISPERSION OF GAS-OIL IN DISTILLED WATER

Experiment Nos. 9 and 10

Dispersed phase fraction : 0.10
Type of agitator : modified Waldhof
Speed of rotation : 1000 rpm
Concentration of Sabacoyl chloride in dispersed phase : 1% v/v

Sl. No.	Size Category (μ m)	Number of Drops Observed		
		DM (expt.No.9)	EM (expt.No.9)	DM (exp.No.10)
1	0-2	673	840	1310
2	2-4	347	300	429
3	4-6	204	133	136
4	6-8	109	102	86
5	8-10	64	67	37
6	10-12	40	26	22
7	12-16	83	58	32
8	16-20	51	48	12
9	20-24	38	20	7
10	24-28	35	13	8
11	28-32	21	10	6
12	32-40	27	9	7
13	40-48	11	4	7
14	48-56	8	0	2
15	56-64	1	0	0
16	64-72	0	0	0
17	72-80	1	0	0
	Total	1713	1630	2101

TABLE A-6: DISPERSION OF n-ALKANES IN DISTILLED WATER

Experiment No. 11

Dispersed phase fraction : 0.08
Type of agitator : Waldhof (modified)
Speed of rotation : 1000 rpm
Concentration of Sabacoyl chloride in dispersed phase : 1% v/v

(Samples collected after 20 minutes from the start of agitation)

Sl. No.	Size Category (μm)	Number of Drops Observed	
		IM	EM
1	0-2	747	589
2	2-4	205	167
3	4-6	75	68
4	6-8	40	42
5	8-10	12	18
6	10-12	11	18
7	12-16	14	18
8	16-20	11	11
9	20-24	5	4
10	24-28	7	2
11	28-32	4	4
12	32-40	5	1
13	40-48	4	0
14	48-56	0	2
15	56-64	2	1
16	64-72	0	0
17	72-80	0	0
18	80-90	0	2
	Total	1142	947

TABLE A-7: DISPERSION OF n.ALKANES IN DISTILLED WATER

Experiment No. 16

Dispersed phase fraction : 0.005
Type of agitator : modified Waldhof
Speed of rotation : 1000 rpm
Concentration of Sabacoyl chloride in dispersed phase : 1% v/v

(Samples collected after 30 minutes from the start of agitation)

Sl. No.	Size Category (μm)	Number of Drops Observed	
		DM	EM
1	0–2	1263	1438
2	2–4	233	213
3	4–6	77	73
4	6–8	40	34
5	8–10	41	24
6	10–12	20	21
7	12–14	11	12
8	14–16	16	12
9	16–18	7	5
10	18–20	10	4
11	20–24	5	13
12	24–28	6	8
13	28–32	8	2
14	32–36	1	2
15	36–40	0	1
16	40–48	2	1
17	48–56	1	0
	Total	1741	1863

APPENDIX B

EFFECT OF DISPERSED PHASE FRACTION AND SPEED OF ROTATION OF MIXER UPON THE DISTRIBUTION OF *n*-ALKANE DROPS IN DISTILLED WATER IN A WALDHOF-AGITATED FERMENTOR.

TABLE B-1: DISPERSION OF 2% n-ALKANES IN DISTILLED WATER USING MODIFIED WALDHOF MIXER

Sl. No.	Size Category (μm)	rpm / Expt.No.	Number of Drops Observed 600 (20)	900 (21)	1200 (43A)	1500 (32D)
1	0-2		589	1180	1255	810
2	2-4		228	233	415	320
3	4-6		90	88	263	273
4	6-8		45	72	148	145
5	8-10		39	55	96	99
6	10-12		25	31	32	53
7	12-14		17	37	36	31
8	14-16		16	45	18	26
9	16-20		25	55	20	27
10	20-24		24	26	12	16
11	24-28		15	13	8	11
12	28-32		12	12	6	4
13	32-40		13	16	2	8
14	40-48		10	3	1	0
15	48-56		2	0	0	0
16	56-64		2	0	0	0
	Total		1152	1866	2312	1823

TABLE B-2: DISPERSION OF 5% n-ALKANES IN DISTILLED WATER USING MODIFIED WALDHOF MIXER

Sl. No.	Size Category (μ m)	Number of Drops Observed			
		rpm	600	900	1200	1500
		Expt.No.	(17)	(18)	(42C)	(32C)
1	0-2		447	612	262	351
2	2-4		220	340	330	223
3	4-6		123	215	292	173
4	6-8		64	141	178	121
5	8-10		50	65	135	76
6	10-12		31	52	79	70
7	12-14		32	68	56	41
8	14-16		28	60	58	17
9	16-20		61	48	49	28
10	20-24		37	34	18	13
11	24-28		38	24	18	15
12	28-32		29	16	12	4
13	32-40		31	22	18	6
14	40-48		12	8	5	4
15	48-56		12	1	0	0
	To tal		1215	1706	1510	1142

TABLE B-3: DISPERSION OF 10% n-ALKANES IN DISTILLED WATER USING MODIFIED WALDHOF MIXER

Sl. No.	Size Category (μm)	Number of Drops Observed				
	rpm Expt.No.	600 (23)	600 (28)	900 (43B)	1200 (41C)	1500 (32A)
1	0-2	600	500	128	249	111
2	2-4	281	122	53	393	223
3	4-6	125	43	36	287	374
4	6-8	73	32	19	216	361
5	8-10	71	17	22	165	315
6	10-12	51	9	18	115	99
7	12-16	83	14	38	131	83
8	16-20	69	12	39	89	30
9	20-24	50	6	24	30	11
10	24-28	42	14	33	17	9
11	28-32	30	6	10	13	3
12	32-40	38	11	12	10	4
13	40-48	17	6	3	6	2
14	48-56	6	5	3	1	1
15	56-64	4	1	0	0	0
16	64-72	2	2	0	0	0
17	72-80	4	0	0	0	0
18	80-90	1	0	0	0	0
	Total	1547	800	438	1722	1626

TABLE B-4: DISPERSION OF 15% n-ALKANES IN DISTILLED WATER USING MODIFIED WALDHOF MIXER

Sl. No.	Size Category (μm)	Number of Drops Observed				
	rpm Expt.No.	600 (26A)	800 (36C)	900 (26B)	1200 (40C)	1500 (32B)
1	0-2	482	235	414	1890	222
2	2-4	185	127	297	361	132
3	4-6	83	70	164	107	151
4	6-8	57	47	146	55	119
5	8-10	45	27	140	45	78
6	10-12	32	12	76	38	31
7	12-16	61	20	88	68	52
8	16-20	44	14	37	28	42
9	20-24	30	10	26	26	36
10	24-28	33	9	12	29	49
11	28-32	13	2	5	12	30
12	32-40	14	5	6	32	31
13	40-48	14	2	3	15	4
14	48-56	3	0	2	0	2
15	56-64	0	0	0	2	0
	Total	1096	580	1416	2708	979

APPENDIX C

EFFECT OF BIOMASS CONCENTRATION UPON THE DISTRIBUTION OF n-ALKANE DROPS IN AQUEOUS MEDIUM IN A WALDHOF AGITATED FERMENTOR

TABLE C-1: DISPERSION OF 5% n-ALKANES IN AQUEOUS MEDIA BY MODIFIED WALDHOF MIXER*

Speed of Agitation: 1200 rpm

Sl. No.	Size Category (μ m)	Cell concentration g/l (dry weight)	Number of Drops Observed					
			0	0.2	0.61	1.03	1.48	1.92
		Experiment No.	(48)	(49)	(50A)	(50B)	(51 A)	(51B)
1	0-2		1350	1112	610	1128	1200	799
2	2-4		396	207	189	236	434	278
3	4-6		91	72	54	74	146	89
4	6-8		49	40	30	47	89	68
5	8-12		34	34	43	34	107	73
6	12-16		16	24	31	18	52	44
7	16-20		8	14	7	12	31	30
8	20-24		12	19	7	9	5	19
9	24-28		4	16	3	5	11	11
10	28-32		5	11	2	4	8	7
11	32-40		12	16	11	6	6	13
12	40-48		11	14	9	7	6	5
13	48-56		15	10	7	5	4	3
14	56-64		9	8	4	1	2	3
15	64-72		8	12	4	1	4	1
16	72-80		7	2	0	-	1	-
17	80-100		2	6	0	-	-	-
18	100-120		1	1	3	-	-	-
	Total		2030	1618	1014	1587	2108	1443

*The vessel and the agitator was similar, but different from those described in Table II-1.1 and Figure 2.1.1.

APPENDIX D

DISTRIBUTION OF n-ALKANE DROPS DISPERSED IN DISTILLED WATER BY A WALDHOF AGITATOR AT DIFFERENT TIMES FROM THE START OF MIXING

TABLE D-1: DISPERSION OF n-ALKANES IN DISTILLED WATER

Dispersed phase fraction: 0.05
Type of agitator: modified Waldhof
Speed of rotation: 800 rpm

Sl. No.	Size Category (μm)	Time(min) Expt.No.	Number of Drops Observed							
			6 (56B)	12 (59B)	15 (58C)	21 (58A)	27 (59A)	30 (57A)	33 (58B)	36 (60B)
1	0-2		96	179	346	93	159	97	158	109
2	2-4		38	87	164	68	73	69	95	54
3	4-6		31	39	55	45	42	38	48	36
4	6-8		32	38	55	43	46	41	52	21
5	8-10		22	23	52	41	17	41	40	29
6	10-12		30	23	35	40	30	55	25	21
7	12-16		70	27	44	81	49	106	56	46
8	16-20		25	27	31	60	30	60	39	48
9	20-24		36	19	25	57	28	43	22	35
10	24-28		35	12	13	55	17	32	22	50
11	28-32		26	8	14	33	17	27	4	37
12	32-36		36	4	15	28	5	13	3	19
13	36-40		18	1	4	17	5	7	4	12
14	40-48		28	5	6	26	8	9	3	11
15	48-56		25	4	6	12	2	2	6	3
16	56-64		10	0	6	1	-	3	3	-
17	64-72		4	3	2	-	-	-	-	-
18	72-80		1	-	-	-	-	-	-	-
	Total		563	499	873	700	528	643	580	531

TABLE D-2: DISPERSION OF n-ALKANES IN DISTILLED WATER

Dispersed phase fraction : 0.05
Type of Agitator : modified Waldhof
Speed of Rotation : 1000 rpm

Sl. No.	Size Category (μm)	Time(min) Expt. No.	Number of Drops Observed 9 (67B)	12 (85B)	18 (66A)	33 (69A)	45 (69B)
1	0-2		75	184	274	378	352
2	2-4		78	81	198	212	319
3	4-6		89	55	157	87	263
4	6-8		77	50	106	109	165
5	8-10		90	68	109	129	142
6	10-12		61	55	63	76	54
7	12-14		56	60	63	50	46
8	14-16		56	55	60	39	48
9	16-20		63	63	77	53	48
10	20-24		42	44	41	35	26
11	24-28		49	30	37	17	11
12	28-32		33	20	7	11	9
13	32-36		24	11	11	7	5
14	36-40		22	4	7	3	2
15	40-48		46	8	9	5	-
16	48-56		9	3	-	-	-
17	56-64		1	1	-	-	-
18	64-72		1	-	-	-	-
	Total		872	792	1219	1211	1490

TABLE D-3: DISPERSION OF n-ALKANES IN DISTILLED WATER

Dispersed phase fraction : 0.05
Type of agitator : modified Waldhof
Speed of rotation : 1200 rpm

Sl. No.	Size Category (μm)	Time(min) Expt.No.	Number of Drops Observed						
			3 (52A)	6 (53A)	9 (86C)	15 (52B)	18 (53B)	21 (87A)	36 (42C)
1	0-2		33	125	239	101	120	548	262
2	2-4		65	88	292	70	139	476	330
3	4-6		40	83	188	82	86	266	292
4	6-8		39	109	64	90	92	117	178
5	8-10		33	103	69	104	90	102	135
6	10-12		30	57	32	97	69	62	79
7	12-16		57	121	63	163	74	85	114
8	16-20		38	93	49	148	40	77	49
9	20-24		35	71	32	72	24	47	18
10	24-28		24	62	30	64	26	37	18
11	28-32		17	44	27	36	20	22	12
12	32-36		10	30	24	29	12	12	11
13	36-40		16	18	11	13	9	2	7
14	40-48		16	26	10	26	8	7	5
15	48-56		10	4	7	-	4	3	-
16	56-64		4	4	2	-	-	1	-
17	64-72		1	2	2	-	-	-	-
18	72-80		1	-	1	-	-	-	-
19	80-90		1	-	-	-	-	-	-
	Total		470	1040	1142	1095	813	1864	1510

TABLE D-4: DISPERSION OF n-ALKANES IN DISTILLED WATER

Dispersed phase fraction : 0.10
Type of agitator : modified Waldhof
Speed of rotation : 800 rpm

Sl. No.	Size Category (μm)	Time(min) Expt.No.	Number of Drops Observed 12 (61A)	15 (63A)	33 (64A)	36 (84C)	39 (64B)	45 (85A)	50 (62B)
1	0-2		210	216	183	188	211	151	179
2	2-4		89	128	133	145	175	111	125
3	4-6		49	85	117	112	133	65	71
4	6-8		45	51	87	61	132	59	99
5	8-10		43	49	103	84	111	64	120
6	10-12		36	42	48	58	56	53	88
7	12-14		30	28	47	52	50	39	68
8	14-16		22	24	47	59	35	36	61
9	16-20		34	72	58	91	69	60	47
10	20-24		36	44	28	52	32	35	32
11	24-28		28	25	18	31	30	16	19
12	28-32		20	18	14	15	12	6	7
13	32-36		11	9	5	14	9	2	8
14	36-40		13	6	5	7	8	2	8
15	40-48		9	5	4	6	6	1	3
16	48-56		10	2	3	4	9	2	4
17	56-64		6	1	3	-	1	1	-
18	64-72		2	1	2	-	-	-	-
	Total		694	806	905	979	1079	703	939

TABLE D-5: DISPERSION OF n-ALKANES IN DISTILLED WATER

Dispersed phase fraction : 0.10
Type of agitator : modified Waldhof
Speed of rotation : 1000 rpm

Sl. No.	Size Category (μm)	Time(min) Expt. No.	Number of Drops Observed 6 (69C)	12 (70B)	15 (73B)	27 (74B)	30 (88C)	33 (74C)	36 (88D)
1	0-2		85	134	93	43	258	31	278
2	2-4		45	137	75	82	284	54	314
3	4-6		46	47	66	154	205	105	229
4	6-8		50	37	114	147	128	133	157
5	8-10		36	37	119	182	177	136	198
6	10-12		26	26	91	131	92	75	84
7	12-14		22	16	84	127	78	79	87
8	14-16		21	21	93	92	50	67	62
9	16-18		27	24	80	77	36	43	73
10	18-20		33	29	61	52	30	40	40
11	20-24		66	66	87	88	37	53	49
12	24-28		75	75	68	71	20	38	34
13	28-32		82	50	41	29	11	21	14
14	32-36		62	40	31	16	9	15	4
15	36-40		62	15	20	5	3	7	1
16	40-48		62	4	17	4	2	3	4
17	48-56		15	1	2	-	-	-	-
	To tal		815	759	1142	1300	1420	905	1626

TABLE D-6: DISPERSION OF n-ALKANES IN DISTILLED WATER

Dispersed phase fraction : 0.10
Type of agitator : modified Waldhof
Speed of rotation : 1200 rpm

Sl. No.	Size Category (μm)	Time (min) / Expt. No.	Number of Drops Observed 7.5 (47B)	12 (90C)	21 (91A)	33 (47D)	36 (41C)
1	0-2		137	318	213	73	249
2	2-4		54	130	91	27	393
3	4-6		33	91	76	18	287
4	6-8		34	71	55	11	216
5	8-10		28	87	63	22	165
6	10-12		18	56	41	18	115
7	12-14		25	32	23	14	75
8	14-16		21	32	30	14	56
9	16-20		28	67	46	31	89
10	20-24		18	50	37	15	30
11	24-28		13	46	38	25	17
12	28-32		9	36	19	9	13
13	32-36		8	22	16	8	8
14	36-40		7	19	10	4	2
15	40-48		8	18	21	3	6
16	48-56		0	11	10	2	1
17	56-64		1	6	3	-	2
18	64-72		1	1	-	-	-
19	72-80		2	1	-	-	-
	Total		445	1094	732	294	1724

TABLE D-7: DISPERSION OF n-ALKANES IN DISTILLED WATER

Dispersed phase fraction : 0.15
Type of agitator : modified Waldhof
Speed of rotation : 800 rpm

Sl. No.	Size Category (μm)	Time (min) / Expt. No.	Number of Drops Observed						
			6 (34A)	12 (36A)	21 (35B)	27 (33C)	30 (34C)	33 (35C)	45 (36C)
1	0-2		64	126	220	154	65	341	235
2	2-4		61	97	153	231	87	251	127
3	4-6		72	62	128	146	119	159	70
4	6-8		33	28	81	125	71	110	47
5	8-12		89	39	139	198	113	180	39
6	12-16		50	32	64	120	47	123	20
7	16-20		41	17	63	65	40	75	14
8	20-24		30	15	65	47	42	41	10
9	24-28		21	16	61	34	25	39	9
10	28-32		18	7	25	17	12	27	2
11	32-40		16	26	32	21	10	23	5
12	40-48		15	12	12	7	7	5	2
13	48-56		7	4	3	4	1	-	-
14	56-64		4	2	1	2	-	-	-
15	64-72		2	-	2	-	-	-	-
16	72-80		2	-	2	-	-	-	-
17	80-90		1	-	-	-	-	-	-
18	90-100		1	-	-	-	-	-	-
	Total		527	483	1051	1171	639	1374	580

TABLE D-8: DISPERSION OF n-ALKANES IN DISTILLED WATER

Dispersed phase fraction : 0.15
Type of agitator : modified Waldhof
Speed of rotation : 1000 rpm

Sl. No.	Size Category (μm)	Time(min) Expt. No.	Number of Drops Observed						
			6 (79A)	9 (81C)	12 (79B)	15 (82A)	27 (83B)	30 (80B)	36 (80C)
1	0-2		117	29	91	103	173	92	32
2	2-4		88	14	71	55	70	77	55
3	4-6		94	23	89	45	50	125	115
4	6-8		95	26	101	45	34	129	109
5	8-10		115	26	85	66	63	157	192
6	10-12		71	19	66	48	50	87	119
7	12-14		61	26	56	46	43	110	121
8	14-16		53	26	55	57	52	106	110
9	16-20		84	56	93	118	135	125	138
10	20-24		82	63	67	94	134	54	65
11	24-28		59	78	51	78	47	40	34
12	28-32		37	60	23	58	24	23	12
13	32-36		30	42	14	37	16	7	6
14	36-40		14	14	13	15	13	10	3
15	40-48		16	18	7	22	8	3	1
16	48-56		8	6	4	5	1	1	-
17	56-64		0	-	3	-	1	-	-
18	64-76		2	-	-	-	-	-	-
	Total		1025	527	889	892	914	1146	1112

TABLE D-9: DISPERSION OF n-ALKANES IN DISTILLED WATER

Dispersed phase fraction : 0.15
Type of agitator : modified Waldhof
Speed of rotation : 1200 rpm

Sl. No.	Size Category (μm)	Time (min) Expt. No.	Number of Drops Observed						
			3 (37A)	12 (40A)	18 (38B)	24 (40B)	30 (38C)	33 (39C)	45 (40C)
1	0-2		75	93	63	194	67	168	1890
2	2-4		132	69	48	71	41	126	361
3	4-6		138	54	43	56	42	165	107
4	6-8		124	38	46	53	37	199	55
5	8-12		229	71	59	108	55	238	83
6	12-16		133	60	61	70	54	146	68
7	16-20		104	19	37	54	39	48	28
8	20-24		69	15	35	40	40	20	26
9	24-28		60	28	53	38	35	12	29
10	28-32		49	22	41	32	24	15	12
11	32-40		65	35	59	48	18	16	32
12	40-48		35	19	14	25	7	4	15
13	48-56		18	5	13	8	2	2	0
14	56-64		9	1	1	4	1	1	2
15	64-72		3	1	0	1	-	1	-
16	72-80		1	0	1	-	-	-	-
17	80-90		4	1	-	-	-	-	-
18	90-100		2	-	-	-	-	-	-
19	100-120		1	-	-	-	-	-	-
	To tal		1251	531	574	802	462	1161	2708

APPENDIX E

POPULATION BALANCE AND GROWTH EQUATIONS

Population Balance Equation :

A droplet present in the n-alkane fermentation system is characterized by its size and the amount of biomass it has on its surface at any time. Hence, the population density of drops can be considered a bivariate function, the variables being v (the volume) and n (the density of biomass on its surface, defined as the amount of biomass per unit area).

The drop-phenomena is considered to be represented by the coalescence-redispersion (C-R) model discussed in Chapter III. Briefly, any two drops present in the system are capable of coalescing with a constant frequency, w. The coalescence is immediately followed by redispersion into two daughter droplets whose sizes are uniformly distributed in statistical sense. The C-R process is assumed to be instantaneous and as a result of this, surface biomass densities on the two drops become uniform. It is also assumed that the drop - phenomena do not cause any exchange of biomass between the two phases and that these do not interfere with mass transfer process. The population balance equation for the coalescence-redispersion model can be easily written as

$$\frac{\partial}{\partial t}\left\{f(v,n,t)\right\} + \frac{\partial}{\partial v}\left\{f(v,n,t)\ \frac{dv}{dt}\right\} + \frac{\partial}{\partial n}\left\{f(v,n,t)\ \frac{dn}{dt}\right\}$$

$$= \iint_{v_1+v_2 \geq v} dv_1\ dv_2 \int_0^{n_{1\,max}} dn_1 w\ g(v_1,v_2;v)\ f(v_1,n_1,t)\ f(v_2,n_2,t)$$

$$- \int_0^{\infty} dv' \int_0^{n_\infty} dn'\ w\ f(v,n,t)\ f(v',n',t) \qquad (E.1)$$

The first term on the right hand side corresponds to the rate of generation of drops due to the C-R events, and the second term represents the rate of loss of drops under consideration, due to coalescence with other drops. $f(v,n,t)$ is the population density of drops, and $f(v,n,t)\ dv\ dn$ represents the fractional number of droplets at any time t having volumes between v and v+dv, and biomass density between n and n+dn, n_2 is the surface biomass density on a drop of volume v_2 which after coalescing with a drop of volume v_1 and surface biomass density n_1, and redispersion will produce two drops having surface biomass density n. By biomass balance, n_2 can be expressed as

$$n_2 = n\left\{\left(\frac{v}{v_2}\right)^{2/3} + \left(\frac{v_1}{v_2} + 1 - \frac{v}{v_2}\right)^{2/3}\right\} - n_1\left(\frac{v_1}{v_2}\right)^{2/3} \qquad (E.2)$$

$n_{1\,max}$ is the maximum surface biomass density on the drop of volume v_1 that is capable of producing after a coalescence-redispersion event with a drop of volume v_2, drops of surface biomass density n; it can be easily shown to be,

$$n_{1\,max} = n\left\{\left(\frac{v}{v_1}\right)^{2/3} + \left(\frac{v_2}{v_1} + 1 - \frac{v}{v_1}\right)^{2/3}\right\} \qquad (E.3)$$

Population balance equations for the case of gas-oil systems can be written in a similar way. The population density of drops in this case will be a trivariate function of drop volume v, surface biomass density n, and concentration of consumable substrate S in the drop.

Growth Equations for n-Alkane Fermentation:

For a single droplet

$$\frac{d}{dt}(\rho_s v) = -\frac{\mu_{max}}{Y} n.A - k_m (S_{eq}' - S').A \qquad (E.4)$$

$$\frac{d}{dt}(A.n) = \mu_{max}\, n.A + k_a(n_\infty - n)\, n'.A - k_d\, n.A \qquad (E.5)$$

where A is the interfacial area of a drop of volume v, n_∞ is the maximum surface biomass concentration. The quantities with primes correspond to the continuous phase.

Material balance for biomass and substrate in the continuous phase leads to:

$$\frac{d}{dt}(V_c \cdot S') = -\frac{\mu_{max}}{Y}\,\frac{S'}{k_s' + S'}\, n' V_c + \int_0^\infty \int_0^{n_\infty} k_m\, A(S_{eq}' - S')\, f(v,n,t)\, dn\, dv \qquad (E.6)$$

$$\frac{d}{dt}(V_c n') = \mu_{max}\,\frac{S'}{k_s' + S'}\, n' V_c - \int_0^\infty \int_0^{n_\infty} \left[k_a\, n'(n_\infty - n) - k_d n\right] A\, f(v,n,t)\, dn\, dv \qquad (E.7)$$

If N_o is the total number of drops present in the system and a subscript i denotes each drop, discretized forms of Equation (E.4) to (E.7) can be written as

$$\frac{d}{dt}(\rho_s v_i) = -\frac{\mu_{max}}{Y} n_i A_i - k_m (S_{eq}' - S') A_i \quad \forall i = 1,2,\ldots,N_o \qquad (E.8)$$

$$\frac{d}{dt}(A_i n_i) = \mu_{max} n_i A_i + k_a (n_\infty - n_i) n' A_i - k_d n_i A_i \quad \forall i = 1,2,\ldots,N_o \qquad (E.9)$$

$$\frac{d}{dt}(V_c S') = -\frac{\mu_{max}}{Y} \frac{S'}{k_s' + S'} n' V_c + \sum_{i=1}^{N_o} k_m A_i (S_{eq}' - S') \qquad (E.10)$$

$$\frac{d}{dt}(V_c n') = \mu_{max} \frac{S'}{k_s' + S'} n' V_c - \sum_{i=1}^{N_o} \left\{ k_a n' (n_\infty - n_i) - k_d n_i \right\} A_i \qquad (E.11)$$

On non-dimensionalizing these equations we get,

$$\frac{d}{d\tau} x_i = - a_1 x_i^{2/3} y_i - a_2 (1-x') x_i^{2/3} \quad \forall i=1,2,\ldots,N_o \qquad (E.12)$$

$$\frac{d}{d\tau} y_i = y_i + a_4 (1-y_i) y' - a_3 y_i - \frac{2}{3} \frac{y_i}{x_i} \frac{dx_i}{d\tau} \quad \forall i=1,2,\ldots,N_o \qquad (E.13)$$

$$\frac{d}{d\tau} x' = - \frac{x'}{a_{k'} + x'} a_5 y' + a_2 a_5 (1-x') \sum_{i=1}^{N_o} x_i^{2/3} \qquad (E.14)$$

$$\frac{d}{d\tau} y' = \frac{x'}{a_{k'} + x'} y' + a_1 \sum_{i=1}^{N_o} x_i^{2/3} \left\{ a_4 (1-y_i) y' - a_3 y_i \right\} \qquad (E.15)$$

where

$$x_i = \frac{v_i}{V_c}, \quad y_i = \frac{n_i}{n_\infty}, \quad x' = \frac{S'}{S_{eq'}}, \quad y' = \frac{n'}{Y \rho_s}, \quad \tau = t\, \mu_{max}$$

$$a_1 = \frac{n_\infty}{Y \rho_s V_c^{1/3}}, \quad a_2 = \frac{k_m}{\mu_{max} V_c^{1/3}} \frac{S_{eq'}}{\rho_s}, \quad a_3 = \frac{k_d}{\mu_{max}},$$

$$a_4 = \frac{k_a Y \rho_s}{\mu_{max}}, \quad a_5 = \frac{\rho_s}{S_{eq'}}, \quad a_{k'} = \frac{k_{s'}}{S_{eq'}}, \quad \alpha = (36\pi)^{1/3}$$

Assuming a quasi-steady state for substrate concentration in the continuous phase

$$x' = \frac{-B + \sqrt{B^2 + 4a_{k'}}}{2} \qquad \text{(E.16)}$$

where $B = -1 + a_{k'} + \dfrac{y'}{a_2 \sum_{i=1}^{N_o} x_i^{2/3}}$

Unless stated otherwise, values of these parameters used in simulations, were:

$\rho_s = 0.85$ g/cm^3 substrate

v_o = average volume of drops at the start of simulation

$= 1 \times 10^{-8}$ cm^3

$\phi = 0.10$

n_o = initial surface biomass density = 0.0 gm/cm^2

$n_\infty = 2 \times 10^{-4}$ gm/cm^2

$\mu_{max} = 0.75$ hr^{-1}

$k_{s'} = 2 \times 10^{-6}$ gm substrate/L$_{CP}$

$k_a = 0.013\ l_{CP}/gm\ cell_{DW}/hr$

$k_d = 0.75\ hr^{-1}$

$S_o = S_{eq'} = 2 \times 10^{-6}$ gm substrate/L_{CP}

$Y = 0.85$ gm $cell_{DW}$/gm substrate

$k_m = 9$ cm/hr

$CRF = 10\ hr^{-1}$

$N_o = 10$ or 20 depending upon whether initial DSD is Dirac delta or uniform (and exponential).

$N_s = 15$

Growth Equations for Gas-Oil Fermentation:

Equations corresponding to (E.8) to (E.11) are

$$\frac{d}{dt}(v_i S_i) = -\frac{\mu_{max}}{Y}\frac{S_i}{k_s + S_i} n_i A_i - k_m (S_{eq_i'} - S') A_i \quad \forall\, i=1,2,\ldots,N_o \qquad (E.17)$$

$$\frac{d}{dt}(A_i n_i) = \mu_{max}\frac{S_i}{k_s+S_i} n_i A_i + k_a(n_\infty - n_i)n' A_i - k_d n_i A_i \quad \forall\, i=1,2,\ldots,N_o \qquad (E.18)$$

$$\frac{d}{dt}(V_c S') = -\frac{\mu_{max}}{Y}\frac{S'}{k_{s'}+S'} n' V_c + \sum_{i=1}^{N_o} k_m A_i (S_{eq_i'} - S') \qquad (E.19)$$

$$\frac{d}{dt}(V_c n') = \mu_{max}\frac{S'}{k_{s'}+S'} n' V_c - \sum_{i=1}^{N_o}\left\{k_a n'(n_\infty - n_i) - k_d n_i\right\} A_i \qquad (E.20)$$

where $S_{eq_i'}$ is the continuous phase substrate concentration in equilibrium with drop i, and is expressed as

$$S_{eq_i'} = S_i \frac{S_{eq'}}{S_o}$$

On non-dimensionalizing these equations, we get

$$\frac{d}{d\tau} x_i = - a_1 y_i \frac{x_i}{a_k + x_i} z_i^{-1/3} - a_2(1-y') z_i^{-1/3} \quad \forall i=1,\ldots,N_o \qquad (E.21)$$

$$\frac{d}{d\tau} y_i = y_i \frac{x_i}{a_k+x_i} + a_4 y'(1-y_i) - a_3 y_i \quad \forall i=1,\ldots,N_o \qquad (E.22)$$

$$\frac{d}{d\tau} x' = - a_5 y' \frac{x'}{a_{k'}+x'} + a_2 a_5 \sum_{i=1}^{N_o} z_i^{2/3}(x_i-x') \qquad (E.23)$$

$$\frac{d}{d\tau} y' = y' \frac{x'}{a_{k'}+x'} - a_1 \sum_{i=1}^{N_o} z_i^{2/3} \left\{ a_4 y'(1-y_i) - a_3 y_i \right\} \qquad (E.24)$$

where $\tau = t \mu_{max}$, $x_i = \frac{S_i}{S_o}$, $y_i = \frac{n_i}{n_\infty}$, $z_i = \frac{v_i}{V_c}$,

$x' = \frac{S'}{S_{eq'}}$, $y' = \frac{n'}{Y S_o}$,

$a_1 = \frac{n_\infty}{Y S_o V_c^{1/3}}$, $a_2 = \frac{k_m}{\mu_{max} V_c^{1/3}} \frac{S_{eq'}}{S_o}$, $a_3 = \frac{k_d}{\mu_{max}}$

$a_4 = \frac{k_a Y S_o}{\mu_{max}}$, $a_5 = \frac{S_o}{S_{eq'}}$, $a_k = \frac{k_s}{S_o}$, $a_{k'} = \frac{k_{s'}}{S_{eq'}}$

Assuming a quasi-steady state for substrate concentration in the continuous phase

$$x' = \frac{-B + \sqrt{B^2 + 4a_{k'} C}}{2} \qquad (E.25)$$

where $B = -C + a_{k'} + \frac{y'}{a_2 \sum_{i=1}^{N_o} z_i^{2/3}}$; $C = \frac{\sum_{i=1}^{N_o} z_i^{2/3} x_i}{\sum_{i=1}^{N_o} z_i^{2/3}}$

Unless stated otherwise, values of these parameters used in simulations were:

$\rho_s = 0.85$ gm$_{substrate}$/cm^3

$S_o = 0.17$ gm$_{substrate}$/cm$^3_{DP}$

$v_o = 1 \times 10^{-8}$ cm^3

$\phi = 0.10$

$n_o = 0.0$ gm cell$_{DW}$/cm^2

$n_\infty = 2.0 \times 10^{-4}$ gm cell$_{DW}$/cm^2

$\mu_{max} = 0.75$ hr^{-1}

$k_{s'} = 2 \times 10^{-6}$ gm substrate/L$_{CP}$

$k_s = 0.17$ gm substrate/cm$^3_{DP}$

$k_a = 0.013$ L$_{CP}$/gm cell$_{DW}$/hr.

$k_d = 0.75$ hr^{-1}

$S_o' = S_{eq'} = 2 \times 10^{-6}$ gm substrate/L$_{CP}$

$Y = 0.85$ gm cell$_{DW}$/gm$_{substrate}$

$k_m = 9.0$ cm/hr

$CRF = 10$ hr^{-1}

$N_o = 10$ or 20 depending upon initial DSD

$N_s = 15$

* * *

APPENDIX F

ALGORITHM FOR MONTE-CARLO SIMULATION

Population balance equation (E.1) when solved with the growth equations (E.4 to E.7), is capable of giving rise to the growth behavior in n-alkane fermentation systems. However, analytical solution to these equations is very complex due to the following considerations:

1. i. Population balance equation is coupled with the growth equations.
   ii. The growth equations for the dispersed phase are coupled in themselves and with those for the continuous phase.
2. i. Population balance equation is a nonlinear integro-partial differential equation with the population density, f, appearing under multiple integral signs in two different terms with variable limits.
   ii. The growth equations for the dispersed and the continuous phases are also non linear.

The prediction of growth behavior of gas-oil fermentation systems is one order of magnitude more complex because the population density of drops in this case is a trivariate function, the variables being v (the volume), S (the substrate concentration), and n (the surface biomass density).

Monte-Carlo simulation procedure can, however, be conveniently used to analyse the problem under consideration, provided care is taken to see that the simulation procedure reproduces the physical process as closely as possible. It can be done by following exactly the course of events as is proposed by the model. The method is not only simple but also provides for incorporation of more complicated models for the particulate phenomena. A Monte-Carlo simulation procedure suitable to the problem at hand was developed by Shah (1974) and will be utilized here.

The Methodology of Simulation:

Hydrocarbon fermentation systems fall into a general category popularly known as 'particulate systems'. The systems consist of particles undergoing random phenomena which affect the properties of these particles. The random phenomena could be either monoparticle, i.e. those involving only one particle at a time, or multiparticle. Examples of monoparticle events are breakage, birth and death, entry and exit from the system, etc. Of multiparticle events, only biparticle random phenomena like two particle coalescence, collision, etc. are important. Events involving more than two particles at a time are not very frequent and notof much interest in systems of particles like drops and bubbles. The random phenomena are specified in terms of frequencies of their occurrence which may be functions of properties of the

particles taking part in the event, and of environmental variables like speed of agitation, power input, dispersed phase fraction, temperature, shape and size of the vessel, and the agitator, etc. The random phenomena may be accompanied by growth of particles also. Both of these affect the state of the system. Growth causes a continuous change in state while change due to random phenomena occurs abruptly at discrete time points at different intervals. Thus, the specification of the dynamic behavior of the system requires statement of (a) initial conditions, (b) frequency of random events, and (c) growth behavior of the particles.

State of the particulate system at any time is specified by the number of particles and their individual properties. Evolution takes place by a sequence of random events between which growth takes place. The time between the two successive random events is a random variable and is termed 'interval of quiescence' (IQ). IQ is the period during which no random event takes place and its probability distribution depends upon the frequency of events and the properties of existing particles. The simulation proceeds by generating a sequence of IQ and updating the properties of the particles to the end of each IQ when a random event takes place and causes an abrupt change in the properties of the particles involved. It is assumed that the random event occurs infinitely fast. A sufficient number of repetitions will allow the estimation of the required quantities.

The hydrocarbon fermentation model under consideration envisages only coalescence-redispersion events accompanied by growth of microbes and consumption of substrate. These random events are biparticle in nature. The frequency of this event is denoted by q and may depend upon the properties of the two particles involved. Thus,

$$q \equiv q\,(x(t),\ y(t)) \tag{F.1}$$

It is defined by,

$$\Pr\left[\text{a given particle of property x interacts with another particle of property y in the time interval t and t+dt}\right] = q(x,y)\,dt + o(dt) \tag{F.2}$$

Let the state of the system at any time be described as,

$$A_t = \left\{x_i(t),\ i = 1,2,\ldots,N(t)\right\} \tag{F.3}$$

where $N(t)$ is the total number of particles at time t, and x_i is the property of the ith particle. $N(t)$ remains constant in the present investigation due to the specific nature of the drop-interactions proposed. q is also assumed to be constant and same for all the particles. The algorithm for this simulation has been developed in detail by Shah (1974).

The probability distribution of IQ may be derived in the following manner:

Let T be a random variable representing time between two successive biparticle events. If $P(T/A_t)$ is the probability

that no biparticle event occurs between time t and $t+\tau$, given the state of the system A_t at time t,

$$P(\tau/A_t) = P(T>\tau/A_t) \qquad (F.4)$$

From the definition,

$$P(\tau + d\tau\,|_{A_t}) = P(\tau\,|_{A_t}).\ \Pr(\text{no biparticle event occurs between } \tau \text{ and } \tau + d\tau)$$

$$= P(\tau\,|_{A_t}) \left[1 - \sum_{j=1}^{N(t)-1} \sum_{k=j+1}^{N(t)} q\{x_j(t), x_k(t)\}\, d\tau \right] \qquad (F.5)$$

The summation term accounts for all the possible pairs of particle population and will be valid only if $N(t) \geq 2$.

Dividing by $d\tau$ and taking the limit $d\tau \to 0$,

$$\frac{d}{d\tau} P(\tau\,|_{A_t}) = - P(\tau\,|_{A_t}) \sum_{j=1}^{N(t)-1} \sum_{k=j+1}^{N(t)} q\{x_j(t), x_k(t)\} \qquad (F.6)$$

which leads to,

$$P(\tau\,|_{A_t}) = \exp\left[- \int_t^{t+\tau} \sum_{j=1}^{N(t)-1} \sum_{k=j+1}^{N(t)} q\{x_j(t'), x_k(t')\}\, dt' \right] \qquad (F.7)$$

because by definition,

$$P(0\,|_{A_t}) = 1.$$

The cumulative probability distribution of T is related to P by,

$$F(\tau|_{A_t}) = \Pr(T \leq \tau|_{A_t})$$

$$= 1 - \Pr\left[T > \tau|_{A_t}\right]$$

$$= 1 - P\left[\tau|_{A_t}\right]$$

Therefore,

$$F(\tau|_{A_t}) = 1 - \exp\left[-\int_{t}^{t+\tau} \sum_{j=1}^{N(t)-1} \sum_{k=j+1}^{N(t)} q\left\{x_j(t'), x_k(t')\right\} dt'\right] \qquad (F.8)$$

Similarly, the conditional probability for a particular pair (i,j) to be involved in the biparticle event is obtained as follows:

Define an indicator variable, u, such that

$u = (i,j)$ if the particles of properties x_i and x_j undergo the biparticle event

Since the required probability is proportional to $q(x_i, x_j)$, we have,

$$\Pr\left[u = (i,j) \Big|_{A_t, T}\right] = \frac{q(x_i, x_j)}{\sum_{k=1}^{N(t)-1} \sum_{l=k+1}^{N(t)} q(x_k, x_l)} \qquad (F.9)$$

The coalesced drops again redisperse into two daughter droplets whose sizes could be $\{x; (x_i+x_j-x)\}$. The probability for formation of a daughter droplet of size x is given by,

$$M = \Pr\left[X \leq x \,\middle|\, A_t, T, u = (i,j)\right] = \frac{x}{x_i + x_j} \qquad (F.10)$$

Starting from an initial state, realization of the population process of a batch two-phase microbial propagator consists of sampling of the following representative sequence $T_1, u_1, M_1;\ T_2, u_2, M_2;\ T_3, u_3, M_3;\ \ldots\ .$

* * *

APPENDIX G

SAMPLE PHOTOGRAPH OF DETERGENT STABILIZED O/W DISPERSION, TAKEN FROM n-ALKANE-WATER-WALDHOF AGITATED SYSTEM